

REPLIES TO REVIEWERS

We would like to thank the reviewers for their constructive comments that helped improve our manuscript. Further we give our response to the comments of both reviewers point by point:

RC: Reviewer Comments, AC: Authors Comments and reply

R1 refers to Reviewer 1 and R2 to Reviewer 2

Replies to Reviewer 1

RC General Comments:

This manuscript presents a DEB-bioaccumulation model for microplastics. The model was calibrated and corroborated with field data available in the North Sea and Northern Ionian Sea, showing some skill in reproducing the (few) available observations. The topic is of interest to the readership of this Journal. The manuscript is very well written and clear. The model, the simulations and the analyses are robust and discussed thoroughly. I have a number of comments that I reported in the pdf version of the manuscript that I am attaching to this review. Here I will mention just two moderate concerns of mine regarding this work. 1) The authors used an ocean-colour chlorophyll product as input of the DEB model. However, this product might be biased in optically complex coastal waters, such as the Southern North Sea considered in this manuscript. The issue is relevant, because the authors pointed out the impact of the high chlorophyll concentration on the results they obtained in the North Sea. I recommend that the author discuss the reliability of the chlorophyll product they used. For example, they could compare the ocean colour product with in situ chlorophyll data from the ICES database (<https://www.ices.dk/marine-data/data-portals/Pages/default.aspx>), or with the NSBC climatology (<https://icdc.cen.uni-hamburg.de/1/daten/ocean/knsc-hydrographic0/>) 2)The authors should point out and discuss a bit more extensively some flaws in the results of their simulations and analysis (e.g. the overestimation of the observed MCs in Figure 6, and the mismatch between the regression results and the data at two sites in Figure 13). I appreciated that these flaws were clearly mentioned in the conclusions. I don't think that these issues compromised the value of the work. More minor to moderate issues are mentioned in the attached pdf of the manuscript.

AC Reply

We would like to thank R1 for carefully reading the manuscript and the very useful comments. With regard to the two moderate concerns:

1) The satellite dataset that we used presented a much better spatial and temporal coverage in our study area, as compared to other available datasets, such as the regional CHL-a satellite product, recommended by the reviewer (CMEMS, OCEANCOLOUR_ATL_CHL_L3_REP_OBSERVATIONS_009_067). As demonstrated in several previous studies (i.e. Sara et al., 2011, 2012, Monaco & McQuaid, 2018) it is crucial to

include daily CHL-a data to force the DEB model, in order to properly simulate the daily fluctuations of the environmental forcing data and thus the MPs accumulation.

In order to assess the reliability of the chlorophyll product that we used, we have followed the reviewer's recommendation and compared the ocean color product as an input of the DEB model, with in situ data available from the ICES database (<https://www.ices.dk/marine-data/data-portals/Pages/default.aspx>). Specifically, we used the in situ chlorophyll-a (CHL-a) data from the ICES database, that is derived from the surface layer (0-3m depth), and covers our study period of 2007-2011. A mean value, regarding depth, was computed, as representative of the upper surface layer. The in situ CHL-a data, which are included within our study area (Sec. 2.4, Southern North Sea, 51.08°-51.44° N, 2.19°-3.45° E) were averaged spatially in order to fit the "box model" of our study. Apparently some days were missing during this time period (2007-2011), while some days there were more than one measurement and then mean daily values were computed. The results from the comparison are presented also in Fig. 1 of the revised manuscript, along with the used satellite data (CMEMS-Globcolour, OCEANCOLOUR_ATL_CHL_L4_REP_OBSERVATIONS_009_098). The used satellite data are in quite good agreement with the available in situ data, presenting relatively small error (RMSE and correlation coefficient computed). The result of this comparison is shown also at the attached Fig.1 here.

The same comparison was conducted also with the regional CHL-a satellite product, suggested by the reviewer (CMEMS, OCEANCOLOUR_ATL_CHL_L3_REP_OBSERVATIONS_009_067), against the in situ data described above. We attached the Fig. 2 (only here) that shows the result of this comparison. The statistical analysis resulted in relatively higher RMSE and lower correlation coefficient, as compared to the one computed with the other (Globcolour) dataset.

Therefore, given also the better spatial and temporal coverage, we concluded that the satellite dataset that we used is optimal in our study area and time period.

2) Changes were made according to the reviewer's comment at the corresponding parts throughout the manuscript. Specifically, we have pointed out and discussed more extensively some flaws in the results of our simulations and analysis, namely the overestimation of the observed MPs in Figure 6, and the mismatch between the regression results and the data at two sites in Figure 13 of the manuscript. These points are listed in detail below, based on the corresponding comments of R1 in the manuscript.

All the line numbers written in RC are the line numbers of the R1's attached pdf manuscript, while the line numbers in AC correspond to the revised manuscript.

RC: line 15 replace "by" with "in"

AC: line 16 done.

RC: line 19 add "mussel"

AC: line 20 done.

RC: line 22 How long was the time window?

AC: line 24-25 the information was added “after 4 years and 1 year simulation”.

RC: line 35 "those": is it referred to MPs or sources?

AC: line 37 it is referred to MPs and was replaced with “those particles”.

RC: line 56 replace “from” with “at”

AC: line 58 done.

RC: line 194-195 please clarify what you mean with "represented", in this context

AC: line 196-197 the clarification was done by adding additional information in this sentence “assuming that all parameters referred to silt (or inedible particles) are applicable also to MPs particles”

RC: line 240 this implies that the last term in eq. 18 has the dimension of "particles" (C), rather than C/time. Please check the units

AC: line 242-252 The Reviewer is right. We reconstructed the Eq. 18 adding a parameter k_f (d^{-1}) in the third term that represents the post-ingestive selection mechanism utilized by the mussel to incorporate indigestible material (i.e. MPs) into faeces. This parameter is calibrated at a constant value for both study areas and illustrates the mussel’s mechanism to discriminate between particles in the gut based on physicochemical criteria according to Ward et al. (2019) review study. This parameter also compensates the units of the third term of Eq. 18 to C/time.

The whole paragraph was reconstructed to adjust the new information (line 242-254) of the revised manuscript.

RC: line 244 This should be defined just before eq. 18, to help the reader understanding the equation

AC: line 238-240 done.

RC: line 250 chlorophyll-a concentration includes large to pico functional groups of phytoplankton. Are all the groups suitable to feed mussels? If not, please clarify the limitation of this assumption in the context of your work.

AC: line 264-268 The information was added about the size limitations of the suspended matter that a mussel is able to filter.

RC: line 251 Has this result of Hatzonikolakis have general validity, or was it referred to a particular location/experiment/condition? Please discuss the extent to which this result can be reliable in the context of your application

AC: line 269-276 Although the result of Hatzonikolakis et al. (2017) was referred to a particular location/condition, the same result has been demonstrated also in other studies (i.e. Troost et al., 2010) referred to different locations and conditions. Considering that POC contributes to the mussel diet when the CHL-a concentration is low enough (Troost et al., 2010) and that our study areas

(North Sea is a more eutrophic environment and N. Ionian Sea refers to mussel farm and thus suitable conditions regarding CHL-a) do not present low Chl-a values, CHL-a can be assumed to be the dominant food source of mussels. The relevant information was added in these lines of the revised manuscript.

RC: line 258-260 Why did you not use the regional chlorophyll product available for the North West Shelf-Seas in the CMEMS catalogue? I think the regional product would have been preferable, because it takes account of the complexity of the optical waters in the coastal North Sea.

AC: line 287-296 This question has been answered in our first comment under the general R1's comment. In this part we added the result of the comparison between the used satellite dataset and the available in situ data from the ICES database. The in situ data were also added in Fig. 1 of the revised manuscript. For more details about the comparison between the recommended regional chlorophyll product and the in situ data, the reader may see the first AC reply.

RC: line 266 Similar to my previous question: why did you not use the CMEMS product for the Mediterranean Sea?

AC: line 305-311 The chosen CHL-a dataset was found preferable, as compared with other available remote sensing datasets (i.e. CMEMS chlorophyll product for Mediterranean Sea), since it presented a better spatial and temporal coverage (Hourany et al., 2019, Garnesson et al., 2019). Unfortunately, available in situ data are very scarce in the study area and therefore an extended comparison between remote and in situ data could not be conducted. However, we have compared the used satellite data (Globcolour) and the proposed product (CMEMS for Mediterranean Sea) with very few available (unpublished) in situ data, which were obtained in the framework of WFD (Water Framework Directive data kindly provided by Georgia Assimakopoulou) (Fig. 3 attached here). The few available CHL-a data in our study area (N 39.49°-39.65°, E 20.09°-20.23°) - specifically "Station Igoumenitsa" (N 39.5°, E 20.2281°) and "Station Kalamas" (N 39.6°, E 20.1439°)- were sampled at 2 m depth, covering the time period of our study (November 2014 to December 2015). The sampling dates were the same in both stations (8-Dec-14, 8-Mar-15, 12-Dec-15), allowing us to compute the mean CHL-a dataset (final 3 values) representative of our "box model". The comparison between the used satellite dataset, the proposed (regional) satellite product and the few in situ data showed the better temporal coverage and a slightly lower error for our satellite dataset (Globcolour) than the regional CMEMS product (Fig. 3 here).

RC line 272 Worth mentioning that PFT satellite products for your study regions were provided by Di Cicco et al., 2017 and Brewin et al 2017 and are now an operational product of CMEMS

AC line 315 the references were added.

RC line 281 Are you sure? Looking at your data I would say the peak is in Spring, isn't it? See also, e.g., Widdicombe et al. (2010), Journal of Plankton Research (although that paper refers to the English Channel)

AC line 322-325 the whole sentence has been clarified. We referred to the rivers discharge peaking at winter period (Van Beusekom et al., 2009), and not to the CHL-a concentration and/or productivity, which indeed peaks at spring season in the North Sea study area (shown also at Fig. 1 of the manuscript).

RC line 407 can you assume that the behavior of the model is close to linear within this range of parameter variation? In fact, SI is meaningful if the linear approximation is adequate

AC line 450-451 The R1's concern is justifiable, since we are aware of the general nonlinear effect of some parameters (i.e. temperature) on the DEB model; however within this range of parameter variation, we assumed that the model approximates the linear behavior. Our intention was to examine if the perturbed variables/parameters have an effect (or not) on the simulated MPs accumulation, in order to proceed with the development of the regression model, relating directly the environmental MPs concentration with the variables/parameters that had high effect on model's result (CHL-a, temperature and the mussel's weight and MPs load) (Eq. 20 of the manuscript). Nonetheless, the same method (sensitivity index, SI) has been also applied in other studies, which intended to examine the model's sensitivity on specific variables/parameters regarding the mussel growth (Casas and Bacher, 2006, Rosland et al., 2009, Béjaoui-Omri et al., 2014, Hatzonikolakis et al., 2017).

RC line 430 the format could be better

AC line 477 the format was changed.

RC line 430 Please define C. Does it represent OBSERVATIONS of C in the environment?

AC line 480 done. C represents the simulated MPs accumulation in the mussel.

RC line 446 Seems to me that Fig 4 is referred to before Figure 3. Please revise the order of the figures

AC line 493 done.

RC line 447 can you provide an estimate of the error, please?

AC line 494 A standard deviation was estimated by tuning the model with various X_k values and comparing the model's simulation with the available field data. The model's result with the estimated value range ($X_k = 8 \pm 1.5 \text{ mg m}^{-3}$) was in agreement with the field data and within their standard deviation.

RC line 453 Was the French site a clean one?

AC line 499-505 The sentence was revised to better justify the high value of X_k , regarding the food quality of the mussel's diet. Apart from the fact that the French site presented lower CHL-a concentrations compared to our study area (North Sea), the DEB model applied at the French site, did not include inedible particles in the mussel's food (so it was assumed clean of inedible particles). On the other hand, in our study the inedible particles (i.e. MPs) have been incorporated in the mussel's diet through the modified relation of the functional response f (Eq. 5, Table 1 in the manuscript), which regulates the assimilation rate and thus the mussel's growth (see also lines 202-208 in the manuscript). Consequently, the higher value of X_k in our study area, reflects the lower quality food and affects the half-saturation constant (X_k) according to Kooijman (2006).

RC line 464 This is not coherent with your comment of Figure 1 that CHL peaked in winter (which in fact I think was wrong)

AC See also the corresponding comment above. The comment was referred to the rivers discharge and not to the CHL-a peak. It was rephrased as mentioned, in lines 322-325 of the revised manuscript.

RC line 480 this reference comes after figure 4: please revise

AC line 532 done.

RC line 492 Please mention that the model overestimated the data range explicitly. It seems like the model reproduced a seasonal increase that was not observed.

AC line 547-548 R1's comment was considered and discussed here and also throughout the whole manuscript at the corresponding parts, as recommended.

RC line 495 Is this explanation quantifiable?

AC line 551-554 This explanation was quantified, discussed and compared with our model's result.

RC line 498-500 This sounds quite a speculation that goes too far. at the end of the day, you calibrated the model to fit the equations to the data.

AC 557-562 the whole sentence was revised, including the model's overestimation in the North Sea simulation.

RC line 500 not really in agreement in the North Sea

AC 557-562 This was commented.

RC line 554 Please mention here in the text and discuss later in the manuscript that in the North Sea the range of variability of the data and model uncertainty do not really overlap significantly at the time of the observations.

AC line 613-615 R1's comment was mentioned here and discussed in the corresponding parts of the manuscript (see also the specific parts discussed in the following comments).

RC line 594 please describe briefly the results shown in figure 13 (e.g. general overlapping of regressed and observed C, except in Hastings and Plymouth)

AC line 664-675 We described the results of Fig. 13 and discussed thoroughly about the possible explanation of the two exceptions (Hastings and Plymouth).

RC line 614-615 Please rephrase.

AC line 689-691 We rephrased the whole sentence.

RC line 623 Which approach? The seasonally variable approach? Please clarify this sentence

AC line 696-704 this was referred to our applied approach with the daily CHL-a fluctuations. In fact, it was further clarified by adding a sentence describing the evolution step that we made, by applying a daily variable approach.

RC line 627 Please remind the reader which figures presented these results.

AC line 706 done.

RC line 630 Please mention and discuss the model overestimation of MP in Figure 6.

AC line 706-712 We would like to thank R1 for the comment, as it allowed us to interpret better our results and compare further the observed field data with the model's result, regarding not only the MPs accumulation in the mussel but also the MPs elimination after 24 hours of depuration. The comment was mentioned and discussed thoroughly.

RC line 641-643 Not clear to me why this sentence is relevant here. Please clarify.

AC line 726-729 R1 is right. We also found this sentence irrelevant here, so it was deleted. The information of this sentence has been communicated to the reader earlier in the relevant part (Sec. 3.3 of the manuscript).

RC line 646-647 This sounds an over-stretched statement. please provide more evidence

AC line 731-734 We rephrased it and provided more evidence, as recommended.

RC line 662 Am I wrong, or Cenv is the dependent variable and C the predictor, in eq. 20?

AC line 751 R1 is right. This was a misprint and was corrected.

RC line 663 But in Hastings and Plymouth, why?

AC line 757-759 This was clearly stated and an explanation was suggested. The specific issue was discussed more in lines 664-675, as mentioned in a previous comment reply.

RC line 670-674 quite long sentence, please consider to split it in 2.

AC line 766-771 done.

RC line 677 Please specify what data you are talking about. MP in mussels, right?

AC line 773 This was done. Yes, we were referred to MPs in mussels.

RC line 686 overstatement. In figure 6 the data are clearly overestimated

AC line 782-784 The sentence was rephrased, including the overestimation statement.

RC line 687 replace "to be close to reality" with "to represent the natural variability"

AC line 785 done.

RC line 693 Here I do not understand: Cenv is highly variable because it is naturally variable, or because there are huge observational errors? please clarify

AC line 790-795 We clarified this by adding a sentence. We thank R1 for the comment.

RC line 729 Is this info relevant?

AC line 833 The information was deleted as we also found it irrelevant.

RC line 745 approximated? considered indirectly?

AC line 851 We replaced it with “considered indirectly”.

RC line 747-752 the logical flow of these last sentences was rather unclear to me. Please consider rephrasing this part.

AC line 851-859 We rephrased these sentences.

RC line 756-757 This is a strong critic, which I appreciate and don't consider a crucial flaw. However, such critic was not as much evident in the presentation and discussion of the results (e.g. Figure 6?). Please report the model flaw also in the presentation and discussion of the results.

AC line 864-865 This sentence was rephrased. The model flaws were reported and discussed extensively at the corresponding parts throughout the whole manuscript (i.e. presentation and discussion of the results, see also above comments reply).

RC line 772-774 I found that the sentence included redundant information, thus I suggested some changes. Please feel free to reject my suggestions

AC line 881-883 We rephrased the sentence, adjusting some changes.

RC page 40 (Figures) Can't you plot just the bottom x-axis, in black? (the upper one is redundant)

AC page 43 Fig. 8 done.

Replies to Reviewer 2

RC General Comments:

In the current manuscript, a Dynamic Energy Budget model is developed aiming to simulate the uptake and excretion rate of microplastics, by two species of mussels at two different regions (North Sea and N. Ionian Sea). The authors claim that the biophysical regime (in this case chlorophyll and sea surface temperature) influences the accumulation rates in filter feeders.

Overall, I think that the paper is well-written, without any major issues or inaccuracies. I appreciate the clear figures that allow following the manuscript. The literature is well cited and extensive. I truly enjoyed reading it; the authors have put substantial efforts in preparing their manuscript. I am, thus, recommending a few minor comments/ suggestions for their consideration. My only semi-major comment, which does not impact the overall research output, is about the overestimation of the satellite derived chlorophyll concentrations at the southern North Sea. Please see the specific comment in the next section.

AC Reply

We would like to thank R2 for his time and considerations and for carefully reading the manuscript and providing useful comments. With regard to the semi-major comment:

Since this was one of the two moderate concerns of R1, we have already examined and discussed the reliability of the satellite derived chlorophyll concentrations that were used at the southern North Sea. We compared the used satellite data (CMEMS-Globcolour), as well as, the regional satellite product (CMEMS product for the North West Shelf-Seas) with the available in situ data (ICES database) (see Fig. 1 and Fig.2 attached here). We concluded that the satellite data used, have a better spatial and temporal coverage and relatively lower error as compared to the regional CHL-a product. For more details, the reader may also see the first reply in R1's comment.

All the line numbers written in RC are the line numbers referred to the original manuscript (written in R2's review), while the line numbers in AC correspond to the revised manuscript.

Abstract

RC line 7: MavroLithari should read Mavrolithari or Mavro Lithari.

AC line 7: it should read Mavro Lithari, so we corrected it.

RC line 29-30: "... with MPs accumulation in mussel's soft tissue, temperature and chlorophyll-a." . The sentence does not flow well. Please revise.

AC line 31-32 R2 is right, so we rephrased the sentence.

Introduction

RC: It flows very well, with informative and well-referenced text. The novelty of the current study is clear.

Line 95 (and 97): DEB has been abbreviated in the abstract, please check the journal rules (if abbreviated in the abstract, is there a need to be abbreviated in the text too?).

Once you find out the rule, please apply to the species *M. edulis* and *M. galloprovincialis* (lines 96/97).

AC We would like to thank R2.

According to the journal rules, abbreviations need to be defined in the abstract and then again at the first instance in the rest of the text. We followed this rule and abbreviated the DEB in the abstract and then at the first instance (line 97). The same was applied also for the species (abstract and line 99-100).

Materials and Methods

RC line 112: The North Sea is a marginal sea rather a semi-enclosed environment (clear openings and influence from the Atlantic from both sides).

AC line 116 The suggestion was done. "semi-enclosed" was replaced with "marginal".

RC line 180: DEB is abbreviated again – please revise.

AC line 184 R2 is right, this was corrected.

RC line 250: chlorophyll-a concentrations (CHL-a, an index of phytoplankton biomass).

AC line 266: done.

RC line 258: in the future, please consider using the OC-CCI Chl-a product, which is a better product for coastal regions. Also available in Copernicus.

AC line 289-298 We have already discussed the reliability of the satellite product that we used in our study area for the specific time period above (in our first reply to R1 and R2 comments) and concluded that the used satellite CHL-a data were suitable for the specific place and time period. However, we thank R2 for the kind recommendation and we will consider this in a future relevant study.

RC line 265: it should read (i.e. SeaWiFS, MERIS, MODIS, VIIRS and OLCI-a). All these are abbreviations and not just names.

AC line 301 R2 is right and we corrected it.

RC: Please provide a simple reasoning why two different products of Chl-a were used for the two different study areas.

AC: This question has been answered also earlier in R1's comment ("why did you not use the CMEMS product for the Mediterranean Sea?"). We provide the same answer here for the reader's convenience:

"AC: line 305-311 The answer was included to the added part of the revised manuscript. Moreover, to justify our reply to R1's question we compared the used satellite data (Globcolour) and the proposed product (CMEMS for Mediterranean Sea) with very few available in situ data, which were obtained in the framework of WFD (Water Framework Directive data kindly provided by Georgia Assimakopoulou). Unfortunately, there are not enough available in situ data for the specific area (Fig. 3 attached here). The available few CHL-a data are included in our study area (N 39.49°-39.65°, E 20.09°-20.23°) - specifically "Station Igoumenitsa" (N 39.5°, E 20.2281°) and "Station Kalamas" (N 39.6°, E 20.1439°) - and sampled at 2 m depth, covering the time period of our study (November 2014 to December 2015). The sampling dates were the same in both stations (8-Dec-14, 8-Mar-15, 12-Dec-15), allowing us to compute the mean CHL-a dataset (final 3 values) representative of our "box model". The comparison between our used satellite data, the proposed satellite product and the few in situ data showed a better temporal coverage and a slightly lower error for our satellite dataset (Globcolour) than the proposed CMEMS product (Fig. 4 here)"

RC line 275: $_{-0.88}$ mg chl-a m⁻³ = should read $_{-0.88}$ mg m⁻³. Please change throughout.

AC This was changed throughout the manuscript.

RC line 282: sea surface temperature has been already abbreviated, please use the abbreviation (i.e. SST)

AC line 327 done.

RC line 325: "...Pouvreau et al., 2006).In order to..." insert a space after the punctuation mark (full stop).

AC line 370 done.

RC line 278 and Figure 1: it is a bit worrying to observe such high chlorophyll values in the coastal North Sea region. In reality, this environment is eutrophic (no doubt) and certainly very high concentrations are expected. However, your North Sea region belongs to CASE II waters, where algorithms tend to overestimate chlorophyll concentrations. In optically-complex Case II waters, Chl-a can not readily be distinguished from particulate matter and/or yellow substances (dissolved organic matter) and so global chlorophyll algorithms are less reliable. This has to be communicated to the readers.

Please add a few sentences to acknowledge the issue. To facilitate your revision, you will find this reference very useful:

International Ocean-Colour Coordinating Group – IOCCG (2000), Remote sensing of ocean colour in coastal, and other optically-complex waters, Rep. Int. Ocean-Colour Coord. Group 3, edited by S. Sathyendranath, Dartmouth, N. S., Canada. The IOCCG reports are freely available and Open-Access.

AC line 289-298 We justified the satellite product that we used in previous comments and added a few sentences to acknowledge the issue as requested. Also the above suggested reference was added.

RESULTS

RC line 448: please use the same units (they are the same after all $\text{mg m}^{-3} = \text{g l}^{-1}$)

AC line 497 this was corrected.

END.

Figures in Replies to Reviewers document

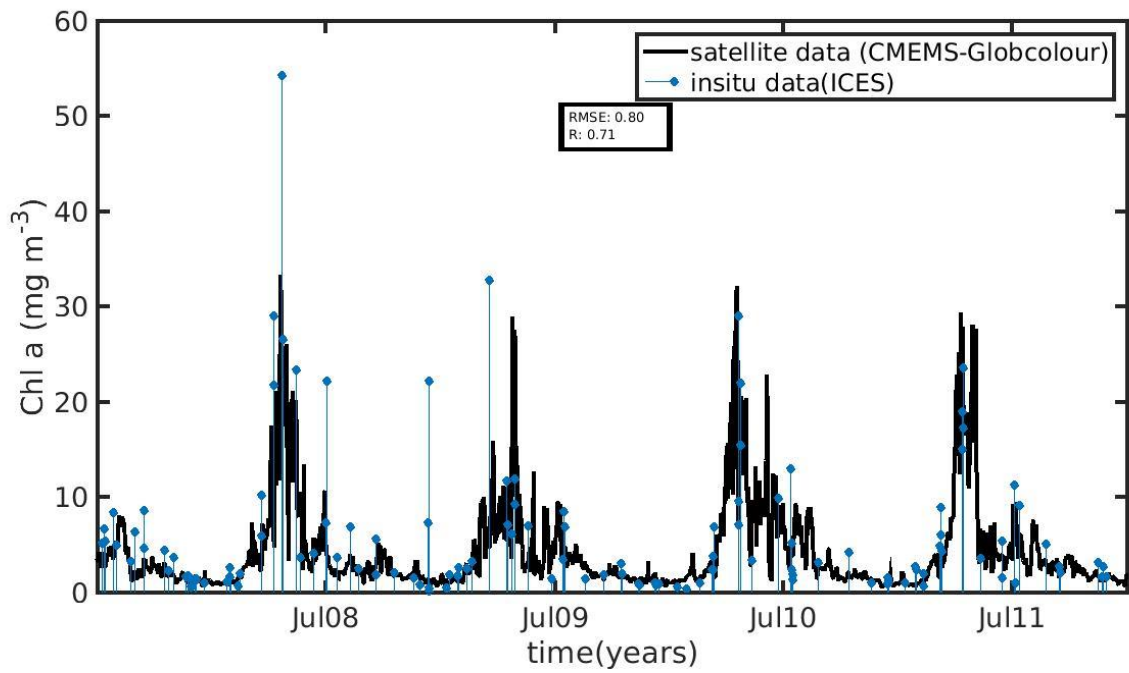


Fig.1. Comparison between the satellite data (CMEMS-Globcolour) with the available in situ data (ICES database)

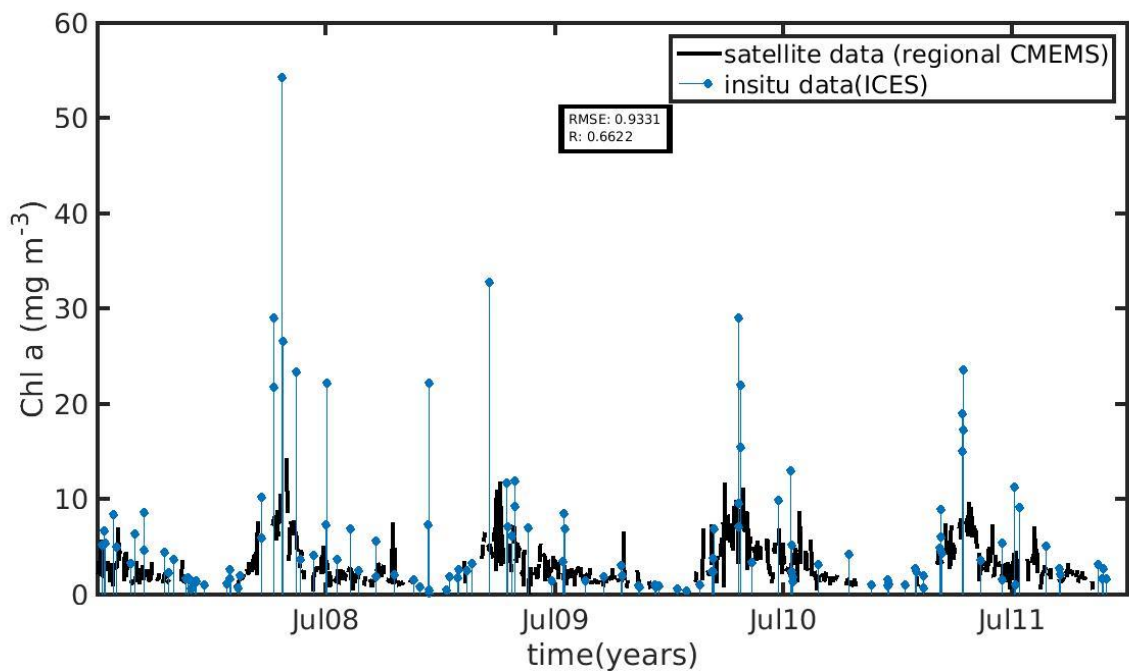


Fig. 2. Comparison between the satellite data (regional CMEMS) with the available in situ data (ICES database).

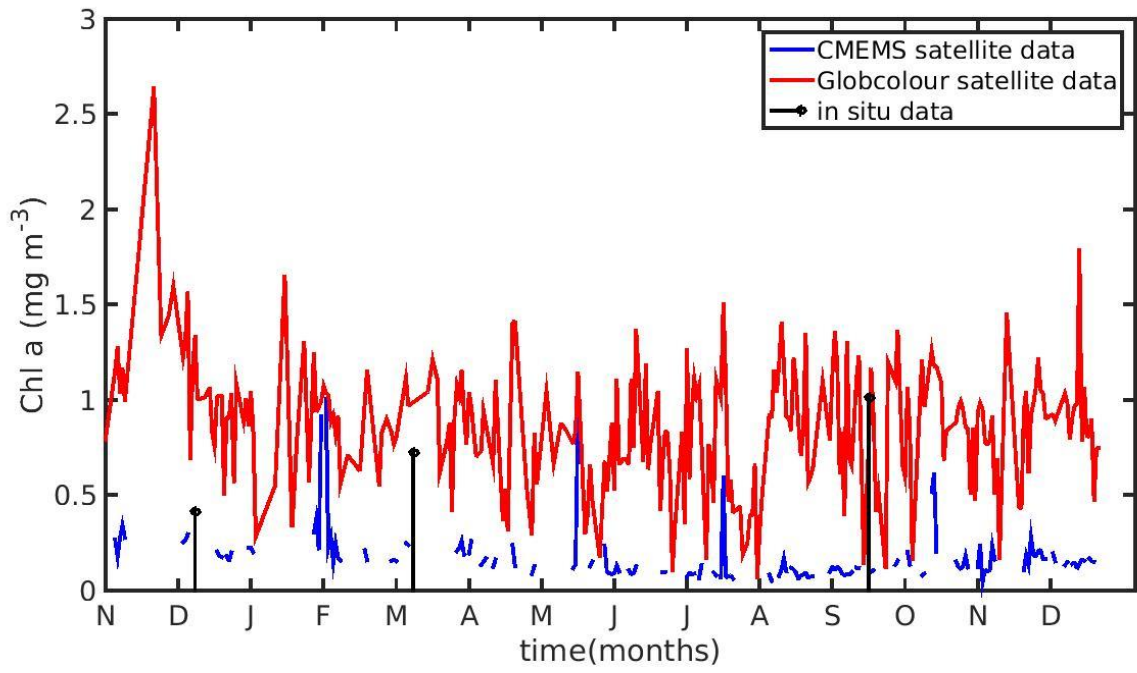


Fig. 3. Comparison between the Globcolour satellite data, the CMEMS satellite data for the Mediterranean Sea and the (few) available in situ data.

Modelling mussel (*Mytilus spp.*) microplastic accumulation.

Natalia Stamataki^{1,2,3}, Yannis Hatzonikolakis^{2,4}, Kostas Tsiaras², Catherine Tsangaris²,
George Petihakis³, Sarantis Sofianos¹, George Triantafyllou^{2,*}

¹Department of Environmental Physics, National and Kapodistrian University of Athens, 15784 Athens, Greece

²Hellenic Centre for Marine Research (HCMR), Athens-Sounio Avenue, Mavro Lithari, 19013 Anavyssos,
Greece

³Hellenic Centre for Marine Research (HCMR), 71003 Heraklion, Greece

⁴Department of Biology, National and Kapodistrian University of Athens, 15784, Greece

*Corresponding author: gt@hcmr.gr

Abstract: Microplastics (MPs) are a contaminant of growing concern due to their widespread distribution and interactions with marine species, such as filter feeders. To investigate the MPs accumulation inby wild and cultured mussels, a Dynamic Energy Budget (DEB) model was developed and validated with the available field data of *Mytilus edulis* (*M. edulis*, wild) from the North Sea and *Mytilus galloprovincialis* (*M. galloprovincialis*, cultured) from the Northern Ionian Sea. Towards a generic DEB model, the site-specific model parameter, half saturation coefficient (X_k) was applied as a power function of food density for the cultured mussel, while for the wild mussel it was calibrated to a constant value. The DEB-accumulation model simulated the uptake and excretion rate of MPs, taking into account of environmental characteristics (temperature and chlorophyll-a). An accumulation of MPs equal to 0.5364 particles individual⁻¹ (fresh tissue mass 1.9 g) and 0.91 particles individual⁻¹ (fresh tissue mass 3.34 g) was simulatedfound for the wild and cultured mussel after 4 years and 1 year respectively, in agreement with the field data. The inverse experiments investigating the depuration time of the wild and cultured mussel in a clean from MPs environment showed a 90% removal of MPs load after 2.53 and 124 days, respectively. Furthermore, sensitivity tests on model parameters and forcing functions highlighted that besides MPs concentration, the accumulation is highly depended on temperature and chlorophyll-a of the surrounding environment. For this reason, an empirical equation was found, directly relating directly the environmental concentration of MPs in seawater, with the seawater's temperature, chlorophyll-a and the MPs accumulation in mussel's soft tissue MPs load, temperature and chlorophyll-a.

1. Introduction

Microplastic particles (MPs) are synthetic organic polymers with size below 5 mm (Arthur et al., 2009) that originate from a variety of sources including ~~mainly~~: those particles that are manufactured for particular household or industrial activities, such as facial scrubs, toothpastes and resin pellets used in the plastic industry (primary MPs), and those formed from the fragmentation of larger plastic items (secondary MPs) (GESAMP, 2015). Eriksen et al. (2014) estimated that more than 5 trillion microplastic particles, weighing over 250,000 tons, float in the oceans. Due to their composition, density and shape, MPs are highly persistent in the environment and are, therefore, accumulating in different marine compartments at increasing rates: surface and deeper layers in the water column, as well as at the seafloor and within the sediments (Moore et al., 2001, Lattin et al., 2004, Thompson, 2004, Lusher, 2015). Since the majority of MPs entering the marine environment, originate from the land (i.e. land-fills, littering of beaches and coastal areas, rivers, floodwaters, untreated municipal sewerage, industrial emissions), the threat of MPs pollution in the coastal zone puts considerable pressure on the coastal ecosystems (Cole et al., 2011, Andrady, 2011). In recent years, initiatives under various projects (i.e. CLAIM, DeFishGear) target at evaluating the threat and impact of marine litter pollution; the European framework of JERICO-RI focuses on a sustainable research infrastructure in the coastal area to support the monitoring, science and management of coastal marine areas (<http://www.jerico-ri.eu/>). In the framework of JERICO-NEXT, a recent study addressed the environmental threats and gaps ~~with~~ monitoring programmes in European coastal waters, including the marine litter (i.e. MPs) as one of the most commonly identified threat to the marine environment and highlighted the need for improved monitoring of the MPs distribution and their impacts in European coastal environments (Painting et al., 2019).

Numerous studies have revealed that MPs are ingested either directly or through lower trophic prey by animals ~~at~~ from all levels of the food web; from zooplankton (Cole et al., 2013), small pelagic fishes and mussels (Digka et al., 2018a) to mesopelagic fishes (Wieczorek et al., 2018) and large predators like tuna and swordfish (Romeo et al., 2015). Microplastic ingestion by marine animals can potentially affect animal health and raises toxicity concerns, since plastics can facilitate the transfer of chemical additives and/or hydrophobic organic contaminants to biota (Mato et al., 2001, Rios et al., 2007, Teuten et al., 2007, 2009, Hirai et al., 2011). Human, as a top predator, is also contaminated by MPs (Schwabl et al., 2019). Mussel and small fishes that are commonly consumed whole, without removing digestive tracts, where MPs are concentrated, are among the most likely pathways for MPs to embed in the human diet (Smith et al., 2018). Especially regarding marine organisms (i.e. mussels), it is notable that the levels of their contamination has been added

69 to the European database (www.ecsafeseafooddbase.eu) as an environmental variable of growing
70 concern, reflecting the health status (Marine Strategy Framework Directive (MSFD) Descriptor 10
71 – Marine Litter (Decision 2017/848/EU)) (De Witte et al., 2014, Vandermeersch et al., 2015, Digka
72 et al., 2018a). Today, a series of studies have denoted the presence of MPs in mussels' tissue
73 intended for human consumption (Van Cauwenberghe and Janssen, 2014, Mathalon and Hill, 2014,
74 Li et al., 2016, 2018, Hantoro et al., 2019). For instance, in a recent study, Li et al. (2018) sampled
75 mussels from coastal waters and supermarkets in the U.K and estimated that a plate of 100g
76 mussels contains 70 MPs that will be ingested by the consumer. The presence of MPs in mussels
77 has been also demonstrated during laboratory trials in their faeces, intestinal tract (Von Moos et al.,
78 2012, Van Cauwenberghe et al., 2015, Wegner et al., 2012, Khan and Prezant, 2018), as well as in
79 their circulatory system (Browne et al., 2008). Other laboratory studies showed several effects of
80 microplastic ingestion in laboratory exposed mussels, including histological changes, inflammatory
81 responses, immunological alterations, lysosomal membrane destabilization, reduced filtering
82 activity, neurotoxic effects, oxidative stress effects, increase in hemocyte mortality, dysplasia,
83 genotoxicity and transcriptional responses (reviewed by Li et al., 2019). However, the tested
84 concentrations of MPs in laboratory experiments are frequently unrealistic, being several orders of
85 magnitude higher (2 to 7 orders of magnitude) than the observed seawater concentrations (Van
86 Cauwenberge et al., 2015, Lenz et al. 2016).

87 Mussels, through their extensive filtering activity, feed on planktonic organisms that have
88 similar size with MPs (Browne et al., 2007) and considering also their inability to select particles
89 with high energy value (i.e. phytoplankton) during filtration (Vahl, 1972, Saraiva et al., 2011a),
90 they are directly exposed to MPs' contamination. Recent studies suggest a positive linear
91 correlation between MPs concentration in mussels and surrounding waters (Capolupo et al., 2018,
92 Qu et al. 2018, Li et al. 2019). The filtering activity of mussels, which directly affects the resulting
93 MPs accumulation, is a complicated process that is controlled by other factors (food availability,
94 temperature, tides etc.).

95 The purpose of the present work is to study the accumulation of MPs ~~inby the~~ mussels and
96 reveal relations between ~~the~~ accumulated concentrations in mussels' soft parts and environmental
97 features. In this context, an accumulation model was developed based on Dynamic Energy Budget
98 theory (DEB, Kooijman , 2000) and applied in two different regions, in two different modes of life
99 (wild and cultivated): in the North Sea (~~Mytilus-~~ *E~~du~~lis* (*M. edulis*), wild) and in the Northern
100 Ionian Sea (~~Mytilus-~~ *gGal*loprovincialis (*M. galloprovincialis*), cultivated). DEB theory provides all
101 the necessary detail to model the feeding processes and aspects of the mussel metabolism, taking
102 into account the impact of the environmental variability on the simulated individual. Apart from
103 modell~~ing~~ the growth of bivalves (Rosland et al., 2009, Sara et al., 2012, Thomas et al., 2011,

104 Saraiva et al., 2012, Hatzonikolakis et al., 2017, Monaco & McQuaid, 2018), DEB models have
105 been used to study other processes as well, such as bioaccumulation of PCBs (Polychlorinated
106 Biphenyls) and POPs (Persistent Organic Compounds) (Zaldivar, 2008), trace metals (Casas and
107 Bacher, 2006) and the impact of climate change on individual's physiology (Sara et al., 2014).
108 However, to our knowledge this is the first time that a DEB-based model is used to assess the
109 uptake and excretion rates of MPs in mussels.

110
111

112 2. Materials and Methods

113

114 2.1 Study areas and field data

115

116 The North Sea is a marginal large semi-enclosed sea on the continental shelf of north-west
117 Europe with a total surface area of 850,000 km² and is bounded by the coastlines of 9 countries.
118 The sea is shallow (mean depth 90 m), getting deeper towards the north (up to 725 meters) and the
119 semi-diurnal tide (tidal range 0-5 m) is the dominant feature of the region (Otto et al., 1990). Major
120 rivers, such as Rhine, Elbe, Weser, Ems and Thames discharge into the southern part of the sea
121 (Lacroix et al., 2004), making this area a productive ecosystem. In this study, the area is limited
122 along the French, Belgian and Dutch North Sea coast (N 50.98°-51.46°, W 1.75°-3.54°). This is
123 located close to harbors, where shipping, industrial and agricultural activity is high, putting
124 considerable pressure on the ecological systems of the region (Van Cauwenberghe et al., 2015).

125 The MPs concentration in mussels' tissue and seawater that were used to validate and force
126 the model respectively at its North Sea implementation were derived from Van Cauwenberghe et al.
127 (2015). Van Cauwenberghe et al. (2015) examined the presence of MPs in wild mussels (*M. edulis*),
128 and thus collected both biota and water at 6 sampling stations along the French, Belgian and Dutch
129 North Sea coast in late summer of 2011. *M. edulis* (mean shell length: 4 ± 0.5 cm and wet weight
130 (w.w.): 2 ± 0.7 g) and water samples were randomly collected on the local breakwaters, in order to
131 assess the MPs concentration in the organisms and their habitat. MPs were present in all analyzed
132 samples, both organisms and water. Seawater samples (N=12) had MPs (<1mm) on average 0.4 ±
133 0.3 particles L⁻¹ (range: 0.0 – 0.8 particles L⁻¹) and *M. edulis* contained on average 0.2 ± 0.3
134 particles g⁻¹w.w. (or 0.4 ± 0.3 particles individual⁻¹) (Van Cauwenberghe et al., 2015). The size
135 range of MPs found within the mussels was 20-90 µm (size <1 mm).

136 The Northern Ionian Sea is located in the transition zone between the Adriatic and Ionian Sea.
137 The long and complex coastline, presents a high diversity of hydrodynamic and sedimentary
138 features. Rivers discharging into the Northern Ionian Sea include Kalamas/Thyamis (Greece) and
139 Butrinto (Albania) (Skoulikidis et al., 2009), making the area suitable for aquaculture. Small
140 farming sites and shellfish grounds are operating in Thesprotia (northwestern Ionian Sea)
141 (Theodorou et al., 2011). The main source of marine litter inputs in the area originates from
142 anthropogenic activities that mainly include shoreline tourism and recreational activities, poor
143 wastewater management, agricultural practices, fisheries, aquacultures and shipping (Vlachogianni
144 et al., 2017; Digka et al., 2018a). According to Politikos et al. (2020), the area around the Corfu
145 island (Northern Ionian Sea) is characterized as a retention area of litter particles probably due to
146 the prevailing weak coastal circulation. Furthermore, a northward current on the east Ionian Sea
147 facilitates the transfer of litter particles towards the Adriatic Sea, which has been characterized as a
148 hotspot of marine litter and one of the most affected areas in the Mediterranean Sea (Pasquini et al.,
149 2016, Vlachogianni et al., 2017, Liubartseva et al., 2018, Politikos et al., 2020).

150 The field data used to validate the model output in the N. Ionian Sea were obtained from
151 Digka et al. (2018b, 2018a). In the framework of the “DeFishGear” project, mussels (*M.*
152 *galloprovincialis*) were collected by hand from a long line type mussel culture farm in Thesprotia
153 (N 39.606567° E 20.149421°), in summer 2015 (end of June/July) at a sampling depth up to 3 m
154 (Digka et al., 2018a). The average MPs accumulation was calculated from a total population of 40
155 mussels originated from the farm, with 18 of them found contaminated with MPs (46.25%). The
156 average load of MPs (size <1 mm) per mussel (mean shell length 5.0 ± 0.3 cm) was 0.9 ± 0.2
157 particles individual⁻¹ and the size of MPs found in the mussel’s tissue ranged from 55 to 620 μm .
158 Both clean and contaminated mussels were included in the calculated mean value in order to
159 represent the mean state of the contamination level for the individual inhabiting the study area.

160 The seawater concentration of MPs for the N. Ionian Sea implementation was obtained from
161 Digka et al. (2018b) and the DeFishGear project results ([http://www.defishgear.net/project/main-](http://www.defishgear.net/project/main-lines-of-activities)
162 [lines-of-activities](http://www.defishgear.net/project/main-lines-of-activities)). In total, 12 manta net tows were conducted in the region, collecting a total
163 number of $n_1=2,027$ particles on October 2014 and $n_2=1,332$ on April 2015, leading to an average
164 of 280 particles per tow with size <1 mm and >330 μm (Digka et al., 2018b). In order to estimate
165 the mean MPs concentration in the region, expressed as particles per volume, the dimensions of the
166 manta net (W 60 cm H 24 cm, rectangular frame opening, mesh size 330 μm) and the sampling
167 distance of each tow (~2 km) were used by multiplying the sample surface of the net by the trawled
168 distance in meters (Maes et al., 2017), which resulted in a mean MPs concentration of 1.17 particles
169 m^{-3} (233,333 particles km^{-2}). Moreover, in the wider region of the Adriatic Sea, Zeri et al. (2018)
170 found a mean density of $315,009 \pm 568,578$ particles km^{-2} (1.58 ± 2.84 particles m^{-3}), out of which

171 34% sized <1 mm. A relatively high value of standard deviation (one order of magnitude higher
172 than the mean value) is adopted (0.0012 ± 0.024 particles L^{-1}), considering that the mussel farm is
173 established in an enclosed gulf and close to the coast, since, according to Zeri et al. (2018), the
174 abundance of MPs is one order of magnitude higher in inshore (<4 km) compared to offshore
175 waters (>4 km). Furthermore, it may be assumed that the adopted range (standard deviation is also
176 multiplied by a factor of 2) includes also the smaller particles sized between 50 μm and < 330 μm ,
177 which have been found in mussel's tissue (Digka et al., 2018a), but were overlooked during the
178 seawater sampling due to the manta net's mesh size (> 330 μm). According to Enders et al. (2015)
179 the relative abundance of small particles (50- 300 μm) compared to particles larger than 300 μm is
180 approximately 50%.

181

182 2.2 DEB model description

183

184 In the present study, a ~~DEB~~Dynamic Energy Budget (DEB, Kooijman, 2000, 2010) model is
185 used as basis to simulate the accumulation of MPs by mussels. In DEB theory (Kooijman, 2000),
186 the energy assimilated through food by the simulated individual is stored in a reserve compartment
187 from where a fixed energy fraction κ is allocated for growth and somatic maintenance, with a
188 priority for maintenance. The remaining energy ($I - \kappa$) is spent on maturity maintenance and
189 reproduction. The individual's condition is defined by the dynamics of three state variables: energy
190 reserves E (joules), structural volume V (cm^3) and energy allocated to reproduction R (joules). The
191 energy flow through the organism is controlled by the fluctuations of the available food density and
192 temperature characterizing the surrounding environment.

193 The DEB model implemented here is an extended version of the model described in
194 Hatzonikolakis et al. (2017), where the growth of the Mediterranean mussel is simulated ~~by~~ taking
195 into account only the assimilation rate of the individual. Since the present study focuses on
196 ~~simulating~~ the MPs accumulation, it is crucial to include a detailed representation of the mussel's
197 feeding mechanism. In this context, the DEB model was extended by including the clearance (C_r),
198 filtration (\dot{p}_{XiF}) and ingestion (\dot{p}_{XiI}) rates of the mussel, following Saraiva et al. (2011a), assuming
199 that all parameters referred to silt (or inedible particles) are applicable also to MPs particles with
200 MPs represented by the silt variable. In this approach, a pre-ingestive selection occurs between
201 filtration and ingestion, returning the rejected material in the water through pseudofaeces (J_{pfi}).
202 Consequently, energy is assimilated through food while the non-assimilated particles are excreted
203 through the faeces production (J_f). The model's equations, variables and parameters are shown in
204 Table 1, 2 and 3 respectively. The scaled functional response f (Eq. 5, Table 1), which regulates the

205 assimilation rate, is modified following Kooijman (2006) to include an inorganic term representing
206 the non-digestible matter i.e. microplastics: $f = X/(X + K_y)$ and $K_y = X_K \cdot (1 + Y/Y_K)$ where Y
207 and Y_k are the concentration of MPs, converted from particles L^{-1} to $g\ m^{-3}$ (Everaert et al., 2018) and
208 the half saturation coefficient of inorganic particles here represented by MPs ($g\ m^{-3}$), respectively.
209 Thus, the assimilation rate that is regulated by f is decreasing when the concentration of MPs is
210 increased. The same approach is followed by other authors who considered inedible particles in the
211 mussel's diet (Ren, 2009, Troost et al., 2010). During the filtration process the same clearance rate
212 for all particles is used ($\{\dot{C}_R\}$), representing the same searching rate for food that depends on the
213 organism maximum capacity ($\{\dot{C}_{Rm}\}$) and environmental particle concentrations (Vahl, 1972,
214 Widdows et al., 1979, Cucci et al., 1989). During the ingestion process the mussel is able to
215 selectively ingest food particles and reject inedible material, in order to increase the organic content
216 of the ingested material (Kiørboe & Møhlenberg, 1981, Jørgensen et al., 1990, Prins et al., 1991,
217 Maire et al., 2007, Ren, 2009, Saraiva et al., 2011a). This selection is reflected by the different
218 binding probabilities adopted for each type of particle (ρ_1 for algae particles and ρ_2 for inorganic
219 particles i.e. MPs, see Eq. 14 and table 3). The equations representing the feeding processes handle
220 each type of particle separately, while there is interference between the simultaneous handling of
221 different particle types (Eq. 12-14, Table 1) (Saraiva et al., 2011a). Finally, during the assimilation
222 process, suspended matter (i.e. MPs) that the mussel is not able to assimilate due to its different
223 chemical composition from the reserve compartment (Saraiva et al., 2011a) or incipient saturation
224 at high algal concentrations (Riisgard et al., 2011) results in the faeces production (Eq. 16, Table 1).
225

226 2.3 Microplastics accumulation sub-model

227
228 With the DEB model as a basis, a sub-model describing the ~~microplastics~~ (MPs) accumulation
229 by the mussel was developed, assuming that the presence of MPs in the ambient water does not
230 cause a significant adverse effect on the organisms' overall energy budget, in accordance with
231 laboratory experiments, conducted in mussel species (Van Cauwenberghe et al., 2015: *Mytilus*
232 *edulis*, Santana et al., 2018: mussel *Perna perna*). Additionally, it was assumed that the mussel
233 filtrates MPs present in the water, without the ability of selecting between the high energetic valued
234 particles and the MPs during the filtration process (Van Cauwenberghe et al., 2015, Von Moos et
235 al., 2012, Browne et al., 2008, Digka et al., 2018a among others). The uptake of MPs from the
236 environment is taken into account through the process of clearance/filtration rate, while the
237 excretion of the contaminant is derived from two processes: (i) pseudofaeces production and (ii)
238 faeces production. The resulting MPs accumulation is influenced by external environmental factors

239 (MPs concentration, food availability, temperature) and internal biological processes (clearance,
240 filtration, ingestion, growth). ~~All these are described by~~ the following differential equation
241 describes the change of the individual MPs accumulation (C , particles individual⁻¹), taking into
242 account the processes mentioned above:

$$\frac{dC}{dt} = C_{env} \cdot \dot{C}_R - \dot{J}_{pf2} - k_f \cdot \frac{J_f}{p_{X1I}} \cdot C \quad (\text{Eq. 18})$$

246 where \dot{C}_R is the clearance rate for water (L h⁻¹), containing a concentration of MPs C_{env} (particles L⁻¹).
247 The terms of \dot{J}_{pf2} and $\frac{J_f}{p_{X1I}}$ represent the elimination rate of MPs through pseudofaeces (particles
248 h⁻¹) and the non-dimensional rate of faeces production with respect to the ingestion rate,
249 respectively (see Table 1, Eq. 15-16). The parameter k_f represents the post-ingestive selection
250 mechanism utilized by the mussel to incorporate indigestible material (i.e. MPs) into faeces and was
251 calibrated using the available field data of mussel's MPs accumulation from both study areas (Table
252 3). Mussel is able to discriminate among particles in the gut based on size, density and chemical
253 properties of the particles (i.e. between microalgae and inorganic material) and thus to eliminate
254 them through faeces (Ward et al., 2019a and references therein). In this context, the pseudofaeces
255 production incorporates the rejected MPs prior to the ingestion, while the faeces production
256 includes MPs that are rejected along with the food particles that are not assimilated by the mussel.
257 The model's time step has been set to one hour in order to capture the dynamics of the rapidly
258 changing processes, such as feeding and excretion.

259 ~~The accumulation of MPs in the individual is represented by the state variable C (particles~~
260 ~~individual⁻¹) which is computed at every model time step. This has been set to one hour, in order to~~
261 ~~properly resolve the dynamics of the rapidly changing processes, such as feeding and excretion.~~

262 2.4 Environmental drivers

263
264 Besides MPs concentration in the seawater, the DEB model is forced by sea surface
265 temperature (SST) and food availability, ~~represented defined by~~ chlorophyll-a concentrations
266 (CHL-a, an index of phytoplankton biomass). *M. edulis* has been demonstrated to filter suspended
267 particles greater than 1µm, a size class that includes all of the phytoplankton, zooplankton and
268 much of the detritus (Vahl, 1972, Mohlenberg and Riisgard, 1978, Saraiva et al., 2011a, Strohmeier
269 et al., 2012), including even aggregated picoplankton-size particles (i.e. marine snow) (Kach and
270 Ward, 2008, Ward and Kach, 2009). CHL-a has been considered the most reliable food quantifier
271 for the calculation of DEB shellfish parameters (Pouvreau et al., 2006, Sara et al., 2012,

272 [Hatzonikolakis et al., 2017 and references therein](#)). Hatzonikolakis et al. (2017) have tested the
273 performance of the model, considering also particulate organic carbon (POC) in the mussel's diet,
274 which, however, did not have an important impact on the model's skill against field data [in the](#)
275 [Mediterranean Sea study areas. This outcome agrees with Troost et al. \(2010\) demonstration that](#)
276 [POC contributes to the mussel's diet when CHL-a concentrations are low at the southwest of](#)
277 [Netherlands. Thus, in the present study, only CHL-a is considered as the available food source for](#)
278 [mussels originated from the Southern North Sea and the Northern Ionian Sea. Thus, only CHL-a, is](#)
279 ~~considered as the available food source~~. For both study areas SST and CHL-a are derived from
280 daily satellite data, a method also used by other authors (i.e. Thomas et al., 2011, Monaco &
281 McQuaid, 2018).

282 In the North Sea, SST data were obtained from daily satellite images provided by Copernicus
283 Marine Environmental Monitoring Service (CMEMS) at 0.04 degree spatial resolution, ~~and~~ CHL-a
284 data [obtained](#) from the [Globcolour](#) daily multi-sensor product provided by CMEMS ~~Globecolour~~
285 ~~database~~ at 1 km spatial resolution, [based on the OC5 algorithm of Gohin et al. \(2002\)](#)
286 (<http://marine.copernicus.eu/>, generated using CMEMS Products, production center ACRI-ST). The
287 environmental forcing data (SST, CHL-a) were averaged over the study area (51.08°-51.44° N,
288 2.19°-3.45° E), covering the period 2007-2011 (5 years), in order to realistically simulate the wild
289 mussel's growth harvested ~~in~~ late summer 2011 (Van Cauwenberghe et al., 2015). [It is notable](#)
290 [that the study area of the North Sea belongs to CASE II waters \(coastal region\), where algorithms](#)
291 [tend to overestimate CHL-a concentrations. In optically-complex Case II waters, CHL-a cannot](#)
292 [readily be distinguished from particulate matter and/or yellow substances \(dissolved organic matter\)](#)
293 [and so global chlorophyll algorithms are less reliable \(IOCCG, 2000\). However, the CHL-a dataset](#)
294 [that was used was found in good agreement with available in situ data from ICES database](#)
295 [\(https://www.ices.dk/data/Pages/default.aspx\)](https://www.ices.dk/data/Pages/default.aspx) for the specific study area and time period, (Fig. 1),
296 [showing a relatively smaller bias and better time-space coverage, as compared with other tested](#)
297 [remote sensing datasets \(not shown\) \(i.e. regional chlorophyll product available for the North West](#)
298 [Shelf-Seas in the CMEMS catalogue, https://resources.marine.copernicus.eu/\).](#)

299 In the North Ionian Sea, daily satellite SST data were also obtained from the CMEMS
300 database for the Mediterranean Sea with 0.04 degree spatial resolution, [while CHL-a daily data](#)
301 [were derived from the Globcolour multi-sensor \(i.e. SeaWiFS, MERIS, MODIS, VIIRS and OLCI-](#)
302 [a\) merged product \(http://globcolour.info\) at 1 km spatial resolution based on the OC5 algorithm](#)
303 ~~suitable for coastal regions (Gohin et al., 2002) while CHL-a data were derived from the merged~~
304 ~~product of many satellites (i.e. SeaWiFs, Meris, Modis, Viirs and Olei a) provided by Globecolour~~
305 ~~web interface (http://globcolour.info) at a daily temporal resolution and 1 km spatial resolution~~. The
306 forcing data were averaged over the study area (N 39.49°-39.65°, E 20.09°-20.23°) covering the

307 period 2014-2015 (2 years), when the cultured mussel is ready for the market. The chosen CHL-a
308 dataset was found preferable, as compared with other available remote sensing datasets (i.e.
309 CMEMS chlorophyll product for Mediterranean Sea), since it presented a better spatial and
310 temporal coverage (Hourany et al., 2019, Garnesson et al., 2019) and a slightly lower error, as
311 compared with the very few available in situ data in the study area (not shown). Unfortunately,
312 these were very scarce and therefore an extended comparison between remote and in situ data could
313 not be conducted. The satellite derived CHL-a data were estimated based on the OC5 algorithm of
314 Gohin et al. (2002) in both study areas, which is regarded as suitable for coastal waters. Satellite
315 data have facilitated large scale ecological studies by providing maps of phytoplankton functional
316 types and sea surface temperature (Raitsos et al., 2005, 2008, 2012, 2014, Palacz et al., 2013, Di
317 Cicco et al., 2017, Brewin et al., 2017). The daily environmental forcing data are shown in Fig. 1
318 and Fig. 2 for the North Sea and the N. Ionian Sea, respectively. The two coastal environments
319 present some important differences regarding both CHL-a and SST. Specifically, in the N. Ionian
320 Sea, CHL-a is relatively low (annual mean $\sim 0.88 \text{ mg-chl-a m}^{-3}$) and peaks during winter (maximum
321 $\sim 2.64 \text{ mg-chl-a m}^{-3}$ at December 2014), while in the North Sea CHL-a is about four times higher
322 (annual mean $4.25 \text{ mg-chl-a m}^{-3}$), peaking in April every year (maximum range $29.44\text{-}33.38 \text{ mg}$
323 chl-a m^{-3}), as soon as light availability reaches a critical level (Van Beusekom et al., 2009). The
324 higher productivity during spring season in the North Sea is related with the nutrient inputs from the
325 English Channel, the North Atlantic and particularly the river discharge of nutrient-rich waters
326 along the Belgian-French-Dutch coastline, which that peaks earlier, during winter period (Van
327 Beusekom et al., 2009). The SSTsea surface temperature peaks during August in both areas (Fig. 1
328 and Fig. 2), but is significantly higher in the N. Ionian Sea (maximum 28.8°C), as compared to the
329 North Sea (maximum $18\text{-}19.3^{\circ}\text{C}$).

330 The environmental concentration of MPs, C_{env} (particles L^{-1}) was obtained also at a daily time
331 step as randomly generated values of the Gaussian distribution that is determined by the mean value
332 and standard deviation of the observed field data (0.4 ± 0.3 particles L^{-1} , North Sea, Van
333 Cauwenberghe et al., 2015, 0.0012 ± 0.024 particles L^{-1} , N. Ionian Sea, Digka et al., 2018a).
334 Considering that these values originate from surface waters and that mussels live in the near surface
335 layer (0-5 m), C_{env} is estimated as a mean value of the upper layer with the methods described by
336 Kooi et al. (2016), who studied the vertical distribution of MPs, considering an exponential
337 decrease with depth. Specifically, in the N. Ionian Sea, mussels were collected from a depth up to 3
338 m (Digka et al., 2018a), while in the North Sea (Van Cauwenberghe et al., 2015), there is no
339 information and thus a maximum depth of 5 m is adopted.

340 In the North Sea simulation, the effect of tides is taken into account by considering that the
341 mussel originated from the intertidal zone, is submerged 12 hours during the day (Van

342 Cauwenberghe et al., 2015). In the N. Ionian Sea simulation, tides are not considered, given the
343 very small tide amplitude (few centimeters) in the Mediterranean (i.e. Sara et al., 2011;
344 Hatzonikolakis et al., 2017) and thus the cultured mussel is assumed permanently submerged. *In*
345 *situ* hourly tide data (2007-2011) from the coastal zone of the region (Dunkerque station N
346 51.04820°, E 2.36650°) obtained from Coriolis and Copernicus data provider
347 (<http://marine.copernicus.eu>, <http://www.coriolis.eu.org>), showed that mussels experience
348 alternating periods of aerial exposure and submergence at approximately every 6 hours (2 high and
349 2 low tides). During aerial exposure the model suspends the feeding processes (Sara et al., 2011)
350 and simulates metabolic depression (Monaco & McQuaid, 2018) where, the Arrhenius thermal
351 sensitivity equation (Eq. 9) is corrected by a metabolic depression constant ($M_d = 0.15$), a value
352 representative for *M. galloprovincialis* and here applied also for *M. edulis*. In the present study, the
353 mussel's body temperature change during low tide is ignored, inducing a model error. The mussel's
354 body temperature (i.e. surrounding water temperature for submerged mussels) during air exposure
355 depends on many factors, such as solar radiation, air's temperature, wind speed and wave height,
356 according to studies investigating the temperature effect on intertidal mussels (Kearney et al., 2010,
357 Sara et al., 2011). However, the present study aims to primarily examine the MPs accumulation and
358 thus the intertidal mussel's body temperature was not thoroughly examined. Nonetheless, the time
359 that the mussel is able to filter, ingest and excrete the suspended matter (i.e. food and MPs particles)
360 and the effect on the mussel's growth through the modified relation of $k(T)$ are included, since the
361 assimilation process occurs whether the mussel is submerged or not (Kearney et al., 2010).

362 2.5 Parameter values

363

364 Most of the DEB model parameters were obtained from Van der Veer et al. (2006) and are
365 referred to the blue mussel *M. ~~edulis~~ edulis* in the northeast Atlantic (see Table 3 for the exceptions).
366 This assumption has also been adopted in previous studies which showed that this parameter set for
367 *M. edulis* applies also for *M. galloprovincialis* (i.e. Casas and Bacher, 2006, Hatzonikolakis et al.,
368 2017). The half saturation coefficient X_k represents the density of food at which the food uptake rate
369 reaches half of its maximum value and should be treated as a site – specific parameter (Troost et al.,
370 2010, Pouvreau et al., 2006). In order to estimate the value of X_k , a different approach was followed
371 for each study area.

372 For the North Sea simulation, X_k was tuned so that the simulated individual has the recorded
373 size at the corresponding estimated age (Van Cauwenberghe et al., 2015) growing with the
374 representative growth rates of wild *M. edulis* at the region (Saraiva et al., 2012, Sukhotin et al.,
375 2007). For the N. Ionian Sea simulation, an alternative method was adopted, aiming to generalize

376 the DEB model to overcome the problem of site-specific parameterization. The DEB model was
377 tuned against literature field data for cultured mussels originated from different areas in the
378 Mediterranean and Black Seas, where the average CHL-a concentration ranged between 1.0 and 5.0
379 $\mu\text{g-chl-}\underline{\text{a}}\text{mg m}^{-3}$, and one X_k value was found for each area. The four areas used, their characteristics
380 and the corresponding value of X_k adopted, are shown in Table 4. These values of X_k are related to
381 the prevailing CHL-a concentration of each area ([CHL-a]) through three different functions:
382 linear: $f(x) = a * [CHL - a] + b$ exponential: $f(x) = a * \exp(b * [CHL - a])$ and power: $f(x) =$
383 $a * [CHL - a]^b + c$. The curve fitting app of Matlab (Matlab R2015a) was used for the
384 determination of a, b and c of each function taking into account the 95% confidence level. The
385 score of each function regarding the somatic/mussel growth simulation in all four regions is tested
386 through target diagrams (Jolliff et al., 2009) by computing the bias and unbiased root-mean-square-
387 deviation (RMSD) between field and simulated data of all 4 regions and the function with the best
388 score is adopted. A similar approach was followed by Alunno-Bruscia et al. (2011) for the oyster
389 *Crassostrea gigas* in six Atlantic ecosystems who expressed the X_k as a linear function of food
390 density (e.g. phytoplankton). Unfortunately, the approach described for the N. Ionian Sea
391 simulation could not be applied in the North Sea, as the limited amount of growth data from the
392 literature for wild *M. edulis* in similar environments did not permit a statistically significant fit of a
393 similar function ($X_k = f(chl - a)$).

394

395 **2.6 Simulation of reproduction-Initialization of the model**

396

397 The reproductive buffer (R) is assumed to be completely emptied at spawning ($R = 0$)
398 (Sprung, 1983, Van Haren et al., 1994). In order to simulate mussel's spawning, the gonado-
399 somatic index (GSI) defined as gonad dry mass over total dry flesh mass was computed at every
400 model's time step (Eq. 17 Table 1; the water content of the fresh tissue mass was assumed 80%
401 according to Thomas et al. (2011)). Spawning was induced by a critical value of GSI (GSI_{th} , Table
402 3) and a minimum temperature threshold (T_{th}) at each study area, obtained from the literature. In the
403 North Sea implementation, T_{th} was set at 9.6 °C (Saraiva et al., 2012), while in the N. Ionian Sea, at
404 15 °C (Honkoop and Van der Meer, 1998). This kind of formulation for the spawning event in
405 bivalves has been used in previous studies (i.e. Pouvreau et al., 2006, Troost et al., 2010, Thomas et
406 al., 2011, Monaco & McQuaid, 2018). The simulated abrupt losses of the mussel's tissue mass
407 correspond to spawning events and the model's prediction was compared with the available
408 literature data regarding the spawning period in each study area. Theodorou et al. (2011)
409 demonstrated that the spawning events occur during winter for *M. galloprovincialis* in the mussel

410 farms of Greece, while in the North Sea the spawning period for *M. edulis* is extended from the end
411 of April until the end of June (Sprung, 1983, Cardoso et al., 2007).

412 In both areas, the model was initialized so that the simulated individual is in the juvenile
413 phase ($V < V_p$; Table 3) and the reproductive buffer can be considered to be empty ($R = 0$) (Thomas
414 et al., 2011). As stated by Jacobs et al. (2015) amongst others, juvenile mussels (*M. edulis*) range
415 between 1.5-25 mm in size. Specifically, in the North Sea the settlement of mussel larvae (*M.*
416 *edulis*) takes place in June and the juveniles grow to a maximum size of 25 mm within 4 months
417 (Jacobs et al., 2014). In the N. Ionian Sea, the operating mussel farms follow the life cycle of *M.*
418 *galloprovincialis*, starting the operational cycle each year by dropping seed collectors from late
419 November until March and the juvenile mussels grow up to 6-6.5cm after approximately one year
420 according to the information obtained from the local farms in the region and Theodorou et al.
421 (2011). The initial fresh tissue mass was distributed between the structural volume (V) and reserves
422 energy (E). Energy allocated to those two compartments was firstly constrained by the initial length
423 (L) and then energy allocated to V was in Eq.10 (Table 1). The initial value of E was set so that the
424 simulated individual has an initial weight that corresponds to the juvenile phase ($V < V_p$) (Table 5).
425 Finally, for both model implementations, the initial accumulation of MPs in the mussel's tissue (C)
426 was set to zero.

427

428 2.7 Simulation Runs

429 The DEB-accumulation model simulates at an hourly basis the growth and MPs accumulation
430 of the wild mussel from the North Sea and the cultured mussel from the N. Ionian Sea. Initially, a
431 model run is performed at each study area during the periods July 2007 to August 2011 (4 years) for
432 the North Sea simulation and late November 2014 to January 2016 (~ 1 year) for the N. Ionian Sea
433 simulation. Additionally, the inverse simulations were performed in order to evaluate the depuration
434 phase of both cultured and wild mussel, by setting the environmental MPs concentration equal to
435 zero ($C_{env}=0$), after a period of 1 year simulation at the N. Ionian Sea, when the cultured mussel has
436 the appropriate size for market, and after 4 years at the North Sea, when literature field data are
437 available (Van Cauwenberghe et al., 2015). In this simulation, the mussel's gut clearance is
438 achieved by the excretion of MPs through faeces (3rd term of Eq. 18), and thus it is necessary to
439 maintain the existence of food in the mussel's environment in order to ensure that the feeding-
440 excretion processes will occur.

441 Furthermore, to examine the model's uncertainty related to the environmental MPs
442 concentration, a series of 15 and 13 simulations were performed in the North Sea and N. Ionian Sea

443 respectively, adopting different constant values of C_{env} within the observed range of each area.
444 Finally, the effect of the environmental forcing data and some model's parameters on the resulting
445 MPs accumulation by both mussels was explored through sensitivity experiments. These were
446 used to derive a new function that predicts the level of MPs pollution in the environment.

447

448 2.8 Sensitivity tests and Regression analysis

449 The effect of the environmental data (CHL-a, temperature, C_{env}) and two parameters
450 representative of mussel's growth (X_k, Y_k) on the MPs accumulation by the mussel for each study
451 area was examined through sensitivity experiments with the DEB-accumulation model. Each
452 variable (CHL-a, T, C_{env}) and parameter (X_k, Y_k) was perturbed by $\pm 10\%$ to examine their effect on
453 the simulated MPs accumulation, and the results of each run were analyzed using the sensitivity
454 index (SI), SI which calculates the percentage change of the mussel's MPs accumulation $SI =$
455 $\frac{1}{n} \sum_{t=1}^n \frac{|C_t^1 - C_t^0|}{C_t^0} \cdot 100$ (%), where n is the simulated time steps, C_t^0 is the MPs accumulation predicted
456 with the standard simulation at time t and C_t^1 is the MPs accumulation with a perturbed
457 variable/parameter at time t ; for details see Bacher and Gangnery, (2006). The same method has
458 been also applied to other studies, which examined the model's sensitivity on specific
459 variables/parameters regarding the mussel growth (Casas and Bacher, 2006, Rosland et al., 2009,
460 Béjaoui-Omri et al., 2014, Hatzonikolakis et al., 2017). In order to also examine the effect of tides,
461 in the North Sea implementation, the sensitivity experiments were conducted twice: the first time
462 assuming that the mussel is permanently submerged and the second time assuming that the mussel
463 is periodically exposed to the air.

464 Preliminary sensitivity experiments showed that the MPs accumulation is highly depended on
465 the prevailing conditions regarding the CHL-a, temperature and C_{env} and the mussel's growth that is
466 regulated by the half saturation coefficient (X_k). Therefore an attempt was made using the model's
467 output to describe the MPs accumulation as a function of these variables through a custom
468 regression model:

$$469 \quad y = b_1 * W + b_2 * \exp\left(\frac{1}{T}\right) + b_3 * \frac{1}{[CHL-a]} + b_4 * C_{env} \quad (\text{Eq. 19})$$

470 where y (particles/individual) is the response variable and represent the predicted MPs
471 accumulation by the mussel; W (g) the mussel's fresh tissue mass, T (K) the sea surface
472 temperature, CHL-a and C_{env} are the concentrations of chlorophyll-a and MPs in the water
473 respectively, which are the predictor variables. The values of coefficients $b_1, b_2, b_3,$ and b_4 are

474 calculated using the nonlinear regression function (nlinfit, Matlab R2015a) which attempts to find
475 values of the parameters b that minimize the least squared differences between the model's MPs
476 accumulation output C and the predictions of the regression model $y = f(W, T, [chl\ a], C_{env}, b)$.

477 The ultimate aim of this analysis, once coefficients are determined, is to use [Eq. equation 19](#) to
478 obtain the environmental MPs concentration:

$$C_{env} = \frac{1}{b_4} * \left(C - b_1 * W - b_2 * \exp\left(\frac{1}{T}\right) - b_3 * \frac{1}{[CHL-a]} \right)$$

480 (Eq. 20)

481 which could be a very useful tool to predict the MPs concentration in the environment, when all
482 involved variables are known ([mussel size](#), [mussel's accumulated MPs \(C\)](#), [wet weight \(W\)](#)
483 temperature [\(T\)](#) and CHL-a), using the mussel as a potential bioindicator (Li et al., 2016, Li et al.,
484 2019). The score of this custom model was tested by applying Eq. 20 in our study areas and 6 more
485 areas around the U.K., where information of mussel's wet weight and both mussels' and
486 environment's MPs load is available (Li et al., 2018). CHL-a and temperature, which were not
487 included in Li et al. (2018), were obtained from daily satellite images (same source as in the North
488 Sea, see 2.4 section), covering the period that the mussels were harvested (Li et al., 2018).

489

490 **3. Results**

491

492 **3.1 Growth simulations**

493

494 The growth simulations of *M. edulis* and *M. galloprovincialis* for the North Sea and the N.
495 Ionian Sea are shown in Fig. [34](#) and Fig. [45](#) respectively. In the North Sea implementation, X_k was
496 tuned to a constant value: $X_k = 8 \text{ mg-ehl-a m}^{-3}$ ($\pm 1.5 \text{ mg m}^{-3}$). The fitted value was [slightly](#) higher, as
497 compared to the one ($X_k = 3.88 \text{ mg m}^{-3} \text{ } \mu\text{g-ehl-a l}^{-1}$) used by Casas and Bacher (2006) in productive
498 areas of the French Mediterranean shoreline (average CHL-a concentration $1.45 \text{ mg m}^{-3} \text{ } \mu\text{g-ehl-a l}^{-1}$
499 maximum peak at $20 \text{ mg m}^{-3} \text{ } \mu\text{g-ehl-a l}^{-1}$), [as a consequence of given](#) the [even](#) higher productivity in
500 the North Sea (average CHL-a concentration $4.25 \text{ mg m}^{-3} \text{ } \mu\text{g-ehl-a l}^{-1}$; maximum peak at $\sim 33.40 \text{ mg}$
501 $\text{m}^{-3} \text{ } \mu\text{g-ehl-a l}^{-1}$). The high value of X_k could also be explained by the presence of [silt and other](#)
502 inedible particles (i.e. MPs) which [led result](#) to lower quality food in the mussel's diet compared
503 with an [assumed](#) "clean [of inedible particles](#)" [site environment](#) (Kooijman, 2006, Ren, 2009). [In the](#)
504 [present study the inedible particles \(i.e. MPs\) have been incorporated in the mussel's diet through](#)

505 the modified relation of the functional response f (Eq. 5, Table 1), which regulates the assimilation
506 rate and thus the mussel's growth. However, the DEB model applied at the French site, did not
507 account inedible particles in the mussel's food. Furthermore, it has been reported that wild mussels
508 grow considerably slower than farmed mussels (~1.7 times) (Sukhotin and Kulakowski, 1992) and
509 thus, a higher value of X_k promotes a lower mussel growth, which is the case of the North Sea
510 mussel. The simulated mussel shell length after 4 years, in August, is 4.35 cm and the fresh tissue
511 mass is 1.87 gr, in agreement with Van Cauwenberghe et al. (2015) and other studies conducted on
512 wild mussels (Sukhotin et al., 2007, Saraiva et al., 2012, MarLIN, 2016). In particular, Saraiva et al.
513 (2012) found that after 16 years of simulation, the wild mussel of the Wadden Sea (North Sea) is 7
514 cm long, while according to Bayne and Worrall (1980) a mussel with shell length 4 cm corresponds
515 to the age of 4 years, in agreement with the current study. The simulated growth presents a strong
516 seasonal pattern, being higher during spring and summer season, as compared to autumn and
517 winter, which is consistent with the seasonal cycle of temperature and CHL-a concentration, for a
518 typical year in the region (Fig. 1). The increase of food availability and temperature during spring
519 (April) results in high mussel growth for a 4-month period, while the decrease of CHL-a from
520 summer until the end of the year, in conjunction with the temperature decrease in autumn, result in
521 a lower mussel growth. Spawning events that occurred each year in late~~between the end of~~ April-
522 early and beginning of May (30 April-2 May) each year, are responsible for the sharp decline in
523 mussel's fresh tissue mass, shown in Fig. 4 (Handa et al., 2011; Zaldivar, 2008) and in agreement
524 with the literature (Sprung, 1983, Cardoso et al., 2007, Saraiva et al., 2012). The predicted weight
525 loss due to spawning was around 7% at the first year of simulation, while the second, third and
526 fourth year the percentage of weight loss increased gradually to 8.3%, 12.6% and 14.4%
527 respectively. Bayne and Worrall (1980) demonstrated that the weight losses on spawning for
528 individuals of 1 g weight vary between 2.1% and 39.8%, presenting a weight-specific increase with
529 size.

530 In the N. Ionian Sea implementation, X_k is applied as a function of CHL-a concentration
531 through the method described in section 2.5. The target diagram showing the performance of each
532 tested function (linear: $f(x) = a * [CHL - a] + b$, where $a = 0.959$ and $b = -1.420$;
533 exponential: $f(x) = a * \exp(b * [CHL - a])$ where $a = 0.2$ and $b = 0.567$; power: $f(x) = a * [CHL - a]^b + c$ where $a = 0.01$, $b = 3.529$ and $c = 0.480$) is shown in Figure 53. The linear
534 and power function of X_k present a good skill, with the power function leading to the most
535 successful simulation of the cultured mussel's growth in all four areas (diagram marks for mussel
536 length and fresh tissue mass are closer to the target's center). The power function applied in the N.
537 Ionian Sea, resulted in mussel's shell length 5.8 cm and fresh tissue mass 5.92 gr after one year
538 simulation, in agreement with Theodorou et al. (2011). The spawning event occurred at the

540 beginning of December (Theodorou et al., 2011) and was illustrated by a 12.6% tissue mass
541 decline.

542

543 3.2 Microplastics accumulation and depuration phase

544

545 The hourly simulated MPs accumulation by the mussel in the North Sea and N. Ionian Sea are
546 shown in Fig. 6 and Fig. 7 respectively. Calibration of the parameter k_f (1.2 d^{-1}) led to a model
547 which was well fitted to the observed MPs accumulation in the mussel of both study areas. In the
548 North Sea, a 4-year-old wild mussel ($L=4.35 \text{ cm}$, $W=1.87 \text{ g}$) contains 0.5364 particles individual⁻¹
549 in August within the range value found by Van Cauwenberghe et al. (2015) (0.4 ± 0.3 particles
550 individual⁻¹), although the model overestimated the data range reproducing a seasonal increase that
551 was not observed. This is most likely due to the fact ~~It is worth noting~~ that Van Cauwenberghe et al.
552 (2015) allowed a 24 h clearance period, before analyzing the mussels' tissue for MPs, ~~possibly~~
553 resulting in slightly lower MPs accumulation than the model's prediction. The MPs egested through
554 faeces by the 4 year old mussel after 24 h were 0.2 ± 0.2 particles individual⁻¹ (Van Cauwenberghe
555 et al., 2015), which agree also with model's output (0.3 particles individual⁻¹, Fig. 8) regarding the
556 depuration phase and could compensate for the observed difference in mussel's MPs load between
557 the simulated and field data. In the N. Ionian Sea, the simulated MPs accumulation by the cultured
558 mussel with $L=4.858 \text{ cm}$ and $W=3.343 \text{ g}$ was 0.91 particles individual⁻¹ in the end of June~~July~~, in
559 agreement with field observations obtained from Digka et al. (2018a) (0.9 ± 0.2 particles individual⁻¹).
560 Overall, the developed model simulated the MPs accumulation by both mussels in the two
561 different areas, using the same parameter set (see Table 3 for the exceptions), under the assumption
562 that parameters referred to silt particles (i.e. inedible particles) may be used to describe also the
563 MPs accumulation. Both simulations were in good agreement with the available field data, with a
564 small deviation for the North Sea.~~In both regions, the model computed MPs accumulation,~~
565 ~~assuming that the mussel treats MPs as silt particles (i.e. inedible particles) and is in agreement with~~
566 ~~the available field data.~~ -This may lead to the assumption~~suggests~~ that mussels ~~probably~~ present a
567 common behavior against all inedible particles. In model's results, based on the uptake and
568 excretion rates of MPs by the mussels in both study areas, the majority of MPs are rejected through
569 pseudofaeces and fewer through faeces production (not shown). This is in agreement with Woods et
570 al. (2018) who found that most microplastic fibers (71%) were quickly rejected as pseudofaeces and
571 $< 1\%$ excreted in faeces.

572 The small-scale (daily) fluctuations of MPs in the mussel (wild and cultivated) reflect the
573 adopted random variability of the environmental MPs concentration C_{env} and the daily fluctuations

574 | of the environmental forcing (CHL-a, temperature). The large-scale (seasonal) variability follows
575 | mainly the variability of the clearance rate. The seasonal variability of the CHL-a concentration and
576 | temperature greatly determines the variability of the clearance rate and hence the variability of MPs
577 | in the individual. Moreover, the model predicts that mussel's energy needs are increased as it grows
578 | and therefore the clearance rate is increased, resulting in higher MPs accumulation.

579 | The simulated time needed to clean the mussel's gut from the MPs load for both areas is
580 | shown in Fig. 8. In both areas, the cleaning follows an exponential decay, in agreement with
581 | laboratory experiments by Woods et al. (2018). In particular, the model predicts a 90% mussel's
582 | cleaning after ~~284330~~ hours (~~~124~~ days) and ~~5663~~ hours (~~~2.53~~ days) for the N. Ionian Sea and
583 | North Sea respectively. The cleaning process is more rapid in the North Sea simulation, which can
584 | be attributed to the higher CHL-a concentration found in this area, leading to increased production
585 | of faeces by the mussel and hence faster excretion of the accumulated MPs. In the N. Ionian Sea, on
586 | the other hand, the rate of the mussel's cleaning is slower, due to the limited food availability.

587

588 | **3.3 Model's uncertainty regarding the environmental microplastics concentration**

589

590 | The MPs concentration in the environment presents a strong variability in both temporal and
591 | spatial scales. To examine the model's uncertainty related to the environmental MPs concentration
592 | (C_{env}), a series of 15 and 13 simulations were performed in the North Sea and N. Ionian Sea
593 | respectively, adopting different values of C_{env} within the observed range of each area. In the North
594 | Sea, the adopted C_{env} ranged between 0.1 and 0.8 particles L^{-1} with a step of 0.05 (15 runs), while in
595 | the N. Ionian Sea C_{env} ranged between 0.0012 and 0.0252 particles L^{-1} with a step of 0.002 (13
596 | runs). -The mean seasonal values and standard deviation of the 15 simulations in the North Sea and
597 | the mean monthly values and standard deviation of the 13 simulations in the N. Ionian Sea were
598 | computed and plotted in Fig. 9 and Fig. 10, respectively. Each error bar represents the uncertainty
599 | of the simulated accumulation at the specific time, related to the environmental MPs concentration.

600 | In both case studies, the uncertainty of the model appears to increase as the MPs accumulation
601 | is increased. -As the mussel grows in the North Sea, the mean value and standard deviation of MPs
602 | accumulation is increased during the same season every year, illustrating the effect of the mussel's
603 | weight. Moreover, the seasonal variability of the MPs accumulation appears to be related
604 | withshould be caused by the seasonality of CHL-a concentration. This is apparent during each
605 | year's spring: when CHL-a concentration peaks at its maximum value (~30 $mg\ m^{-3}$; see Fig. 1), the
606 | filtration rate is decreased (Riisgard et al., 2003, 2011), leading to lower MPs accumulation by the
607 | mussel and thus lower model's uncertainty. In the N. Ionian Sea, the effect of the mussel's weight is

608 more apparent in the early months (~ 6 months), resulting on higher MPs accumulation and model
609 uncertainty as the mussel grows. Afterwards, the seasonality of both CHL-a concentration and
610 temperature plays the major role. During summer, when the CHL-a concentration is progressively
611 decreased, reaching minimum values (~0.7 mg /m³) and temperature is increased (>20° C), the
612 filtration rate is significantly decreased or stopped, resulting in lower MPs accumulation and lower
613 model's uncertainty. This is in line with studies reporting that the mussel suspends the filtering
614 activity and thus closes its valves until better conditions occur (Pascoe et al., 2009, Rissgard et al.,
615 2011). Overall, the available field data lie within the model's uncertainty, apart from the North Sea
616 case, where the range of field data variability and model uncertainty dot not overlap significantly at
617 the time of the observations for both study areas.

618 Moreover, to evaluate the scenario adopted with the set-up of the previous experiments
619 (random C_{env} at a daily time step) 3 additional model runs are performed in each study area,
620 adopting each time different stochastic sequences of daily random C_{env} values within the observed
621 range, which is considered to reflect the high spatial and temporal variability of the environmental
622 MPs concentration. The mean value and standard deviation of these “stochastic” runs lie most of
623 the time within the standard deviation of the overall model's uncertainty in both case study areas
624 (Fig. 9 and Fig. 10).

625

626 **3.4 Sensitivity and Regression analysis results**

627

628 The results of the sensitivity experiments regarding the MPs accumulation by the mussels are
629 shown in Fig. 11 and 12 for the North Sea and N. Ionian Sea respectively. The comparison between
630 the intertidal and subtidal mussel of the North Sea revealed that both +10% and -10% perturbation
631 of CHL-a and X_k have a slightly lower effect on the MPs accumulation by the intertidal mussel
632 which is probably attributed to the intermittent feeding periods experienced by the individual due to
633 the tide effect. As far as the temperature effect, both +10% and -10% perturbed value led to higher
634 sensitivity on the MPs accumulation by the intertidal mussel, due to the adopted modified
635 temperature relation during low tide. Especially, if the mussel's body temperature change during air
636 exposure would be considered, the perturbed temperature will probably affect even more the MPs
637 accumulation on the intertidal than the subtidal mussel. The sensitivityeffect of the C_{env} is slightly
638 higher and lower on the MPs accumulation by the intertidal mussel when perturbed either +10%
639 orand -10% is almost the same for the intertidal and subtidal mussel, respectively, however the
640 difference of the sensitivity index (%) between the two mussels (intertidal vs. subtidal) is small,

641 indicating that the environmental MPs concentration affects similarly both mussels, regardless the
642 continuous or intermittent feeding-excretion process.

643 The comparison between the mussel sensitivity indexes in the N. Ionian and the North Sea
644 (in conditions of submergence) study areas reveals some important differences. Generally, most of
645 the perturbed (either +10% or -10%) variables and parameters (i.e. CHL-a, temperature, X_k) present
646 higher sensitivity on the MPs accumulation by the mussel from the N. Ionian Sea. This is attributed
647 to the prevailing environmental conditions and specifically the lower food availability (CHL-a) and
648 the higher temperature range in the N. Ionian Sea compared to the North Sea, which greatly
649 determine the feeding processes, the mussel's growth and hence the MPs accumulation. The
650 perturbed C_{env} in both study areas appears to affect similarly the MPs accumulation on both mussels
651 (\sim 10%), with the small difference (<2%) probably attributed to the higher abundance of
652 seawater's MPs present in the North Sea compared to the N. Ionian Sea. Finally, the half saturation
653 coefficient for the inorganic particles (Y_k) has no effect on the MPs accumulation of both North Sea
654 and N. Ionian Sea mussels, indicating that the amount of inedible particles (i.e. MPs) is relatively
655 low in both areas and thus the Y_k does not affect the way that the organic particles are being
656 ingested (Kooijman, 2006). According to Ren (2009), when the inorganic matter is low, the $K(y)$
657 (Eq. 5; Table 1) is approximately equal to X_k and then Y_k is the least sensitive parameter for the
658 ingestion rate and thus growth.

659 The DEB-accumulation model output was used to determine the coefficients in Eq. 19 by the
660 nonlinear regression analysis: $b_1 = 0.1909 (\pm 0.0006)$, $b_2 = 0.0412 (\pm 0.0019)$, $b_3 = 0.1315 (\pm$
661 $0.0021)$ and $b_4 = 1.1060 (\pm 0.0253)$. The accurate estimation of the confidence intervals for the
662 estimated coefficients (b_1, b_2, b_3, b_4) is indicated by the low confidence intervals, while the mean
663 squared error of the regression model appears also sufficiently small~~are small enough which~~
664 ~~indicates an accurate estimation of them and the mean squared error of the regression model is~~
665 ~~small enough~~ (MSE=0.0523). Subsequently, as shown in Figure 13, Eq. ~~uation~~ 20 may be used to
666 predict the MPs concentration of the environment where mussels live, ~~being~~ in most cases, the
667 predicted MPs concentration is found within the standard deviation of the field data. Two
668 exceptions are shown in Hastings-A and Plymouth areas. The reasons behind these discrepancies
669 may be related to the environmental conditions prevailing in each area at the sampling time. For
670 example, Eq. 20 does not take into account the impact of tides that may affected the mussel's MPs
671 load (C) and the lack of information on the exact sampling date led to using a mean SST and CHL-a
672 value representative of the given sampling time period (Li et al., 2018). Although, Eq. 20 does not
673 account for the tide effect, however, the sensitivity analysis (Fig. 11) showed that the effect of C_{env}
674 on the mussel's MPs accumulation was the same for both intertidal and subtidal mussel in the North
675 Sea. This result may also apply at the two exceptions areas, leading to the assumption that the

676 discrepancies are due to the lack of the ambient temperature and CHL-a information during the
677 sampling date. In any case However, this is just a first rough demonstration of the method and
678 should be implemented in more environments in order to be further validated.

679

680

681 **4. Discussion**

682

683 A DEB-accumulation model was developed and validated with ~~the only available~~ data
684 available from the North Sea and the N. Ionian Sea, to study the MPs accumulation by wild *M.*
685 *edulis* and cultured *M. galloprovincialis*, ~~as they~~ grown in different, representative environments.
686 Although the study is limited by scarce validation data, it should be noted the MPs accumulation
687 model parameter set, except one tuning parameter (k_f), was extracted from the literature (Table 3),
688 assuming it is notable that the accumulation submodel's parameters are extracted from literature
689 (Table 3) illustrating that mussels adopt a common defensive mechanism against inedible particles
690 (i.e. silt, MPs). Thus, the theoretical background constructed by Saraiva et al., (2011a) (based on
691 Kooijman, 2010) regarding the feeding and excretion processes of the mussel remains unspoiled.
692 Through the strong theoretical background of DEB theory, this study highlights that the
693 accumulation of MPs by the mussel is highly depended on the prevailing environmental conditions
694 which control the amount of MPs that the mussel filtrates and excretes.

695 Towards a generic DEB model Beginning with the generalization of the DEB model
696 regarding the site specific parameter X_k in the N. Ionian Sea simulation, the applied function of the
697 half saturation coefficient ($f(x) = a * [CHL - a]^b + c$) successfully captures the physiological
698 responses and thus the growth rate of the cultured mussel at the N. Ionian Sea implementation. In
699 the current study, ~~a demonstration of this method~~ ledis conducted leading to a robust and generic
700 DEB growth model able to simulate robust enough with a sufficiently generic nature for the
701 simulation of the mussel growth in representative mussel habitats of the Mediterranean Sea,
702 covering a range of productivity and sea surface temperature. This approach supports and takes a
703 step further of Bourles et al. (2008) suggestion about a suggested for oyster growth (*Crassostrea*
704 *gigas*) that a seasonally varied half saturation coefficient, demonstrating an improvement could
705 improve the accuracy of the food quantifier. The applied function of X_k considers the daily CHL-a
706 fluctuations, and thus the seasonal variation of the seawater composition. ~~because seawater~~
707 ~~composition is closely related to the season.~~ As more field data becomes available from various
708 environments, the applied ~~such an~~ approach could result to more generic formulations for the site-

709 specific parameter X_k , so that the model could be applied in several areas of interest, where field
710 growth data are absent and/or to simulate the potential mussel growth in the 2D space.

711 The simulation of MPs accumulation by the mussels, using the DEB-accumulation model, is
712 in good agreement with the available field data (Fig. 3 and Fig. 4). The simulated values lie within
713 the observed field data range (mean \pm SD), although the seasonal increase reproduced by the model
714 at the North Sea implementation did not exactly overlap with the field data at the time of
715 observations. This could be attributed to the clearance period (24 h) that allowed mussels to excrete
716 MPs through faeces (0.2 ± 0.2 particles individual⁻¹) before the mussel's tissue analysis (Van
717 Cauwenberghe et al., 2015). The measured loss of mussel's MPs is in agreement with the model's
718 result on the depuration experiment after 24 h. The MPs accumulation by the cultivated mussel
719 (fresh tissue mass 3.3342 g) originated from the N. Ionian Sea with mean $C_{env} = 0.0012 \pm 0.024$
720 particles L⁻¹, is 0.91 particles individual⁻¹ and by the wild mussel (fresh tissue mass 1.87 g) from the
721 North Sea with mean $C_{env} = 0.4 \pm 0.3$ particles L⁻¹ is 0.5364 particles individual⁻¹. If these
722 concentrations are expressed per gram of wet tissue of mussels, the cultivated mussel contamination
723 (0.27 particles g⁻¹w.w.) is comparable with the wild mussel (0.2834 particles g⁻¹w.w.), despite the
724 much lower environmental MPs concentration (C_{env}) in the N. Ionian Sea than the North Sea. This
725 comparison aims to highlight the significant impact of the prevailing environmental conditions
726 (CHL-a and temperature) on the MPs accumulation by the mussels, although they originate from
727 different areas and lived different time period. The generally high abundance of CHL-a in the North
728 Sea simulation, contributes to a reduction of the filtering activity and hence of the MPs
729 accumulation. The threshold algal concentration for reduction of the mussel's filtration rate
730 (incipient saturation) has been found to lie between 6.3 and 10.0 $\text{mg m}^{-3} \mu\text{g chl-a L}^{-1}$ (Riisgard et al.,
731 2011), which is a range comparable to the CHL-a concentrations in the North Sea—ease.
732 Furthermore, in the N. Ionian Sea simulation, the filtration, ingestion, pseudofaeces and faeces
733 production rates are decreased during the summer season when the CHL-a and temperature has
734 downward and upward trend respectively, gradually leading to a decline of the mussel's MPs
735 accumulation. Van Cauwenberghe and Janssen (2014) found that cultivated *M. edulis* from the
736 North Sea contained on average 0.36 ± 0.07 particles g⁻¹w.w., a slightly higher similar value with
737 that found in the present study for the wild mussel of the North Sea (0.2834 particles g⁻¹w.w.). This
738 could be attributed to mussel farms acting as a potential source of MPs contamination for the
739 mussels due to plastic materials (i.e. plastic sock nets and polypropylene long lines) used during
740 cultivation (Mathalon and Hill, 2014, Santana et al., 2018). probably highlights the small
741 contribution of mussel farms as a source of MPs pollution (Santana et al., 2018). Moreover, the
742 intertidal wild mussel (present study) is assumed to filter and excrete MPs half of the time in
743 comparison with the submerged cultured mussel in the North Sea, resulting though in similar

744 accumulation level. The model also predicts the time needed for the 90% gut clearance of both
745 cultured (N. Ionian Sea) and wild (North Sea) mussel to be almost 284330 hours and 5663 hours
746 (equivalent to 124 and 2.53 days) respectively, when MPs contamination is removed from their
747 habitat. This is in line with a series of studies which demonstrated that the depuration time varies
748 between 6-72 hours and can last up to 40 days depending on several factors such as species,
749 environmental conditions (Bayne et al., 1987), size and type of MPs (Browne et al., 2008, Ward and
750 Kach, 2009, Woods et al., 2018, Birnstiel et al., 2019).

751 The strong dependence of food (CHL-a), temperature and seawater's MPs concentration on
752 the MPs accumulation by the mussel, regarding its wet weight, is demonstrated through sensitivity
753 experiments that were used to derive a rather simple nonlinear regression model (Eq. 19). The
754 comparison of the regression model's with the DEB model's output resulted in a quite accurate
755 estimation of the coefficients, which in turn sparked the idea of a 'new' relationship (Eq. 20) that
756 could potentially predict the MPs concentration in the environment (C_{env}) when certain conditions
757 are known (CHL-a, T, C_{env} , W). The latter equation was applied in 8 areas in total (2 from the
758 present study areas and 6 from Li et al. (2018)), with relatively good results since there is general
759 overlapping of regressed and observed MPs concentration in the environment (C_{env}), except for
760 Hastings-A and Plymouth areas, probably due to missing information on the environmental
761 conditions (CHL-a, SST) during the samplingthe predicted value is within the observed range of
762 field data in most regions, suggesting thatmaking the mussels can be used as potential bioindicators.
763 Mussels have been previously proposed as bioindicators for marine microplastic pollution (<1 mm),
764 although the efficient gut clearance and selective feeding behavior limit their quantitative ability
765 (Lusher et al., 2017, Brate et al., 2018, Beyer et al., 2017, Fossi et al., 2018, Li et al., 2019).The
766 ~~very~~ recent study by Ward et al. (2019b) demonstrated that bivalves are poor bioindicators of MPs
767 pollution due to the particle selection during feeding and excretion processes that is based on the
768 physical characteristics of the MPs. Considering that the MPs accumulation is site-dependent~~d~~ and
769 that sampling of mussels is usually easier than seawater (Karlsson et al., 2017, Brate et al., 2018),
770 models like the one described in Eq. 20, ~~that~~ besides the MPs accumulation, take into account also
771 characteristics of the environment, ~~that~~which are crucial for the way that mussels accumulate MPs,
772 This methodpossibly could be possibly used at global level and allow comparisons between various
773 environments. However, the method described should be validated in more environments with more
774 frequent field data to be able to provide secure results.

775 In addition to~~Despite~~ the scarce validation data regarding the MPs accumulation in mussels,
776 ~~in this study~~ has some morethere are some other limitations. First of all, the data regarding the
777 concentration of MPs in the mussels' environment areis also scarce; since MPs is a relatively recent
778 subject of study, the existing knowledge of the spatial and temporal distribution is still quite limited

779 (Law and Thompson, 2014, Browne, 2015, Anderson et al., 2016, de Sa et al., 2018, Smith et al.,
780 2018, Troost et al., 2018). To overcome the lack of environmental MPs time series, a function of
781 randomly generated values within the observed range of each area was applied and its uncertainty
782 was examined through an ensemble forecasting. Specifically, the model's uncertainty due to the
783 environmental MPs concentration (C_{env}) was tested by performing a series of model runs forced by
784 an envelope of representative values of C_{env} . ~~and The~~ results (section 3.3) showed ~~ed~~ that the adopted
785 stochastic scenario simulates ~~ed quite satisfactorily~~ ~~realistically~~ the MPs accumulation by the mussels,
786 lying within the observed field range, although a slight overestimation was found in the North Sea
787 and in agreement with the available field data. The approach used is assumed to represent the
788 natural variability ~~be close to reality~~ since it has been reported that ~~MPs quantification in the water~~
789 ~~is rather a complicated procedure due to the influence of many factors such as tides, wind, wave~~
790 ~~action, ocean currents, river inputs and hydrodynamic features~~ ~~lead~~ ~~resulting~~ to high spatially and
791 temporally variability of MPs distribution even in very small scales (Messinetti et al., 2018,
792 Goldstein et al., 2013). In addition, the nature of the variable C_{env} makes it difficult to estimate,
793 presenting large observational errors, not only due to the intense physical variation but also due to
794 different sampling and analysis techniques that were used. In a future work the DEB-accumulation
795 model could be coupled with a high-resolution MPs distribution model (Kalaroni et al., 2019),
796 being extensively validated against field data that will have been collected and processed according
797 to a common scientifically defined protocol, to overcome this limitation. Moreover, the approach
798 followed in calculating the value of MPs concentration in the near surface layer (0-5m depth) (Kooi
799 et al., 2016), resulted in a representative value of the upper ocean layer. In depth knowledge of the
800 MPs distribution, both horizontally and vertically, is essential to understand and mitigate their
801 impact not only on the various marine compartments but also on the organisms inhabiting those
802 compartments (Van Sebille et al., 2015, Kooi et al., 2016). For that reason, it is important to
803 enhance the monitoring activity especially in the vulnerable coastal environments, adopting
804 integrated cross-disciplinary approaches and monitoring of biological, physical and chemical
805 parameters which provide information on the ecosystem function, in order to improve the
806 assessment of emerging pollutants (i.e. MPs) and their impacts on biota (objective of JERICO-RI
807 framework).

808 ~~Our~~ ~~Further, the~~ assumption that the mussel has the same filtration rate for all particles
809 independently of their chemical composition, size and shape, is a simplification and an open
810 contradictory theme of discussion (see Saraiva et al., 2011a for details). However, in our model
811 application through the model, a pre-ingestive particle selection by the mussel is implied based on
812 the organic-inorganic content of the suspended matter illustrating the different binding probabilities
813 applied for algal and MPs particles during the ingestion process. Through an investigation of wild

814 mussel's faeces and pseudofaeces production in laboratory conditions, Zhao et al. (2018) found that
815 the length of MPs was significantly longer in pseudofaeces than in the digestive gland and faeces.
816 Furthermore, Van Cauwenberghe et al. (2015) demonstrated that mussel's faeces contained larger
817 MPs (15–500 μm) compared to the mussel's tissue (20–90 μm). Apparently, smaller sized MPs
818 seem to be dominant within the mussels in comparison with the size of the MPs in the ambient
819 environment (Li et al., 2018, Qu et al., 2018, Digka et al., 2018b), implying that the mussel is more
820 prone to ingest and retain smaller sized MPs. As an example, Digka et al. (2018b) confirmed that
821 the smaller MPs (<1 mm) occupy the 62.3%, 96.9% and 100% of the total MPs in seawater,
822 sediments and mussels from the N. Ionian Sea respectively. In a future work this selection pattern
823 regarding size, could be simulated by suitable preference weights among different MPs sizes. This
824 will improve the knowledge of the feeding and excretion mechanisms used by the mussels against
825 MPs pollution and the assessment of the ecological footprint (Rist et al., 2019).

826 ~~Our~~ Moreover, the assumption that the contamination by MPs does not affect the energy
827 budget in terms of growth might also be a simplification as this is a subject currently under
828 investigation. Van Cauwenberghe et al. (2015) found that although mussels *M. edulis* exposed to
829 MPs increased their energy consumption, the energy reserves was not affected compared to the
830 control organisms, implying that mussels are able to adopt a defensive mechanism against the
831 suspended inorganic particles (i.e. MPs) (Ward and Shumway, 2004). Furthermore, MPs exposure
832 showed no significant effect on mussel's (*Perna perna*) energy budget, despite its long duration and
833 relatively realistic intensity, leading to the hypothesis that ~~concluding to the assumption of~~ mussels's
834 can acclimate to the MPs exposure ~~acclimation~~ to maintain their ~~its~~ health (Santana et al., 2018). On
835 the contrary, other authors ~~who mainly intended to predict future effects~~, suggested a significant
836 energy shift from reproduction to structural growth and elevated maintenance costs, probably
837 attributed to the reduced energy intake, when the organisms (i.e. oyster *Crassostrea gigas*) were
838 contaminated with high and unrealistic concentration of MPs (Sussarellu et al., 2016). Moreover,
839 Gardon et al. (2018) showed that the overall energy balance of oyster *Pinctada margaritifera* was
840 significantly impacted by the reduced assimilation efficiency in correlation with the exposed dose
841 of MPs and for that reason energy had to be withdrawn from reproduction to compensate for the
842 energy loss. In future dedicated experiments exploring the effects on all components of a DEB
843 model should be carried out considering long-term realistic MPs exposure.

844 Our use of the tide data led to some model bias ~~Furthermore, the tide data as considered in the~~
845 ~~present study impose model's bias~~, since the model does not take into account of the mussel's body
846 temperature change when this is exposed to air ~~was not taken into consideration~~. Assessing the
847 mussel's body temperature requires ~~demand~~ extended experiments in field conditions (Tagliarolo
848 and McQuaid, 2015, Monaco and McQuaid, 2018). The ~~A very recent~~ study by Seuront et al. (2019)

849 along the French coast of the eastern English Channel found no significant correlation between air's
850 and mussel's body temperature, but ~~demonstrated a rather positively~~ significant positive correlation
851 between the body temperature and with the hard substrate's (i.e. rocks) temperature. However, in the
852 present study the tide effect on processes that are affected by the thermal equation ($k(T)$) is
853 considered indirectly through the metabolic depression (details in section 2.4). Sara et al. (2011)
854 ~~following the method developed by Kearney et al. (2010), who~~ coupled a DEB model with a
855 biophysical model (Kearney et al., 2010), incorporating ~~the~~ the change of mussel's body temperature
856 during emersion, by using information of various climatological variables (i.e. solar radiation, air
857 temperature, wind speed, wave height), but ~~the ignored the~~ temperature sensitivity on the
858 physiological processes ~~was ignored~~. In a future study, a combined ~~similar~~ approach by coupling the
859 present DEB-accumulation model with a biophysical model, which includes both the tide effect on
860 the physiological processes and the mussel's body temperature respectively, could be followed and
861 lead to a more detailed simulation of the intertidal mussel's ~~body temperature~~.

862 5. Conclusions

863
864 In a future study the model should be corroborated further by using a larger dataset
865 of validated against more frequent field data regarding the MPs accumulation, with sampling of
866 mussels of among various sizes and life stages. Currently, the model is mainly limited by the
867 insufficient validation, as a larger dataset could be also used for a better model calibration, as for now
868 ~~it cannot be reliable in conducting predictions within accepted precision~~. However, this study
869 provides a new approach in studying the accumulation of MPs by filter feeders and reveals the
870 relations between characteristics of the mussel's surrounding environment and the MPs
871 accumulation, which is presented with high seasonal fluctuations. Additionally, in a future study the
872 DEB-accumulation model will be coupled to with a ~~coupled~~ hydrodynamic-biochemical model (e.g.,
873 Petihakis et al., 2002, 2012, Triantafyllou et al., 2003, Tsiaras et al., 2014, Ciavatta et al., 2019,
874 Kalaroni et al., 2020) and a MPs distribution model (Kalaroni et al., 2019) that will provide fields
875 of temperature, food availability and MPs concentration respectively at the Mediterranean scale,
876 and eventually lead to an integrated representation of the MPs accumulation by mussels (Daewel et
877 al., 2008). This fully coupled model will be downscaled to the Cretan Sea SuperSite, while the
878 parameterization of important biological processes will be redesigned based on the new data which
879 will be acquired in the framework of the JERICO S3 project (<http://www.jerico-ri.eu>). The present
880 study highlights the urgent need for adopting a multi-disciplinary monitoring activity by measuring
881 physical, biological and chemical parameters that are crucial for mapping the MPs distribution,
882 assessing the contamination level of the marine organisms and investigating the impact on the

883 health status. Overall, despite the ~~significant~~ limitations ~~that were~~ mentioned ~~before~~, taken into
884 account that plastics are one of the global hot issues, this particular study could help ~~for the~~ design
885 ~~of~~ next efforts, since it provides indications on the future priority related issues.

886

887 **Author Contribution:**

888 **Natalia Stamataki, Yannis Hatzonikolakis, Kostas Tsiaras, Catherine Tsangaris, George**
889 **Petihakis, Sarantis Sofianos, George Triantafyllou**

890

891 G.T. conceived the basic idea of the present study and was responsible for the management and
892 coordination of the research planning and execution. N.S. and Y.H. developed the model code with
893 the contribution of K.T.. N.S. collected the existing information on the subject and performed the
894 simulations of the present study with the help of Y.H. when needed. G.T., G.P., K.T., Y.H. and N.S.
895 contributed to the interpretation of the results. C.T. provided the field data of the mussel's
896 microplastic accumulation in the North Ionian Sea. N.S. prepared the manuscript, with critical
897 review, commentary and revision contributed from all co-authors.

898

899 **Competing interests:**

900 The authors declare that they have no conflict of interest.

901

902 **Acknowledgments:**

903

904 This work was partially funded by the national project 'Blue growth with innovation and
905 application in Greek Seas' (MIS 5002438) and the EU H2020 CLAIM project (G.A. n° 774586).
906 This study has been conducted using E.U. Copernicus Marine Service Information
907 (<http://marine.copernicus.eu/>). Part of this work was supported by the JERICO- NEXT project. This
908 project has received funding from the European Union's Horizon 2020
909 research and innovation programme under grant agreement no. 654410.

910

911

912

913

References

- 915 Alunno-Bruscia, M., Bourlès, Y., Maurer, D., Robert, S., Mazurié, J., Gangnery, A., Gouletquer, P. and
 916 Pouvreau, S.: A single bio-energetics growth and reproduction model for the oyster *Crassostrea gigas* in six Atlantic
 917 ecosystems, *J. Sea Res.*, 66(4), 340–348, doi:10.1016/j.seares.2011.07.008, 2011.
- 918 Anderson, J. C., Park, B. J. and Palace, V. P.: Microplastics in aquatic environments: Implications for Canadian
 919 ecosystems, *Environ. Pollut.*, 218, 269–280, doi:10.1016/j.envpol.2016.06.074, 2016.
- 920 Andrady, A. L.: Microplastics in the marine environment, *Mar. Pollut. Bull.*, 62(8), 1596–1605,
 921 doi:10.1016/j.marpolbul.2011.05.030, 2011.
- 922 Arthur, C., J. Baker and H. Bamford (eds). Proceedings of the International Research Workshop on the
 923 Occurrence, Effects and Fate of Microplastic Marine Debris. Sept 9-11, 2008. NOAA Technical Memorandum NOS-
 924 OR&R-30, 2009
- 925 Bacher, C. and Gangnery, A.: Use of dynamic energy budget and individual based models to simulate the
 926 dynamics of cultivated oyster populations, *J. Sea Res.*, 56(2), 140–155, doi:10.1016/j.seares.2006.03.004, 2006.
- 927 Bayne, B. and Worrall, C.: Growth and Production of Mussels *Mytilus edulis* from Two Populations, *Mar. Ecol.*
 928 *Prog. Ser.*, 3, 317–328, doi:10.3354/meps003317, 1980.
- 929 Bayne, B. L., Hawkins, A. J. S. and Navarro, E.: Feeding and digestion by the mussel *Mytilus edulis* L.
 930 (*Bivalvia: Mollusca*) in mixtures of silt and algal cells at low concentrations, *J. Exp. Mar. Bio. Ecol.*, 111(1), 1–22,
 931 doi:10.1016/0022-0981(87)90017-7, 1987.
- 932 Béjaoui-Omri, A., Béjaoui, B., Harzallah, A., Aloui-Béjaoui, N., El Bour, M. and Aleya, L.: Dynamic energy
 933 budget model: a monitoring tool for growth and reproduction performance of *Mytilus galloprovincialis* in Bizerte
 934 Lagoon (Southwestern Mediterranean Sea), *Environ. Sci. Pollut. Res.*, 21(22), 13081–13094, doi:10.1007/s11356-014-
 935 3265-1, 2014.
- 936 Beyer, J., Green, N. W., Brooks, S., Allan, I. J., Ruus, A., Gomes, T., Bråte, I. L. N. and Schøyen, M.: Blue
 937 mussels (*Mytilus edulis* spp.) as sentinel organisms in coastal pollution monitoring: A review, *Mar. Environ. Res.*,
 938 130, 338–365, doi:10.1016/j.marenvres.2017.07.024, 2017.
- 939 Birnstiel, S., Soares-Gomes, A. and da Gama, B. A. P.: Depuration reduces microplastic content in wild and
 940 farmed mussels, *Mar. Pollut. Bull.*, 140, 241–247, doi:10.1016/j.marpolbul.2019.01.044, 2019.
- 941 Bourlès, Y., Alunno-Bruscia, M., Pouvreau, S., Tollu, G., Leguay, D., Arnaud, C., Gouletquer, P. and
 942 Kooijman, S. A. L. M.: Modelling growth and reproduction of the Pacific oyster *Crassostrea gigas*: Advances in the
 943 oyster-DEB model through application to a coastal pond, *J. Sea Res.*, 62(2–3), 62–71,
 944 doi:10.1016/j.seares.2009.03.002, 2009.
- 945 Bråte, I. L. N., Hurley, R., Iversen, K., Beyer, J., Thomas, K. V., Steindal, C. C., Green, N. W., Olsen, M. and
 946 Lusher, A.: *Mytilus* spp. as sentinels for monitoring microplastic pollution in Norwegian coastal waters: A qualitative
 947 and quantitative study, *Environ. Pollut.*, 243, 383–393, doi:10.1016/j.envpol.2018.08.077, 2018.
- 948 [Brewin, R., Ciavatta, S., Sathyendranath, S., Jackson, T., Tilstone, G. and Curran, K.: Uncertainty in Ocean-
 949 Color Estimates of Chlorophyll for Phytoplankton Groups, *Front. Mar. Sci.*, 4, doi:10.3389/fmars.2017.00104, 2017.](#)
- 950 [Browne, M. A., Galloway, T. and Thompson, R.: Microplastic-an emerging contaminant of potential concern?,
 951 *Integr. Environ. Assess. Manag.*, 3\(4\), 559–561, doi:10.1002/ieam.5630030412, 2007.](#)
- 952 Browne, M. A., Dissanayake, A., Galloway, T. S., Lowe, D. M. and Thompson, R. C.: Ingested microscopic
 953 plastic translocates to the circulatory system of the mussel, *Mytilus edulis* (L.), *Environ. Sci. Technol.*, 42(13), 5026–
 954 5031, doi:10.1021/es800249a, 2008.
- 955 ~~[Browne, M. A., Galloway, T. and Thompson, R.: Microplastic-an emerging contaminant of potential concern?,
 956 *Integr. Environ. Assess. Manag.*, 3\(4\), 559–561, doi:10.1002/ieam.5630030412, 2007.](#)~~
- 957 Browne, M. A.: Sources and pathways of microplastics to habitats, *Mar. Anthropog. Litter*, 229–244,
 958 doi:10.1007/978-3-319-16510-3_9, 2015.
- 959 Capolupo, M., Franzellitti, S., Valbonesi, P., Lanzas, C. S. and Fabbri, E.: Uptake and transcriptional effects of
 960 polystyrene microplastics in larval stages of the Mediterranean mussel *Mytilus galloprovincialis*, *Environ. Pollut.*, 241,
 961 1038–1047, doi:10.1016/j.envpol.2018.06.035, 2018.
- 962 Cardoso, J. F. M. F., Dekker, R., Witte, J. I. J. and van der Veer, H. W.: Is reproductive failure responsible for
 963 reduced recruitment of intertidal *Mytilus edulis* L. in the western Dutch Wadden Sea?, *Senckenbergiana Maritima*,
 964 37(2), 83–92, doi:10.1007/BF03043695, 2007.

965 Casas, S. and Bacher, C.: Modelling trace metal (Hg and Pb) bioaccumulation in the Mediterranean mussel,
966 *Mytilus galloprovincialis*, applied to environmental monitoring, *J. Sea Res.*, 56(2), 168–181,
967 doi:10.1016/j.seares.2006.03.006, 2006.

968 Ciavatta, S., Kay, S., Brewin, R. J. W., Cox, R., Di Cicco, A., Nencioli, F., Polimene, L., Sammartino, M.,
969 Santoleri, R., Skákala, J. and Tsapakis, M.: Ecoregions in the Mediterranean Sea Through the Reanalysis of
970 Phytoplankton Functional Types and Carbon Fluxes, *J. Geophys. Res. Ocean.*, 124(10), 6737–6759,
971 doi:10.1029/2019JC015128, 2019.

972 [Cole, M., Lindeque, P., Halsband, C. and Galloway, T. S.: Microplastics as contaminants in the marine
973 environment: A review, *Mar. Pollut. Bull.*, 62\(12\), 2588–2597, doi:10.1016/j.marpolbul.2011.09.025, 2011.](#)

974 Cole, M., Lindeque, P., Fileman, E., Halsband, C., Goodhead, R., Moger, J. and Galloway, T. S.: Microplastic
975 ingestion by zooplankton, *Environ. Sci. Technol.*, 47(12), 6646–6655, doi:10.1021/es400663f, 2013.

976 ~~Cole, M., Lindeque, P., Halsband, C. and Galloway, T. S.: Microplastics as contaminants in the marine
977 environment: A review, *Mar. Pollut. Bull.*, 62(12), 2588–2597, doi:10.1016/j.marpolbul.2011.09.025, 2011.~~

978 Cucci, T. L., Shumway, S. E., Brown, W. S. and Newell, C. R.: Using phytoplankton and flow cytometry to
979 analyze grazing by marine organisms, *Cytometry*, 10(5), 659–669, doi:10.1002/cyto.990100523, 1989.

980 Daewel, U., Peck, M. A., Kühn, W., St. John, M. A., Alekseeva, I. and Schrum, C.: Coupling ecosystem and
981 individual-based models to simulate the influence of environmental variability on potential growth and survival of
982 larval sprat (*Sprattus sprattus* L.) in the North Sea, *Fish. Oceanogr.*, 17(5), 333–351, doi:10.1111/j.1365-
983 2419.2008.00482.x, 2008.

984 de Sá, L. C., Oliveira, M., Ribeiro, F., Rocha, T. L. and Futter, M. N.: Studies of the effects of microplastics on
985 aquatic organisms: What do we know and where should we focus our efforts in the future?, *Sci. Total Environ.*, 645,
986 1029–1039, doi:10.1016/j.scitotenv.2018.07.207, 2018.

987 De Witte, B., Devriese, L., Bekaert, K., Hoffman, S., Vandermeersch, G., Cooreman, K. and Robbens, J.:
988 Quality assessment of the blue mussel (*Mytilus edulis*): Comparison between commercial and wild types, *Mar. Pollut.*
989 *Bull.*, 85(1), 146–155, doi:10.1016/j.marpolbul.2014.06.006, 2014.

990 [Di Cicco, A., Sammartino, M., Marullo, S. and Santoleri, R.: Regional Empirical Algorithms for an Improved
991 Identification of Phytoplankton Functional Types and Size Classes in the Mediterranean Sea Using Satellite Data,
992 *Front. Mar. Sci.*, 4, doi:10.3389/fmars.2017.00126, 2017.](#)

993 Digka, N., Tsangaris, C., Kaberi, H., Adamopoulou, A. and Zeri, C.: Microplastic Abundance and Polymer
994 Types in a Mediterranean Environment, Springer Water., 2018b.

995 Digka, N., Tsangaris, C., Torre, M., Anastasopoulou, A. and Zeri, C.: Microplastics in mussels and fish from the
996 Northern Ionian Sea, *Mar. Pollut. Bull.*, 135, 30–40, doi:10.1016/j.marpolbul.2018.06.063, 2018a.

997 [El Hourany, R., Abboud-Abi Saab, M., Faour, G., Mejia, C., Crépon, M., & Thiria, S.: Phytoplankton Diversity
998 in the Mediterranean Sea From Satellite Data Using Self-Organizing Maps, *J. Geophys. Res. Ocean.*, 124\(8\), 5827–
999 5843, doi:10.1029/2019jc015131, 2019.](#)

1000 Enders, K., Lenz, R., Stedmon, C. A. and Nielsen, T. G.: Abundance, size and polymer composition of marine
1001 microplastics $\geq 10 \mu\text{m}$ in the Atlantic Ocean and their modelled vertical distribution, *Mar. Pollut. Bull.*, 100(1), 70–81,
1002 doi:10.1016/j.marpolbul.2015.09.027, 2015.

1003 Eriksen, M., Lebreton, L. C. M., Carson, H. S., Thiel, M., Moore, C. J., Borerro, J. C., Galgani, F., Ryan, P. G.
1004 and Reisser, J.: Plastic Pollution in the World’s Oceans: More than 5 Trillion Plastic Pieces Weighing over 250,000
1005 Tons Afloat at Sea, *PLoS One*, 9(12), doi:10.1371/journal.pone.0111913, 2014.

1006 Everaert, G., Van Cauwenberghe, L., De Rijcke, M., Koelmans, A. A., Mees, J., Vandegehuchte, M. and
1007 Janssen, C. R.: Risk assessment of microplastics in the ocean: Modelling approach and first conclusions, *Environ.*
1008 *Pollut.*, 242, 1930–1938, doi:10.1016/j.envpol.2018.07.069, 2018.

1009 Fossi, M. C., Pedà, C., Compa, M., Tsangaris, C., Alomar, C., Claro, F., Ioakeimidis, C., Galgani, F., Hema, T.,
1010 Deudero, S., Romeo, T., Battaglia, P., Andaloro, F., Caliani, I., Casini, S., Panti, C. and Baini, M.: Bioindicators for
1011 monitoring marine litter ingestion and its impacts on Mediterranean biodiversity, *Environ. Pollut.*, 237, 1023–1040,
1012 doi:10.1016/j.envpol.2017.11.019, 2018.

1013 Gardon, T., Reisser, C., Soyeux, C., Quillien, V. and Le Moullac, G.: Microplastics Affect Energy Balance and
1014 Gametogenesis in the Pearl Oyster *Pinctada margaritifera*, *Environ. Sci. Technol.*, 52(9), 5277–5286,
1015 doi:10.1021/acs.est.8b00168, 2018.

1016 [Garnesson, P., Mangin, A., Fanton d’Andon, O., Demaria, J., & Bretagnon, M.: The CMEMS
1017 GlobColour chlorophyll a product based on satellite observation: multi-sensor merging and flagging strategies, *Ocean
1018 Sci.*, 15\(3\), 819–830, doi:10.5194/os-15-819-2019, 2019.](#)

1019 GESAMP Joint Group of Experts on the Scientific Aspects of Marine Environmental Protection: Sources, fate
1020 and effects of microplastics in the marine environment: a global assessment”, edited by P. J. Kershaw and ed), Reports
1021 Stud. GESAMP, 90(90), 96, doi:10.13140/RG.2.1.3803.7925, 2015.

1022 *GlobColour data (<http://globcolour.info>) used in this study has been developed, validated, and distributed by*
1023 *ACRI-ST, France.*

1024 Gohin, F., Druon, J. N. and Lampert, L.: A five channel chlorophyll concentration algorithm applied to Sea
1025 WiFS data processed by SeaDAS in coastal waters, *Int. J. Remote Sens.*, 23(8), 1639–1661,
1026 doi:10.1080/01431160110071879, 2002.

1027 Goldstein, M. C., Titmus, A. J. and Ford, M.: Scales of spatial heterogeneity of plastic marine debris in the
1028 northeast Pacific Ocean, *PLoS One*, 8(11), 80020, doi:10.1371/journal.pone.0080020, 2013.

1029 Handå, A., Alver, M., Edvardsen, C. V., Halstensen, S., Olsen, A. J., Øie, G., Reitan, K. I., Olsen, Y. and
1030 Reinertsen, H.: Growth of farmed blue mussels (*Mytilus edulis* L.) in a Norwegian coastal area; comparison of food
1031 proxies by DEB modeling, *J. Sea Res.*, 66(4), 297–307, doi:10.1016/j.seares.2011.05.005, 2011.

1032 Hantoro, I., Löhr, A. J., Van Belleghem, F. G. A. J., Widianarko, B. and Ragas, A. M. J.: Microplastics in coastal
1033 areas and seafood: implications for food safety, *Food Addit. Contam. - Part A Chem. Anal. Control. Expo. Risk*
1034 *Assess.*, 36(5), 674–711, doi:10.1080/19440049.2019.1585581, 2019.

1035 Hatzonikolakis, Y., Tsiaras, K., Theodorou, J. A., Petihakis, G., Sofianos, S. and Triantafyllou, G.: Simulation of
1036 mussel *Mytilus galloprovincialis* growth with a dynamic energy budget model in Maliakos and Thermaikos Gulfs
1037 (Eastern mediterranean), *Aquac. Environ. Interact.*, 9, 371–383, doi:10.3354/aei00236, 2017.

1038 Hirai, H., Takada, H., Ogata, Y., Yamashita, R., Mizukawa, K., Saha, M., Kwan, C., Moore, C., Gray, H.,
1039 Laursen, D., Zettler, E. R., Farrington, J. W., Reddy, C. M., Peacock, E. E. and Ward, M. W.: Organic micropollutants
1040 in marine plastics debris from the open ocean and remote and urban beaches, *Mar. Pollut. Bull.*, 62(8), 1683–1692,
1041 doi:10.1016/j.marpolbul.2011.06.004, 2011.

1042 [International Ocean-Colour Coordinating Group – IOCCG, Remote sensing of ocean colour in coastal, and other](#)
1043 [optically-complex waters, Rep. Int. Ocean-Colour Coord. Group 3, edited by S. Sathyendranath, Dartmouth, N. S.](#)
1044 [Canada, 2000.](#)

1045 Jacobs, P., Beauchemin, C. and Riegman, R.: Growth of juvenile blue mussels (*Mytilus edulis*) on suspended
1046 collectors in the Dutch Wadden Sea, *J. Sea Res.*, 85, 365–371, doi:10.1016/j.seares.2013.07.006, 2014.

1047 Jacobs, P., Troost, K., Riegman, R. and van der Meer, J.: Length- and weight-dependent clearance rates of
1048 juvenile mussels (*Mytilus edulis*) on various planktonic prey items, *Helgol. Mar. Res.*, 69(1), 101–112,
1049 doi:10.1007/s10152-014-0419-y, 2015.

1050 Jolliff, J. K., Kindle, J. C., Shulman, I., Penta, B., Friedrichs, M. A. M., Helber, R. and Arnone, R. A.: Summary
1051 diagrams for coupled hydrodynamic-ecosystem model skill assessment, *J. Mar. Syst.*, 76(1–2), 64–82,
1052 doi:10.1016/j.jmarsys.2008.05.014, 2009.

1053 Jørgensen, C., Larsen, P. and Riisgård, H.: Effects of temperature on the mussel pump, *Mar. Ecol. Prog. Ser.*,
1054 64(1/2), 89–97, doi:10.3354/meps064089, 1990.

1055 [Kach, D. and Ward, J.: The role of marine aggregates in the ingestion of picoplankton-size particles by](#)
1056 [suspension-feeding molluscs, Mar. Biol., 153\(5\), 797–805, doi:10.1007/s00227-007-0852-4, 2007.](#)

1057 Kalaroni S, Hatzonikolakis Y, Tsiaras K, Gkanasos A, Triantafyllou G.: Modelling the Marine Microplastic
1058 Distribution from Municipal Wastewater in Saronikos Gulf (E. Mediterranean). *Oceanogr Fish Open Access J.*; 9(1):
1059 555752. DOI: 10.19080/OFOAJ.2019.09.555752, 2019.

1060 Kalaroni, S., Tsiaras, K., Petihakis, G., Economou-Amilli, A. and Triantafyllou, G.: Modelling the
1061 Mediterranean pelagic ecosystem using the POSEIDON ecological model. Part I: Nutrients and chlorophyll-a
1062 dynamics, *Deep. Res. Part II Top. Stud. Oceanogr.*, 171, 104647, doi:10.1016/j.dsr2.2019.104647, 2020.

1063 Karayücel, S., Çelik, M. Y., Karayücel, I. and Erik, G.: Karadeniz’de Sinop İlinde Akdeniz Midyesinin (*Mytilus*
1064 *galloprovincialis* Lamarck, 1819) Sal Sisteminde Büyümesi ve Üretimi, *Turkish J. Fish. Aquat. Sci.*, 10(1), 9–17,
1065 doi:10.4194/trjfas.2010.0102, 2010.

1066 Karlsson, T. M., Vethaak, A. D., Almroth, B. C., Ariese, F., van Velzen, M., Hassellöv, M. and Leslie, H. A.:
1067 Screening for microplastics in sediment, water, marine invertebrates and fish: Method development and microplastic
1068 accumulation, *Mar. Pollut. Bull.*, 122(1–2), 403–408, doi:10.1016/j.marpolbul.2017.06.081, 2017.

1069 Kearney, M., Simpson, S. J., Raubenheimer, D. and Helmuth, B.: Modelling the ecological niche from functional
1070 traits, *Philos. Trans. R. Soc. B Biol. Sci.*, 365(1557), 3469–3483, doi:10.1098/rstb.2010.0034, 2010.

1071 Khan, M. B. and Prezant, R. S.: Microplastic abundances in a mussel bed and ingestion by the ribbed marsh
1072 mussel *Geukensia demissa*, *Mar. Pollut. Bull.*, 130, 67–75, doi:10.1016/j.marpolbul.2018.03.012, 2018.

1073 Kjørboe, T. and Møhlenberg, F.: Particle Selection in Suspension-Feeding Bivalves, *Mar. Ecol. Prog. Ser.*, 5,
1074 291–296, doi:10.3354/meps005291, 1981.

1075 Kooi, M., Reisser, J., Slat, B., Ferrari, F. F., Schmid, M. S., Cunsolo, S., Brambini, R., Noble, K., Sirks, L. A.,
1076 Linders, T. E. W., Schoeneich-Argent, R. I. and Koelmans, A. A.: The effect of particle properties on the depth profile
1077 of buoyant plastics in the ocean, *Sci. Rep.*, 6(1), doi:10.1038/srep33882, 2016.

1078 ~~Kooijman SALM: *Dynamic Energy Budget Theory for Metabolic Organisation*. Cambridge University Press,
1079 Cambridge, 2010.~~

1080 Kooijman, S. A. L. M.: *Dynamic Energy and Mass Budgets in Biological Systems*. Cambridge: Cambridge
1081 University Press, 2000.

1082 Kooijman, S. A. L. M.: Pseudo-faeces production in bivalves, *J. Sea Res.*, 56(2), 103–106,
1083 doi:10.1016/j.seares.2006.03.003, 2006.

1084 ~~Kooijman SALM: *Dynamic Energy Budget Theory for Metabolic Organisation*. Cambridge University Press,
1085 Cambridge, 2010.~~

1086 Lacroix, G., Ruddick, K., Ozer, J. and Lancelot, C.: Modelling the impact of the Scheldt and Rhine/Meuse
1087 plumes on the salinity distribution in Belgian waters (southern North Sea), *J. Sea Res.*, 52(3), 149–163,
1088 doi:10.1016/j.seares.2004.01.003, 2004.

1089 Lattin, G. L., Moore, C. J., Zellers, A. F., Moore, S. L. and Weisberg, S. B.: A comparison of neustonic plastic
1090 and zooplankton at different depths near the southern California shore, *Mar. Pollut. Bull.*, 49(4), 291–294,
1091 doi:10.1016/j.marpolbul.2004.01.020, 2004.

1092 Law, K. L. and Thompson, R. C.: Microplastics in the seas, *Science* (80-.), 345(6193), 144–145,
1093 doi:10.1126/science.1254065, 2014.

1094 Lenz, R., Enders, K. and Nielsen, T. G.: Microplastic exposure studies should be environmentally realistic, *Proc.*
1095 *Natl. Acad. Sci. U. S. A.*, 113(29), E4121–E4122, doi:10.1073/pnas.1606615113, 2016.

1096 ~~Li, J., Qu, X., Su, L., Zhang, W., Yang, D., Kolandhasamy, P., Li, D. and Shi, H.: Microplastics in mussels along
1097 the coastal waters of China, *Environ. Pollut.*, 214, 177–184, doi:10.1016/j.envpol.2016.04.012, 2016.~~

1098 Li, J., Green, C., Reynolds, A., Shi, H. and Rotchell, J. M.: Microplastics in mussels sampled from coastal waters
1099 and supermarkets in the United Kingdom, *Environ. Pollut.*, 241, 35–44, doi:10.1016/j.envpol.2018.05.038, 2018.

1100 Li, J., Lusher, A. L., Rotchell, J. M., Deudero, S., Turra, A., Bråte, I. L. N., Sun, C., Shahadat Hossain, M., Li,
1101 Q., Kolandhasamy, P. and Shi, H.: Using mussel as a global bioindicator of coastal microplastic pollution, *Environ.*
1102 *Pollut.*, 244, 522–533, doi:10.1016/j.envpol.2018.10.032, 2019.

1103 ~~Li, J., Qu, X., Su, L., Zhang, W., Yang, D., Kolandhasamy, P., Li, D. and Shi, H.: Microplastics in mussels along
1104 the coastal waters of China, *Environ. Pollut.*, 214, 177–184, doi:10.1016/j.envpol.2016.04.012, 2016.~~

1105 Liubartseva, S., Coppini, G., Lecci, R. and Clementi, E.: Tracking plastics in the Mediterranean: 2D Lagrangian
1106 model, *Mar. Pollut. Bull.*, 129(1), 151–162, doi:10.1016/j.marpolbul.2018.02.019, 2018.

1107 ~~Lusher, A.: *Microplastics in the marine environment: Distribution, interactions and effects*. *Mar. Anthropog.*
1108 *Litter*, 245–307, doi:10.1007/978-3-319-16510-3_10, 2015.~~

1109 Lusher, A., Bråte, I. L. N., Hurley, R., Iversen, K. and Olsen, M.: Testing of methodology for measuring
1110 microplastics in blue mussels (*Mytilus* spp) and sediments, and recommendations for future monitoring of
1111 microplastics, 87, (7209), doi:10.13140/RG.2.2.24399.59041, 2017.

1112 ~~Lusher, A.: *Microplastics in the marine environment: Distribution, interactions and effects*. *Mar. Anthropog.*
1113 *Litter*, 245–307, doi:10.1007/978-3-319-16510-3_10, 2015.~~

1114 Maes, T., Van der Meulen, M. D., Devriese, L. I., Leslie, H. A., Huvet, A., Frère, L., Robbens, J. and Vethaak,
1115 A. D.: Microplastics baseline surveys at the water surface and in sediments of the North-East Atlantic, *Front. Mar.*
1116 *Sci.*, 4(MAY), doi:10.3389/fmars.2017.00135, 2017.

1117 Maire, O., Amouroux, J. M., Duchêne, J. C. and Grémare, A.: Relationship between filtration activity and food
1118 availability in the Mediterranean mussel *Mytilus galloprovincialis*, *Mar. Biol.*, 152(6), 1293–1307,
1119 doi:10.1007/s00227-007-0778-x, 2007.

1120 MarLIN: The Marine Life Information Network - Common mussel (*Mytilus edulis*). Available from:
1121 <https://www.marlin.ac.uk/species/detail/1421>, 2016.

1122 Mathalon, A. and Hill, P.: Microplastic fibers in the intertidal ecosystem surrounding Halifax Harbor, Nova
1123 Scotia, *Mar. Pollut. Bull.*, 81(1), 69–79, doi:10.1016/j.marpolbul.2014.02.018, 2014.

1124 Mato, Y., Isobe, T., Takada, H., Kanehiro, H., Ohtake, C. and Kaminuma, T.: Plastic resin pellets as a transport
1125 medium for toxic chemicals in the marine environment, *Environ. Sci. Technol.*, 35(2), 318–324,
1126 doi:10.1021/es0010498, 2001.

1127 Messinetti, S., Mercurio, S., Parolini, M., Sugni, M. and Pennati, R.: Effects of polystyrene microplastics on
1128 early stages of two marine invertebrates with different feeding strategies, *Environ. Pollut.*, 237, 1080–1087,
1129 doi:10.1016/j.envpol.2017.11.030, 2018.

1130 [Möhlenberg, F., & Riisgård, H.: Efficiency of particle retention in 13 species of suspension feeding bivalves, *Ophelia*, 17\(2\), 239–246, doi:10.1080/00785326.1978.10425487, 1978.](#)

1132 Monaco, C. J. and McQuaid, C. D.: Applicability of Dynamic Energy Budget (DEB) models across steep
1133 environmental gradients, *Sci. Rep.*, 8(1), doi:10.1038/s41598-018-34786-w, 2018.

1134 Moore, C. J., Moore, S. L., Leecaster, M. K. and Weisberg, S. B.: A comparison of plastic and plankton in the
1135 North Pacific Central Gyre, *Mar. Pollut. Bull.*, 42(12), 1297–1300, doi:10.1016/S0025-326X(01)00114-X, 2001.

1136 Otto, L., Zimmerman, J. T. F., Furnes, G. K., Mork, M., Saetre, R. and Becker, G.: Review of the physical
1137 oceanography of the North Sea, *Netherlands J. Sea Res.*, 26(2–4), 161, doi:10.1016/0077-7579(90)90091-T, 1990.

1138 Painting, S. J., Collingridge, K. A., Durand, D., Grémare, A., Créach, V., Arvanitidis, C. and Bernard, G.:
1139 Marine monitoring in Europe: is it adequate to address environmental threats and pressures?, *Ocean Sci. Discuss.*,
1140 16(1), 1–31, doi:10.5194/os-2019-75, 2019.

1141 Palacz, A. P., St. John, M. A., Brewin, R. J. W., Hirata, T. and Gregg, W. W.: Distribution of phytoplankton
1142 functional types in high-nitrate, low-chlorophyll waters in a new diagnostic ecological indicator model,
1143 *Biogeosciences*, 10(11), 7553–7574, doi:10.5194/bg-10-7553-2013, 2013.

1144 Pascoe, P. L., Parry, H. E. and Hawkins, A. J. S.: Observations on the measurement and interpretation of
1145 clearance rate variations in suspension-feeding bivalve shellfish, *Aquat. Biol.*, 6(1–3), 181–190, doi:10.3354/ab00123,
1146 2009.

1147 Pasquini, G., Ronchi, F., Straffella, P., Scarcella, G. and Fortibuoni, T.: Seabed litter composition, distribution
1148 and sources in the Northern and Central Adriatic Sea (Mediterranean), *Waste Manag.*, 58, 41–51,
1149 doi:10.1016/j.wasman.2016.08.038, 2016.

1150 Petihakis, G., Triantafyllou, G., Allen, I. J., Hoteit, I. and Dounas, C.: Modelling the spatial and temporal
1151 variability of the Cretan Sea ecosystem, *J. Mar. Syst.*, 36(3–4), 173–196, doi:10.1016/S0924-7963(02)00186-0, 2002.

1152 Petihakis, G., Triantafyllou, G., Korres, G., Tsiaras, K. and Theodorou, A.: Ecosystem modelling: Towards the
1153 development of a management tool for a marine coastal system part-II, ecosystem processes and biogeochemical
1154 fluxes, *J. Mar. Syst.*, 94(SUPPL.), 49–64, doi:10.1016/j.jmarsys.2011.11.006, 2012.

1155 Politikos, D. V., Tsiaras, K., Papatheodorou, G. and Anastasopoulou, A.: Modeling of floating marine litter
1156 originated from the Eastern Ionian Sea: Transport, residence time and connectivity, *Mar. Pollut. Bull.*, 150, 110727,
1157 doi:10.1016/j.marpolbul.2019.110727, 2020.

1158 Pouvreau, S., Bourles, Y., Lefebvre, S., Gangnery, A. and Alunno-Bruscia, M.: Application of a dynamic energy
1159 budget model to the Pacific oyster, *Crassostrea gigas*, reared under various environmental conditions, *J. Sea Res.*,
1160 56(2), 156–167, doi:10.1016/j.seares.2006.03.007, 2006.

1161 Prins, T. C., Smaal, A. C. and Pouwer, A. J.: Selective ingestion of phytoplankton by the bivalves *Mytilus edulis*
1162 *L.* and *Cerastoderma edule (L.)*, *Hydrobiol. Bull.*, 25(1), 93–100, doi:10.1007/BF02259595, 1991.

1163 Qu, X., Su, L., Li, H., Liang, M. and Shi, H.: Assessing the relationship between the abundance and properties of
1164 microplastics in water and in mussels, *Sci. Total Environ.*, 621, 679–686, doi:10.1016/j.scitotenv.2017.11.284, 2018.

1165 [Raitsos, D. E., Reid, P. C., Lavender, S. J., Edwards, M. and Richardson, A. J.: Extending the SeaWiFS
1166 chlorophyll data set back 50 years in the northeast Atlantic, *Geophys. Res. Lett.*, 32\(6\), 1–4,
1167 doi:10.1029/2005GL022484, 2005.](#)

1168 [Raitsos, D. E., Lavender, S. J., Mavelias, C. D., Haralabous, J., Richardson, A. J. and Reid, P. C.: Identifying
1169 four phytoplankton functional types from space: An ecological approach, *Limnol. Oceanogr.*, 53\(2\), 605–613,
1170 doi:10.4319/lo.2008.53.2.0605, 2008.](#)

1171 Raitsos, D. E., Korres, G., Triantafyllou, G., Petihakis, G., Pantazi, M., Tsiaras, K. and Pollani, A.: Assessing
1172 chlorophyll variability in relation to the environmental regime in Pagasitikos Gulf, Greece, *J. Mar. Syst.*, 94(SUPPL.),
1173 16–22, doi:10.1016/j.jmarsys.2011.11.003, 2012.

1174 ~~Raitsos, D. E., Lavender, S. J., Mavelias, C. D., Haralabous, J., Richardson, A. J. and Reid, P. C.: Identifying
1175 four phytoplankton functional types from space: An ecological approach, *Limnol. Oceanogr.*, 53(2), 605–613,
1176 doi:10.4319/lo.2008.53.2.0605, 2008.~~

1177 Raitsos, D. E., Pradhan, Y., Lavender, S. J., Hoteit, I., Mcquatters-Gollop, A., Reid, P. C. and Richardson, A. J.:
1178 From silk to satellite: Half a century of ocean colour anomalies in the Northeast Atlantic, *Glob. Chang. Biol.*, 20(7),
1179 2117–2123, doi:10.1111/gcb.12457, 2014.

1180 [Raitsos, D. E., Reid, P. C., Lavender, S. J., Edwards, M. and Richardson, A. J.: Extending the SeaWiFS](#)
1181 [chlorophyll data set back 50 years in the northeast Atlantic, *Geophys. Res. Lett.*, 32\(6\), 1–4,](#)
1182 [doi:10.1029/2005GL022484, 2005.](#)

1183 Ren, J. S.: Effect of food quality on energy uptake, *J. Sea Res.*, 62(2–3), 72–74,
1184 doi:10.1016/j.seares.2008.11.002, 2009.

1185 [Riisgård, H. U., Kittner, C. and Seerup, D. F.: Regulation of opening state and filtration rate in filter-feeding](#)
1186 [bivalves \(*Cardium edule*, *Mytilus edulis*, *Mya arenaria*\) in response to low algal concentration, *J. Exp. Mar. Bio. Ecol.*,](#)
1187 [284\(1–2\), 105–127, doi:10.1016/S0022-0981\(02\)00496-3, 2003.](#)

1188 Riisgård, H. U., Egede, P. P. and Barreiro Saavedra, I.: Feeding Behaviour of the Mussel, *Mytilus edulis* : New
1189 Observations, with a Minireview of Current Knowledge , *J. Mar. Biol.*, 2011, 1–13, doi:10.1155/2011/312459, 2011.

1190 [Riisgård, H. U., Kittner, C. and Seerup, D. F.: Regulation of opening state and filtration rate in filter-feeding](#)
1191 [bivalves \(*Cardium edule*, *Mytilus edulis*, *Mya arenaria*\) in response to low algal concentration, *J. Exp. Mar. Bio. Ecol.*,](#)
1192 [284\(1–2\), 105–127, doi:10.1016/S0022-0981\(02\)00496-3, 2003.](#)

1193 Rios, L. M., Moore, C. and Jones, P. R.: Persistent organic pollutants carried by synthetic polymers in the ocean
1194 environment, *Mar. Pollut. Bull.*, 54(8), 1230–1237, doi:10.1016/j.marpolbul.2007.03.022, 2007.

1195 Rist, S., Steensgaard, I. M., Guven, O., Nielsen, T. G., Jensen, L. H., Møller, L. F. and Hartmann, N. B.: The fate
1196 of microplastics during uptake and depuration phases in a blue mussel exposure system, *Environ. Toxicol. Chem.*,
1197 38(1), 99–105, doi:10.1002/etc.4285, 2019.

1198 Romeo, T., Pietro, B., Pedà, C., Consoli, P., Andaloro, F. and Fossi, M. C.: First evidence of presence of plastic
1199 debris in stomach of large pelagic fish in the Mediterranean Sea, *Mar. Pollut. Bull.*, 95(1), 358–361,
1200 doi:10.1016/j.marpolbul.2015.04.048, 2015.

1201 Rosland, R., Strand, Alunno-Bruscia, M., Bacher, C. and Strohmeier, T.: Applying Dynamic Energy Budget
1202 (DEB) theory to simulate growth and bio-energetics of blue mussels under low seston conditions, *J. Sea Res.*, 62(2–3),
1203 49–61, doi:10.1016/j.seares.2009.02.007, 2009.

1204 Santana, M. F. M., Moreira, F. T., Pereira, C. D. S., Abessa, D. M. S. and Turra, A.: Continuous Exposure to
1205 Microplastics Does Not Cause Physiological Effects in the Cultivated Mussel *Perna perna*, *Arch. Environ. Contam.*
1206 *Toxicol.*, 74(4), 594–604, doi:10.1007/s00244-018-0504-3, 2018.

1207 Sarà, G., Kearney, M. and Helmuth, B.: Combining heat-transfer and energy budget models to predict thermal
1208 stress in Mediterranean intertidal mussels, *Chem. Ecol.*, 27(2), 135–145, doi:10.1080/02757540.2011.552227, 2011.

1209 [Sarà, G., Reid, G. K., Rinaldi, A., Palmeri, V., Troell, M. and Kooijman, S. A. L. M.: Growth and reproductive](#)
1210 [simulation of candidate shellfish species at fish cages in the Southern Mediterranean: Dynamic Energy Budget \(DEB\)](#)
1211 [modelling for integrated multi-trophic aquaculture, *Aquaculture*, 324–325, 259–266,](#)
1212 [doi:10.1016/j.aquaculture.2011.10.042, 2012.](#)

1213 Sarà, G., Milanese, M., Prusina, I., Sarà, A., Angel, D. L., Glamuzina, B., Nitzan, T., Freeman, S., Rinaldi, A.,
1214 Palmeri, V., Montalto, V., Lo Martire, M., Gianguzza, P., Arizza, V., Lo Brutto, S., De Pirro, M., Helmuth, B.,
1215 Murray, J., De Cantis, S. and Williams, G. A.: The impact of climate change on mediterranean intertidal communities:
1216 Losses in coastal ecosystem integrity and services, *Reg. Environ. Chang.*, 14(SUPPL.1), 5–17, doi:10.1007/s10113-
1217 012-0360-z, 2014.

1218 [Sarà, G., Reid, G. K., Rinaldi, A., Palmeri, V., Troell, M. and Kooijman, S. A. L. M.: Growth and reproductive](#)
1219 [simulation of candidate shellfish species at fish cages in the Southern Mediterranean: Dynamic Energy Budget \(DEB\)](#)
1220 [modelling for integrated multi-trophic aquaculture, *Aquaculture*, 324–325, 259–266,](#)
1221 [doi:10.1016/j.aquaculture.2011.10.042, 2012.](#)

1222 Saraiva, S., der Meer, J. van, Kooijman, S. A. L. M. and Sousa, T.: DEB parameters estimation for *Mytilus*
1223 *edulis*, *J. Sea Res.*, 66(4), 289–296, doi:10.1016/j.seares.2011.06.002, 2011b.

1224 Saraiva, S., van der Meer, J., Kooijman, S. A. L. M. and Sousa, T.: Modelling feeding processes in bivalves: A
1225 mechanistic approach, *Ecol. Modell.*, 222(3), 514–523, doi:10.1016/j.ecolmodel.2010.09.031, 2011a.

1226 Saraiva, S., Van Der Meer, J., Kooijman, S. A. L. M., Witbaard, R., Philippart, C. J. M., Hippler, D. and Parker,
1227 R.: Validation of a Dynamic Energy Budget (DEB) model for the blue mussel *Mytilus edulis*, *Mar. Ecol. Prog. Ser.*,
1228 463, 141–158, doi:10.3354/meps09801, 2012.

1229 Schwabl, P., Koppel, S., Königshofer, P., Bucsecs, T., Trauner, M., Reiberger, T. and Liebmann, B.: Detection of
1230 various microplastics in human stool: A prospective case series, *Ann. Intern. Med.*, 171(7), 453–457,
1231 doi:10.7326/M19-0618, 2019.

1232 Seuront, L., Nicastro, K. R., Zardi, G. I. and Goberville, E.: Decreased thermal tolerance under recurrent heat
1233 stress conditions explains summer mass mortality of the blue mussel *Mytilus edulis*, *Sci. Rep.*, 9(1),
1234 doi:10.1038/s41598-019-53580-w, 2019.

1235 Skoulidakis, N. T., Economou, A. N., Gritzalis, K. C. and Zogaris, S.: Rivers of the Balkans, *Rivers Eur.*, 421–
1236 466, doi:10.1016/B978-0-12-369449-2.00011-4, 2009.

1237 Smith, M., Love, D. C., Rochman, C. M. and Neff, R. A.: Microplastics in Seafood and the Implications for
1238 Human Health, *Curr. Environ. Heal. reports*, 5(3), 375–386, doi:10.1007/s40572-018-0206-z, 2018.

1239 Sprung, M.: Reproduction and fecundity of the mussel *mytilus edulis* at helgoland (North sea), *Helgoländer*
1240 *Meeresuntersuchungen*, 36(3), 243–255, doi:10.1007/BF01983629, 1983.

1241 Strohmeier, T., Strand, Ø., Alunno-Bruscia, M., Duinker, A. and Cranford, P.: Variability in particle retention
1242 efficiency by the mussel *Mytilus edulis*, *J. Exp. Mar. Bio. Ecol.*, 412, 96–102, doi:10.1016/j.jembe.2011.11.006, 2012.

1243 Sukhotin, A. A. and Kulakowski, E. E.: Growth and population dynamics in mussels (*Mytilus edulis* L.) cultured
1244 in the White Sea, *Aquaculture*, 101(1–2), 59–73, doi:10.1016/0044-8486(92)90232-A, 1992.

1245 Sukhotin, A. A., Strelkov, P. P., Maximovich, N. V. and Hummel, H.: Growth and longevity of *Mytilus edulis*
1246 (L.) from northeast Europe, *Mar. Biol. Res.*, 3(3), 155–167, doi:10.1080/17451000701364869, 2007.

1247 Sussarellu, R., Suquet, M., Thomas, Y., Lambert, C., Fabioux, C., Pernet, M. E. J., Goïc, N. Le, Quillien, V.,
1248 Mingant, C., Epelboin, Y., Corporeau, C., Guyomarch, J., Robbens, J., Paul-Pont, I., Soudant, P. and Huvet, A.: Oyster
1249 reproduction is affected by exposure to polystyrene microplastics, *Proc. Natl. Acad. Sci. U. S. A.*, 113(9), 2430–2435,
1250 doi:10.1073/pnas.1519019113, 2016.

1251 Tagliarolo, M. and McQuaid, C. D.: Sub-lethal and sub-specific temperature effects are better predictors of
1252 mussel distribution than thermal tolerance, *Mar. Ecol. Prog. Ser.*, 535, 145–159, doi:10.3354/meps11434, 2015.

1253 Teuten, E. L., Rowland, S. J., Galloway, T. S. and Thompson, R. C.: Potential for plastics to transport
1254 hydrophobic contaminants, *Environ. Sci. Technol.*, 41(22), 7759–7764, doi:10.1021/es071737s, 2007.

1255 Teuten, E. L., Saquing, J. M., Knappe, D. R. U., Barlaz, M. A., Jonsson, S., Björn, A., Rowland, S. J.,
1256 Thompson, R. C., Galloway, T. S., Yamashita, R., Ochi, D., Watanuki, Y., Moore, C., Viet, P. H., Tana, T. S.,
1257 Prudente, M., Boonyatumanond, R., Zakaria, M. P., Akkavong, K., Ogata, Y., Hirai, H., Iwasa, S., Mizukawa, K.,
1258 Hagino, Y., Imamura, A., Saha, M. and Takada, H.: Transport and release of chemicals from plastics to the
1259 environment and to wildlife, *Philos. Trans. R. Soc. B Biol. Sci.*, 364(1526), 2027–2045, doi:10.1098/rstb.2008.0284,
1260 2009.

1261 Theodorou, J. A., Viaene, J., Sorgeloos, P. and Tzovenis, I.: Production and Marketing Trends of the Cultured
1262 Mediterranean Mussel *Mytilus galloprovincialis* Lamarck 1819, in Greece , *J. Shellfish Res.*, 30(3), 859–874,
1263 doi:10.2983/035.030.0327, 2011.

1264 Thomas, Y., Mazurié, J., Alunno-Bruscia, M., Bacher, C., Bouget, J. F., Gohin, F., Pouvreau, S. and Struski, C.:
1265 Modelling spatio-temporal variability of *Mytilus edulis* (L.) growth by forcing a dynamic energy budget model with
1266 satellite-derived environmental data, *J. Sea Res.*, 66(4), 308–317, doi:10.1016/j.seares.2011.04.015, 2011.

1267 Thompson, R. C., Olson, Y., Mitchell, R. P., Davis, A., Rowland, S. J., John, A. W. G., McGonigle, D. and
1268 Russell, A. E.: Lost at Sea: Where Is All the Plastic?, *Science* (80-.), 304(5672), 838, doi:10.1126/science.1094559,
1269 2004.

1270 Triantafyllou, G., Petihakis, G. and Allen, I. J.: Assessing the performance of the Cretan Sea ecosystem model
1271 with the use of high frequency M3A buoy data set, *Ann. Geophys.*, 21(1), 365–375, doi:10.5194/angeo-21-365-2003,
1272 2003.

1273 Troost, T. A., Wijsman, J. W. M., Saraiva, S. and Freitas, V.: Modelling shellfish growth with dynamic energy
1274 budget models: An application for cockles and mussels in the Oosterschelde (southwest Netherlands), *Philos. Trans. R.*
1275 *Soc. B Biol. Sci.*, 365(1557), 3567–3577, doi:10.1098/rstb.2010.0074, 2010.

1276 Troost, T. A., Desclaux, T., Leslie, H. A., van Der Meulen, M. D. and Vethaak, A. D.: Do microplastics affect
1277 marine ecosystem productivity?, *Mar. Pollut. Bull.*, 135, 17–29, doi:10.1016/j.marpolbul.2018.05.067, 2018.

1278 ~~Troost, T. A., Wijsman, J. W. M., Saraiva, S. and Freitas, V.: Modelling shellfish growth with dynamic energy~~
1279 ~~budget models: An application for cockles and mussels in the Oosterschelde (southwest Netherlands), *Philos. Trans. R.*~~
1280 ~~*Soc. B Biol. Sci.*, 365(1557), 3567–3577, doi:10.1098/rstb.2010.0074, 2010.~~

1281 Tsiaras, K. P., Petihakis, G., Kourafalou, V. H. and Triantafyllou, G.: Impact of the river nutrient load variability
1282 on the North Aegean ecosystem functioning over the last decades, *J. Sea Res.*, 86, 97–109,
1283 doi:10.1016/j.seares.2013.11.007, 2014.

1284 Vahl, O.: Efficiency of particle retention in *mytilus edulis* L, *Ophelia*, 10(1), 17–25,
1285 doi:10.1080/00785326.1972.10430098, 1972.

1286 van Beusekom, J. E. E., Loebel, M. and Martens, P.: Distant riverine nutrient supply and local temperature drive
1287 the long-term phytoplankton development in a temperate coastal basin, *J. Sea Res.*, 61(1–2), 26–33,
1288 doi:10.1016/j.seares.2008.06.005, 2009.

1289 Van Cauwenberghe, L. and Janssen, C. R.: Microplastics in bivalves cultured for human consumption, *Environ.*
1290 *Pollut.*, 193, 65–70, doi:10.1016/j.envpol.2014.06.010, 2014.

1291 Van Cauwenberghe, L., Claessens, M., Vandegehuchte, M. B. and Janssen, C. R.: Microplastics are taken up by
1292 mussels (*Mytilus edulis*) and lugworms (*Arenicola marina*) living in natural habitats, *Environ. Pollut.*, 199, 10–17,
1293 doi:10.1016/j.envpol.2015.01.008, 2015.

1294 van der Veer, H. W., Cardoso, J. F. M. F. and van der Meer, J.: The estimation of DEB parameters for various
1295 Northeast Atlantic bivalve species, *J. Sea Res.*, 56(2), 107–124, doi:10.1016/j.seares.2006.03.005, 2006.

1296 van Haren, R. J. F., Schepers, H. E. and Kooijman, S. A. L. M.: Dynamic energy budgets affect kinetics of
1297 xenobiotics in the marine mussel *Mytilus edulis*, *Chemosphere*, 29(2), 163–189, doi:10.1016/0045-6535(94)90099-X,
1298 1994.

1299 Van Sebille, E., Wilcox, C., Lebreton, L., Maximenko, N., Hardesty, B. D., Van Franeker, J. A., Eriksen, M.,
1300 Siegel, D., Galgani, F. and Law, K. L.: A global inventory of small floating plastic debris, *Environ. Res. Lett.*, 10(12),
1301 124006, doi:10.1088/1748-9326/10/12/124006, 2015.

1302 Vandermeersch, G., Lourenço, H. M., Alvarez-Muñoz, D., Cunha, S., Diogène, J., Cano-Sancho, G., Sloth, J. J.,
1303 Kwadijk, C., Barcelo, D., Allegaert, W., Bekaert, K., Fernandes, J. O., Marques, A. and Robbens, J.: Environmental
1304 contaminants of emerging concern in seafood - European database on contaminant levels, *Environ. Res.*, 143, 29–45,
1305 doi:10.1016/j.envres.2015.06.011, 2015.

1306 Vlachogianni, T., Anastasopoulou, A., Fortibuoni, T., Ronchi, F. and Zeri, C.: Marine Litter Assessment in the
1307 Adriatic & Ionian Seas. IPA-Adriatic DeFishGear Project, MIO-ECSDE, HCMR and ISPRA. pp. 168 (ISBN: 978-
1308 960-6793-25-7), 2017.

1309 Von Moos, N., Burkhardt-Holm, P. and Köhler, A.: Uptake and effects of microplastics on cells and tissue of the
1310 blue mussel *Mytilus edulis* L. after an experimental exposure, *Environ. Sci. Technol.*, 46(20), 11327–11335,
1311 doi:10.1021/es302332w, 2012.

1312 Ward, J. E. and Kach, D. J.: Marine aggregates facilitate ingestion of nanoparticles by suspension-feeding
1313 bivalves, *Mar. Environ. Res.*, 68(3), 137–142, doi:10.1016/j.marenvres.2009.05.002, 2009.

1314 Ward, J. E. and Shumway, S. E.: Separating the grain from the chaff: Particle selection in suspension- and
1315 deposit-feeding bivalves, *J. Exp. Mar. Bio. Ecol.*, 300(1–2), 83–130, doi:10.1016/j.jembe.2004.03.002, 2004.

1316 [Ward, J., Rosa, M. and Shumway, S.: Capture, ingestion, and egestion of microplastics by suspension-feeding](#)
1317 [bivalves: a 40-year history, *Anthr. Coasts*, 2\(1\), 39–49, doi:10.1139/anc-2018-0027, 2019a.](#)

1318 Ward, J. E., Zhao, S., Holohan, B. A., Mladinich, K. M., Griffin, T. W., Wozniak, J. and Shumway, S. E.:
1319 Selective Ingestion and Egestion of Plastic Particles by the Blue Mussel (*Mytilus edulis*) and Eastern Oyster
1320 (*Crassostrea virginica*): Implications for Using Bivalves as Bioindicators of Microplastic Pollution, *Environ. Sci.*
1321 *Technol.*, 53(15), 8776–8784, doi:10.1021/acs.est.9b02073, 2019b.

1322 Wegner, A., Besseling, E., Foekema, E. M., Kamermans, P. and Koelmans, A. A.: Effects of nanopolystyrene on
1323 the feeding behavior of the blue mussel (*Mytilus edulis* L.), *Environ. Toxicol. Chem.*, 31(11), 2490–2497,
1324 doi:10.1002/etc.1984, 2012.

1325 Widdows, J., Fieth, P. and Worrall, C. M.: Relationships between seston, available food and feeding activity in
1326 the common mussel *Mytilus edulis*, *Mar. Biol.*, 50(3), 195–207, doi:10.1007/BF00394201, 1979.

1327 Wieczorek, A. M., Morrison, L., Croot, P. L., Allcock, A. L., MacLoughlin, E., Savard, O., Brownlow, H. and
1328 Doyle, T. K.: Frequency of microplastics in mesopelagic fishes from the Northwest Atlantic, *Front. Mar. Sci.*, 5(FEB),
1329 doi:10.3389/fmars.2018.00039, 2018.

1330 Woods, M. N., Stack, M. E., Fields, D. M., Shaw, S. D. and Matrai, P. A.: Microplastic fiber uptake, ingestion,
1331 and egestion rates in the blue mussel (*Mytilus edulis*), *Mar. Pollut. Bull.*, 137, 638–645,
1332 doi:10.1016/j.marpolbul.2018.10.061, 2018.

1333 Zaldivar, J. M.: A general bioaccumulation DEB model for mussels. JRC Scientific and Technical Reports, EUR
1334 23626. Office for Official Publications of the European Communities: Luxembourg, ISBN 978-92-79-10943-0 , ii, 31
1335 pp, 2008.

1336 Zeri, C., Adamopoulou, A., Bojanić Varezić, D., Fortibuoni, T., Kovač Viršek, M., Kržan, A., Mandić, M.,
1337 Mazziotti, C., Palatinus, A., Peterlin, M., Prvan, M., Ronchi, F., Siljic, J., Tutman, P. and Vlachogianni, T.: Floating
1338 plastics in Adriatic waters (Mediterranean Sea): From the macro- to the micro-scale, *Mar. Pollut. Bull.*, 136, 341–350,
1339 doi:10.1016/j.marpolbul.2018.09.016, 2018.

1340 Zhao, S., Ward, J. E., Danley, M. and Mincer, T. J.: Field-Based Evidence for Microplastic in Marine
 1341 Aggregates and Mussels: Implications for Trophic Transfer, Environ. Sci. Technol., 52(19), 11038–11048,
 1342 doi:10.1021/acs.est.8b03467, 2018.
 1343

1344

1345 **Tables & Figures**

1346
$$\frac{dE}{dt} = \dot{p}_a - \dot{p}_c \quad (1)$$

1347
$$\frac{dV}{dt} = \frac{k \cdot \dot{p}_c - [\dot{p}_M] \cdot V}{[E_g]} \quad (2)$$

1348
$$\frac{dR}{dt} = (1 - k) \cdot \dot{p}_c - \left[\frac{1-k}{k} \right] \cdot \min(V, V_p) \cdot [\dot{p}_M] \quad (3)$$

1349
$$\dot{p}_a = \{\dot{p}_{Am}\} \cdot f \cdot k(T) \cdot V^{\frac{2}{3}} \quad (4)$$

1350
$$f = \frac{X}{X + K_y}, \quad \text{where } K_y = X_K \cdot \left(1 + \frac{Y}{Y_K}\right) \quad (5)$$

1351
$$\dot{p}_c = \frac{[E]}{[E_g] + k \cdot [E]} \cdot \left(\frac{[E_g] \cdot \{\dot{p}_{Am}\} \cdot k(T) \cdot V^{\frac{2}{3}}}{[E_m]} + [\dot{p}_M] \cdot V \right) \quad (6)$$

1352
$$[E] = \frac{E}{V} \quad (7)$$

1353
$$[\dot{p}_M] = k(T) \cdot [\dot{p}_M]_m \quad (8)$$

1354
$$k(T) = \frac{\exp\left(\frac{T_A - T_A}{T_I - T}\right)}{1 + \exp\left(\frac{T_{AL} - T_{AL}}{T - T_L}\right) + \exp\left(\frac{T_{AH} - T_{AH}}{T_H - T}\right)} \quad (9)$$

1355
$$L = \frac{V^{\frac{1}{3}}}{\delta_m} \quad (10)$$

1356
$$W = d \cdot \left(V + \frac{E}{[E_g]} \right) + \frac{R}{\mu_E} \quad (11)$$

1357
$$\dot{C}_R = \frac{\{\dot{C}_{Rm}\}}{1 + \sum_i^n \frac{X_i \cdot \{\dot{C}_{Rm}\}}{\{\dot{p}_{XiFm}\}}} \cdot k(T) \cdot V^{\frac{2}{3}}, \quad i = \begin{cases} 1 \text{ for } CHL - a \\ 2 \text{ for } MPs \end{cases} \quad (12)^a$$

1358
$$\dot{p}_{XiF} = \dot{C}_R \cdot X_i \quad (13)^a$$

1359
$$\dot{p}_{XiI} = \frac{\rho_{Xi} \cdot \dot{p}_{XiF}}{1 + \sum_i^n \frac{\rho_{Xi} \cdot \dot{p}_{XiF}}{\{\dot{p}_{XiIm}\}}} \quad (14)^a$$

1360
$$\dot{J}_{pfi} = \dot{p}_{XiF} - \dot{p}_{XiI} \quad (15)^a$$

1361
$$\dot{J}_f = \dot{p}_{X1I} - \dot{p}_A \quad (16)$$

$$GSI = \frac{\frac{R}{\mu_E}}{d \cdot \left(V + \frac{E}{[Eg]} \right) + \frac{R}{\mu_E}} \quad (17)$$

1363 Table 1. Dynamic energy budget model: equations. See Table 2 for model variables, Table 3 for parameters and Table
1364 4 for initial values

1365 ^a notation refers to feeding equations handling each type of suspended matter separately (i=1 for algae and i=2 for
1366 microplastics) where units transformation is applied when it is necessary (see Table 3).
1367

Variable	Description	Units
1368 V	Structural volume	cm^3
1369 E	Energy reserves	J
1370 R	Energy allocated to development 1371 and reproduction	J
1372 C	Microplastics accumulation	particles individual ⁻¹
1373 \dot{p}_a	Assimilation energy rate	J d^{-1}
1374 \dot{p}_c	Utilization energy rate	J d^{-1}
1375 \dot{C}_R	Clearance rate	$\text{m}^3 \text{d}^{-1}$
1376 C_{env}	Microplastics concentration	particles L^{-1}
1377 \dot{p}_{XiF}	Filtration rate	J d^{-1} or g d^{-1}
1378 \dot{p}_{XiI}	Ingestion rate	J d^{-1} or g d^{-1}
1379 \dot{J}_{pfi}	Pseudofaeces production rate	J d^{-1} or g d^{-1}
1380 \dot{J}_f	Faeces production rate	J d^{-1}
1381 f	Functional response function	-
1382 X_i	Food or MPs density	mg chl a m^{-3} or g m^{-3}
1383 $[\dot{p}_M]$	Maintenance costs	$\text{J cm}^{-3} \text{d}^{-1}$
1384 T	Temperature	K
1385 $k(T)$	Temperature dependence	-
1386 L	Shell length	cm
1387 W	Fresh tissue mass	g
1388 GSI	Gonado-somatic index	-

1390 Table 2. Dynamic energy budget model: variables

1391

Parameter	Units	Description	Value	Reference
$\{p_{Am}\}$	$\text{J cm}^{-2} \text{d}^{-1}$	Maximum surface area-specific assimilation rate	147.6	Van der Veer et al. (2006)
$\{C_{Rm}\}$	$\text{m}^3 \text{cm}^{-2} \text{d}^{-1}$	Maximum surface area-specific clearance rate	0.096	Saraiva et al. (2011a)
$\{p_{X_1Fm}\}$	$\text{mg chl-a cm}^{-2} \text{d}^{-1}$	Algal maximum surface area-specific filtration rate*	0.1152	Rosland et al. (2009)
$\{p_{X_2Fm}\}$	$\text{g cm}^{-2} \text{d}^{-1}$	Silt maximum surface area-specific filtration rate	3.5	Saraiva et al. (2011a)
$\{p_{X_1Im}\}$	mg chl-a d^{-1}	Algae maximum ingestion rate*	$3.12 \cdot 10^6$	Saraiva et al. (2011b)
$\{p_{X_2Im}\}$	g d^{-1}	Silt maximum ingestion rate	0.11	Saraiva et al. (2011b)
ρ_1	-	Algae binding probability	0.99	Saraiva et al. (2011a)
ρ_2	-	Inorganic material binding probability	0.45	Saraiva et al. (2011a)
k_f	d^{-1}	Post-ingestive losses through faeces	Calibrated	-
X_K	mg chl-a m^{-3}	Half saturation coefficient	Calibrated	-
T_A	K	Arrhenius temperature	5800	Van der Veer et al. (2006)
T_I	K	Reference temperature	293	Van der Veer et al. (2006)
T_L	K	Lower boundary of tolerance rate	275	Van der Veer et al. (2006)
T_H	K	Upper boundary of tolerance rate	296	Van der Veer et al. (2006)
T_{AL}	K	Rate of decrease of upper boundary	45430	Van der Veer et al. (2006)
T_{AH}	K	Rate of decrease of lower boundary	31376	Van der Veer et al. (2006)
$[p_M]_m$	$\text{J cm}^{-3} \text{d}^{-1}$	Volume specific maintenance costs	24	Van der Veer et al. (2006)
$[E_G]$	J cm^{-3}	Volume specific growth costs	1900	Van der Veer et al. (2006)
$[E_m]$	J cm^{-3}	Maximum energy density	2190	Van der Veer et al. (2006)
k	-	Fraction of utilized energy spent on maintenance/growth	0.7	Van der Veer et al. (2006)
V_p	cm^3	Volume at start of reproductive stage	0.06	Van der Veer et al. (2006)
GSI_{th}	-	Gonado-somatic index triggering spawning	0.28	Van der Veer et al. (2006)
δ_m	-	Shape coefficient	0.25	Casas & Bacher (2006)
d	g cm^{-3}	Specific density	1.0	Kooijman (2000)
μ_E	J g^{-1}	Energy content of reserves	6750	Casas & Bacher (2006)
λ	J mg chl-a^{-1}	Conversion factor	2387.73	Rosland et al. (2009)

1419

Table 3. Dynamic energy budget model: parameters

1420 *units mol C converted to mg CHL-a by multiplying with the factor $\frac{12 \cdot 10^3}{50}$ assuming Carbon:CHL-a ratio of 50
 1421 (Hatzonikolakis et al., 2017).

1422

1423

1424

Area	X _k value (mg m ⁻³)	CHL-a range (mg m ⁻³)	CHL-a mean (mg m ⁻³)	Temperature range(°C)	Length after one year±SD (cm)	Reference
Maliakos Gulf	0.72	0.87-5.59	1.80	12.0-26.0	7.06 ± 0.46	Hatzonikolakis et al., 2017
Thermaikos Gulf	0.56	1.04-2.76	1.89	11.5-24.5	7.0 ± 0.47	Hatzonikolakis et al., 2017
Black Sea	Calibrated: 0.96	0.53-16.30	3.07	6.5-25.0	7.5 ± 0.1	Karayucel et al., 2010
Bizerte lagoon	3.829	4.00-7.70	5.20	12.0-28.0	7.26 ± 0.46	Béjaoui-Omri et al., 2014

1425

1426 *Table 4. Half saturation tuned values (X_k) and mussel growth data (Length) in different areas of the Mediterranean and*
 1427 *Black Seas.*

1428

1429

Northern Ionian Sea			North Sea		
Variable	Value		Variable	Value	
Start date	20 Nov 2010		Start date	1 Jul 2007	
L	0.85 cm		L	0.15 cm	
W	0.1938 g		W	0.0055 g	
V	0.0096 cm ³		V	5.3·10 ⁻⁵ cm ³	
E	350 J		E	10 J	
R	0 J		R	0 J	
C	0 particles individual ⁻¹		C	0 particles individual ⁻¹	

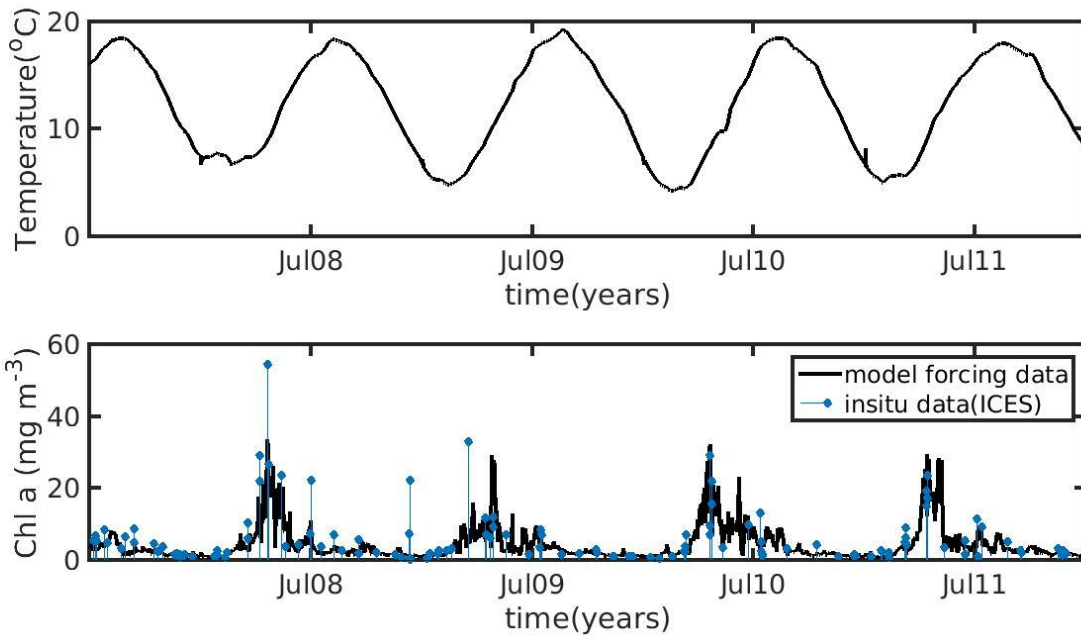
1440 *Table 5. Dynamic energy budget-accumulation model: initial values. L: shell length; W: fresh tissue mass; V: structural*
 1441 *volume; E: energy reserves; R: energy allocated to reproduction; C: Microplastics accumulation*

1442

1443

1444

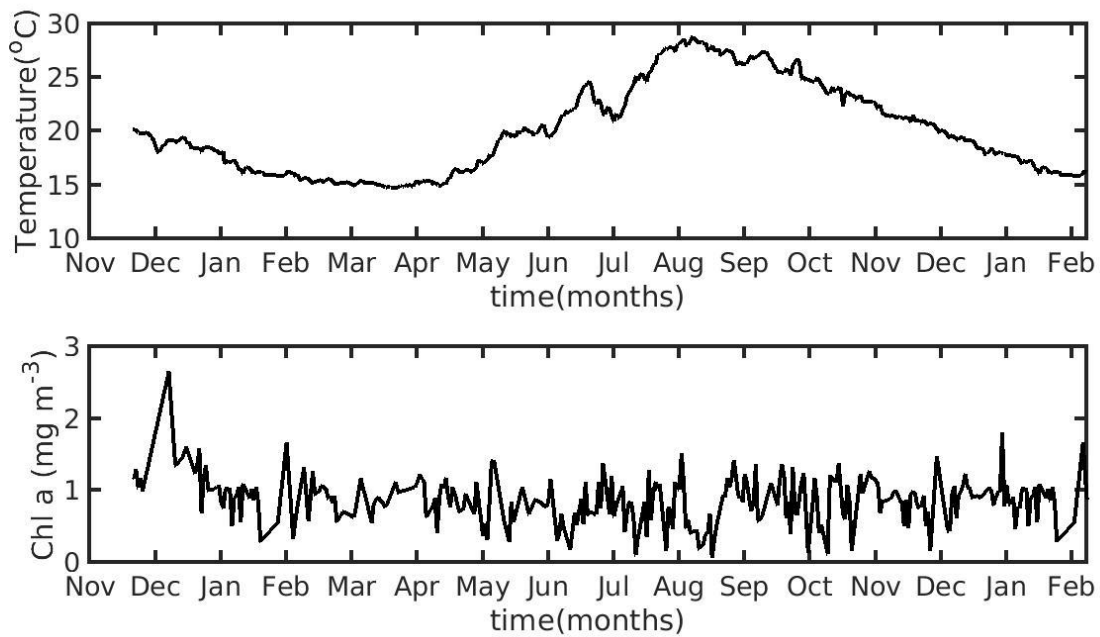
1445



1446

1447 *Fig. 1. Environmental data used for the forcing of the Dynamic Energy Budget model(DEB) in the North Sea*
 1448 *simulation, showing temperature (top) and chlorophyll a concentration against in situ data from the ICES database*
 1449 *(bottom).*

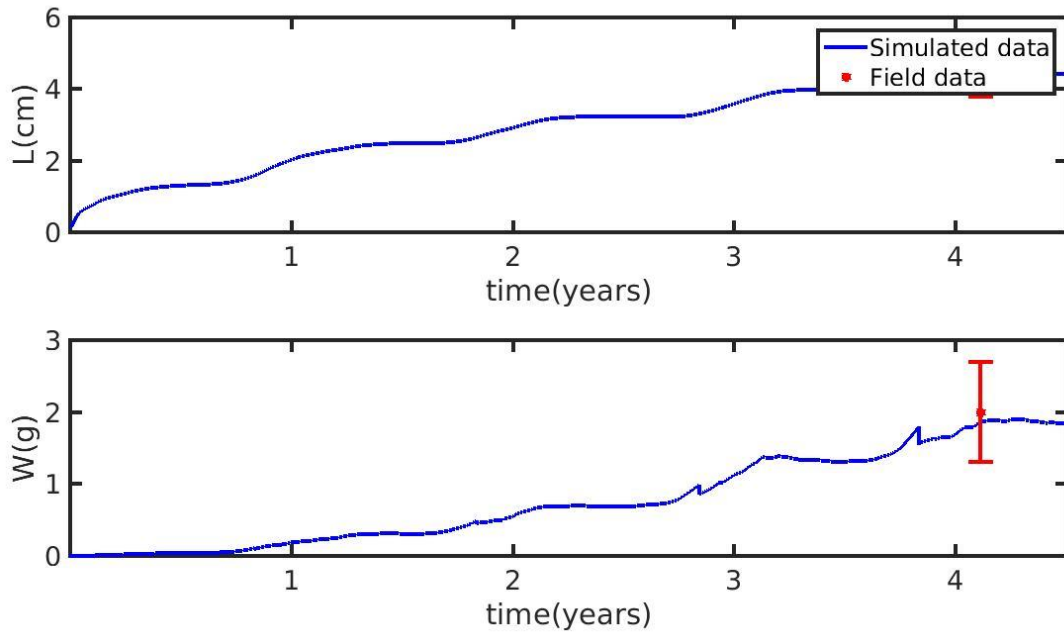
1450



1451

1452 *Fig. 2. Environmental data used for the forcing of the dynamic energy budget model in the Northern Ionian Sea*
 1453 *simulation, showing temperature (top) and chlorophyll a concentration (bottom).*

1454



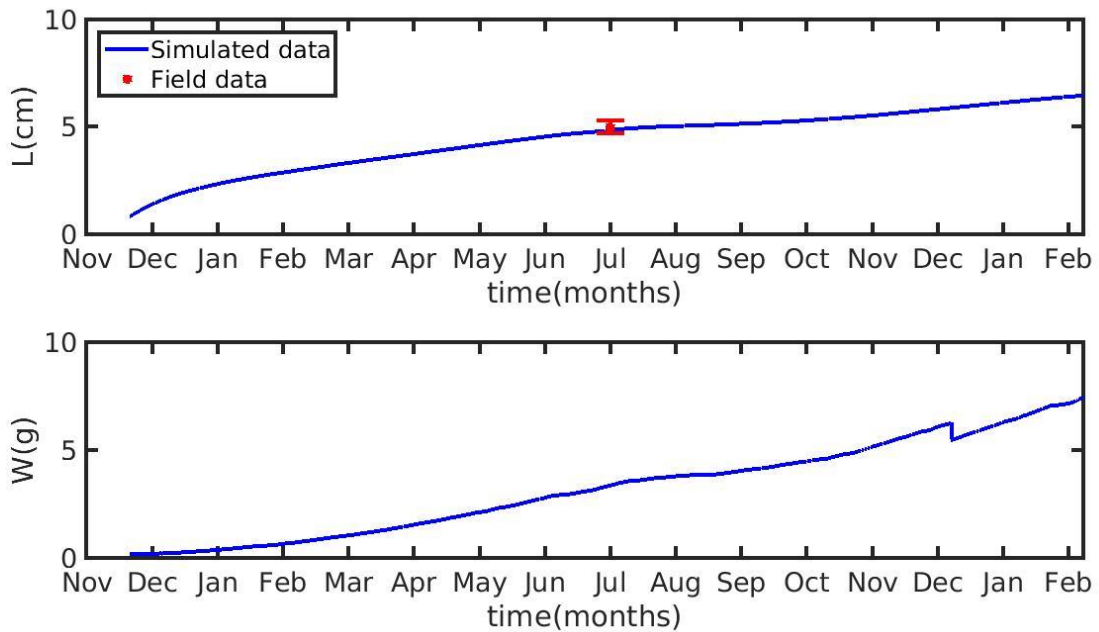
1455

1456

1457

1458

Fig. 3. Simulated mussel shell length (L) (top) and fresh tissue mass (W) (bottom) against North Sea data (red star: mean \pm SD), using chlorophyll a ($X = [CHL-a]$) in the mussel diet.

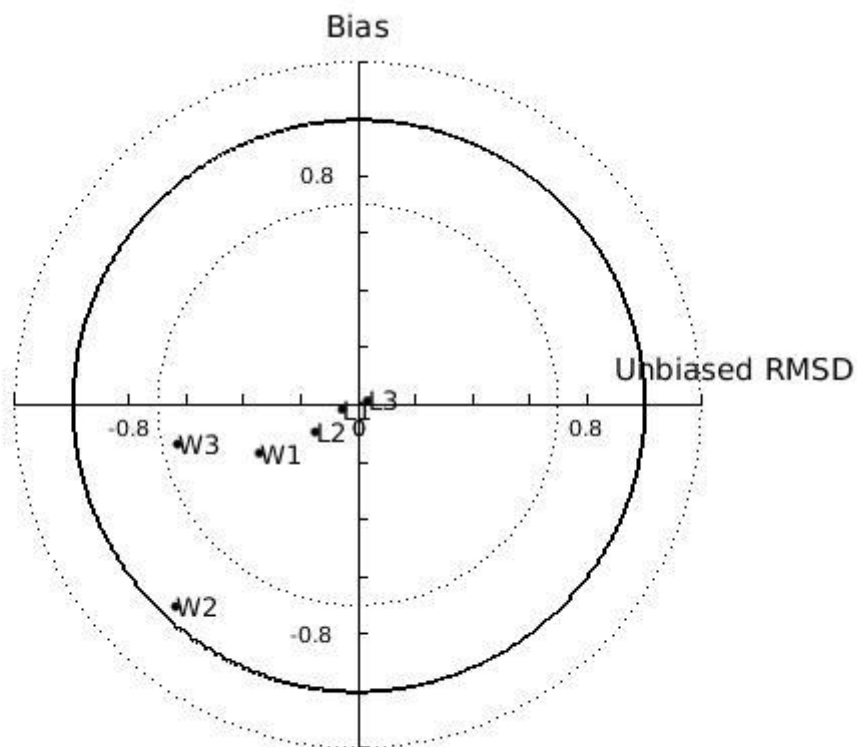


1459

1460

1461

Fig. 4. Simulated mussel shell length (L) (top) and fresh tissue mass (W) (bottom) against North Sea data (red star: mean \pm SD), using chlorophyll a ($X = [CHL-a]$) in the mussel diet

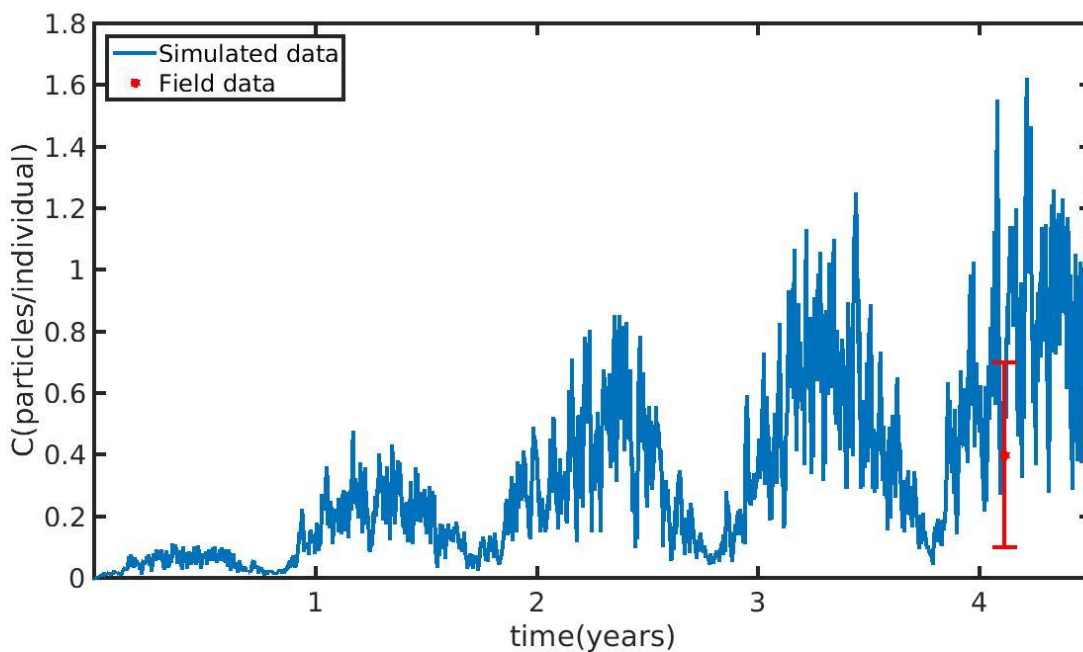


1462

1463 | *Fig. 53. Target diagram of simulated shell length (L) and fresh mass tissue weight (W) against field data from*
 1464 *Thermaikos and Maliakos Gulf (eastern Mediterranean Sea), Black Sea and Bizerte Lagoon (southwestern*
 1465 *Mediterranean Sea), using the **power** (L_1 , W_1), **exponential** (L_2 , W_2) and **linear** (L_3 , W_3) function of the half saturation*
 1466 *coefficient. The model bias is indicated on the y-axis while the unbiased root-mean-square-deviation (RMSD) is*
 1467 *indicated on the x-axis.*

1468

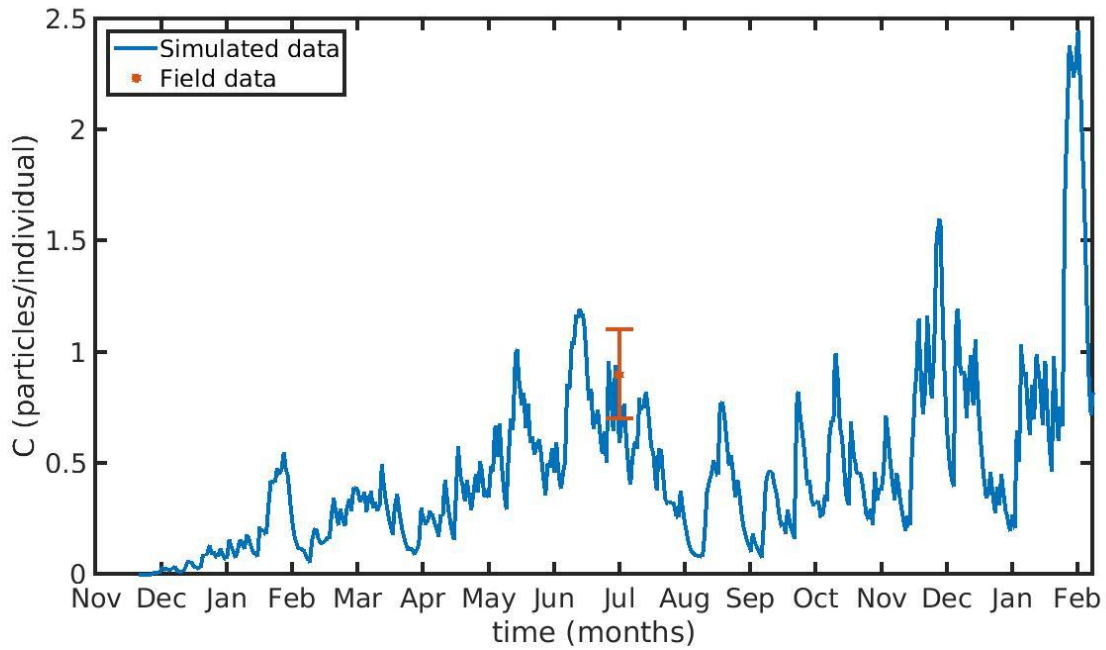
1469



1470

1471 Fig.6. Microplastics (MPs) accumulation by the mussel (blue line) against field data (red star: mean \pm SD), using daily
1472 environmental concentration of MPs (C_{env} mean value \pm SD: 0.4 ± 0.3 particles L^{-1}) in the North Sea.

1473

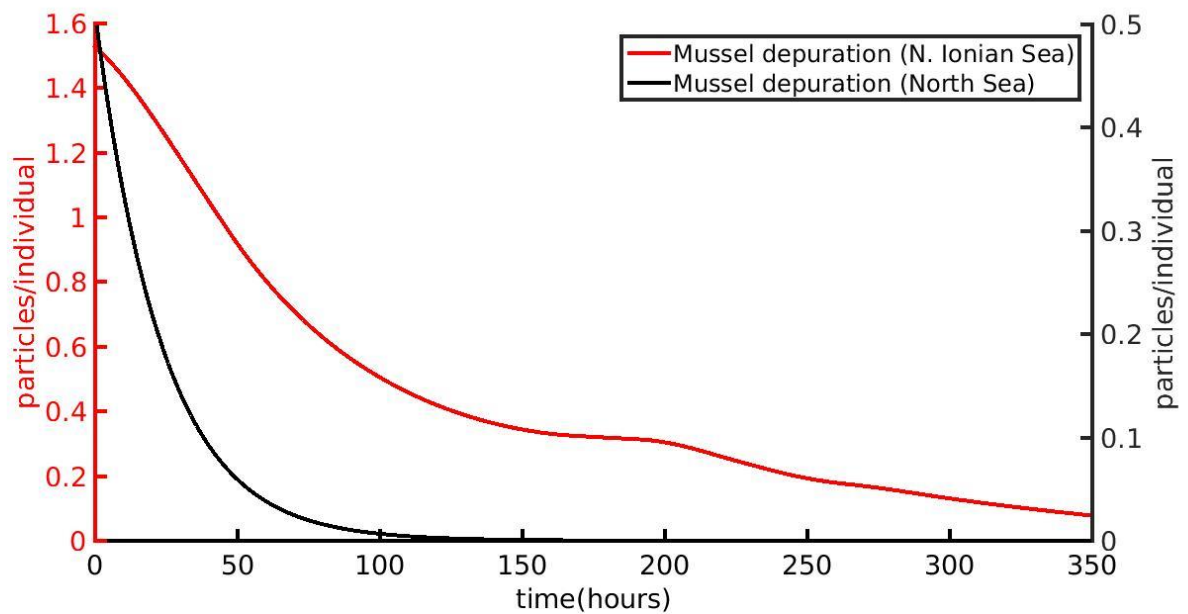


1474

1475 Fig. 7. Microplastics (MPs) accumulation by the mussel (blue line) against field data (red star: mean value \pm SD),
1476 using daily environmental concentration of MPs (C_{env} mean value \pm SD: 0.0012 ± 0.024 particles L^{-1}) in the Northern
1477 Ionian Sea.

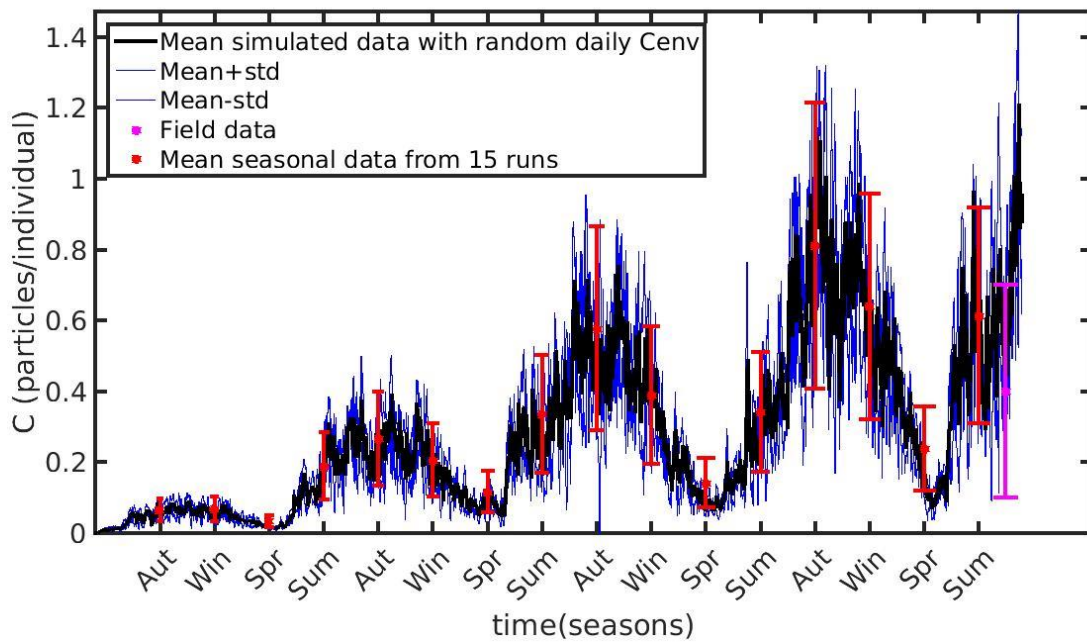
1478

1479



1480

1481 Fig. 8. Depuration phase of the cultured *Mytilus galloprovincialis* (red line) and wild *Mytilus edulis* (black line) using
1482 zero environmental concentration of microplastics ($C_{env}=0$) after 1 year and 4 years of simulation time at the Northern
1483 Ionian Sea and North Sea respectively.

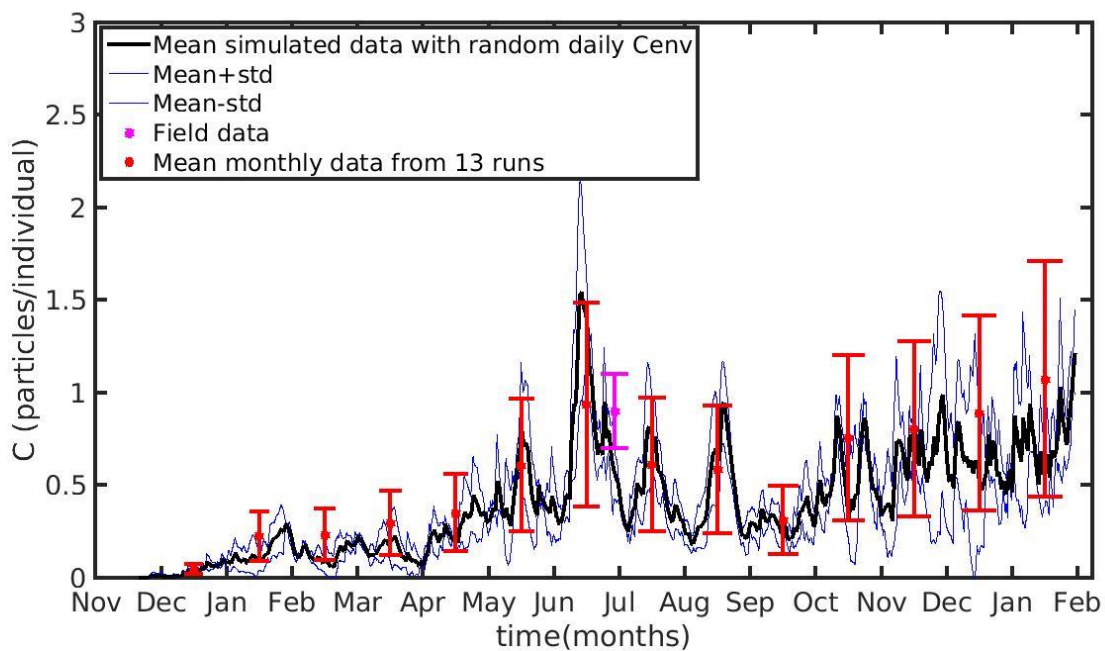


1485

1486 *Fig.9. Mean seasonally values and standard deviation of microplastics (MPs) accumulation (red error bars: mean*
 1487 *value \pm SD) by the mussel in North Sea derived from 15 model runs with different constant values of environmental*
 1488 *MPs concentration (C_{env} range: 0.1-0.8 particles L^{-1}); Mean hourly simulated data (black line) and standard deviation*
 1489 *(blue lines) of microplastics accumulation derived from 3 model runs with stochastic sequences of daily random C_{env}*
 1490 *values.*

1491

1492

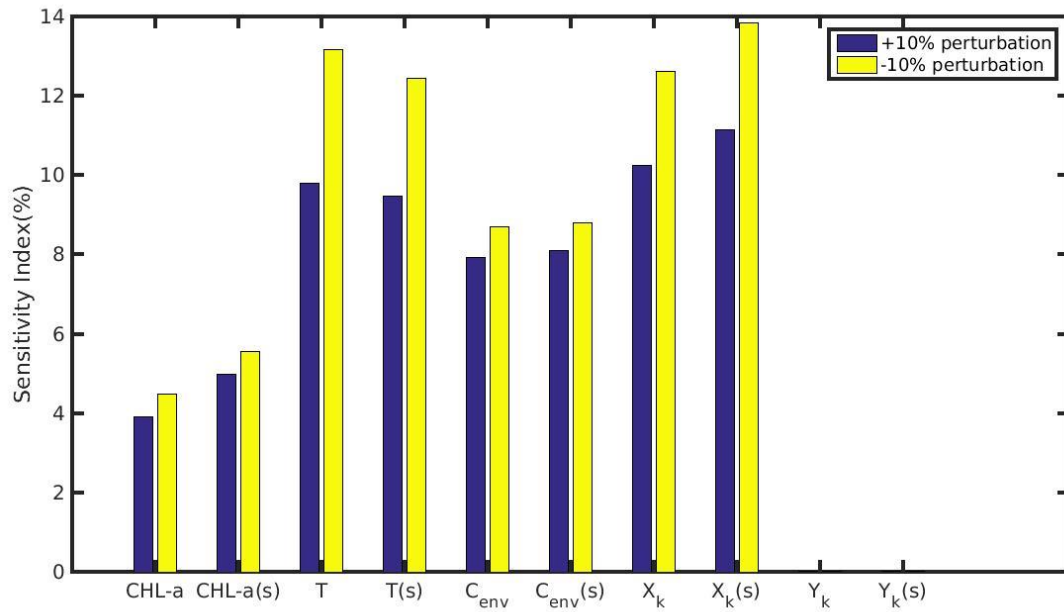


1493

1494 *Fig. 10. Mean monthly values and standard deviation of microplastics accumulation (red error bars: mean value \pm SD)*
 1495 *by the mussel in Northern Ionian Sea derived from 13 model runs with different constant values of environmental MPs*
 1496 *concentration (C_{env} range: 0.0012-0.024 particles L^{-1}); Mean hourly simulated data (back line) and standard deviation*

1497 (blue lines) of microplastics accumulation derived from 3 model runs with stochastic sequences of daily random C_{env}
 1498 values.

1499

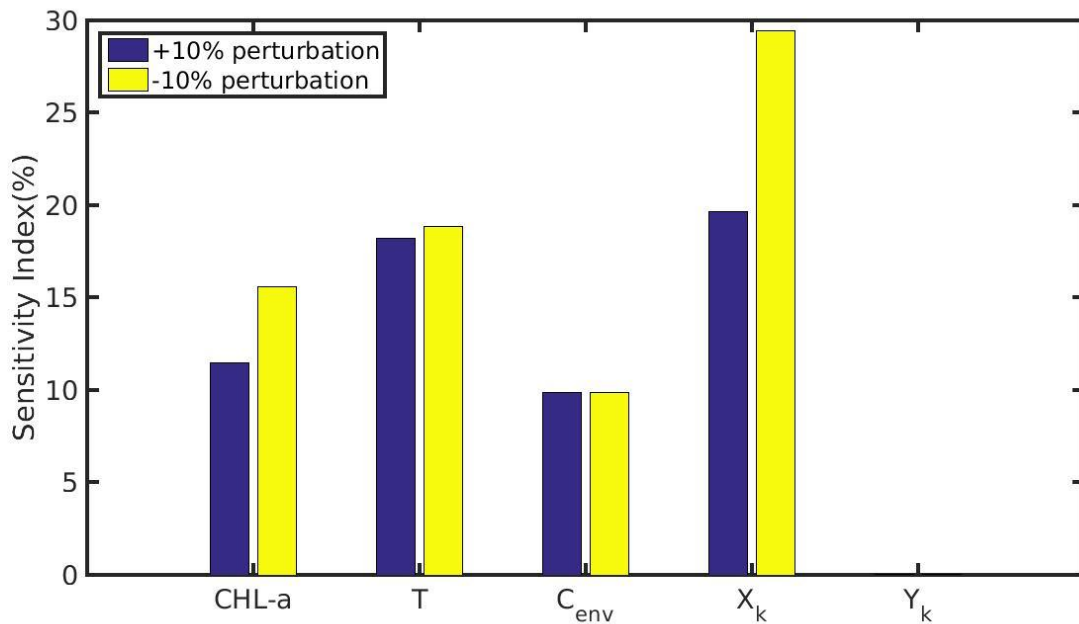


1500

1501 Fig. 11. Sensitivity index of MPs accumulation on the wild mussel of the North Sea when variables (CHL-a,
 1502 temperature, C_{env}) and parameters (X_k , Y_k) are perturbed $\pm 10\%$. The notation (s) refers to the permanently submerged
 1503 mussel.

1504

1505



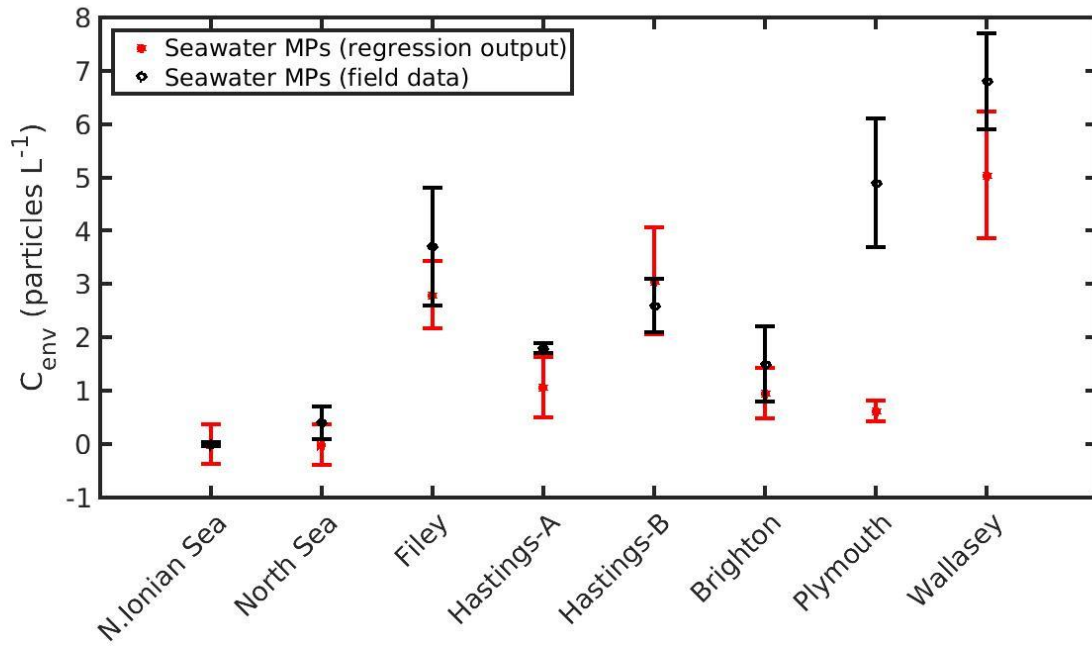
1506

1507 Fig. 12. Sensitivity index of MPs accumulation on the cultured mussel of the Northern Ionian Sea when variables
 1508 (CHL-a, temperature, C_{env}) and parameters (X_k , Y_k) are perturbed $\pm 10\%$.

1509

1510

1511



1512

1513

1514

Fig. 13. Prediction of seawater microplastics concentration by using Eq. 20 for the Northern Ionian Sea, North Sea (present study) and 6 areas around U.K. (Filey, Hastings-A&B, Brighton, Plymouth, Wallasey; Li et al. (2018)).

Modelling mussel (*Mytilus spp.*) microplastic accumulation.

Natalia Stamataki^{1,2,3}, Yannis Hatzonikolakis^{2,4}, Kostas Tsiaras², Catherine Tsangaris²,
George Petihakis³, Sarantis Sofianos¹, George Triantafyllou^{2,*}

¹Department of Environmental Physics, [National and Kapodistrian](#) University of Athens, 15784 Athens, Greece

²Hellenic Centre for Marine Research (HCMR), Athens-Sounio Avenue, Mavro Lithari, 19013 Anavyssos, Greece

³Hellenic Centre for Marine Research (HCMR), 71003 Heraklion, Greece

⁴Department of Biology, [National and Kapodistrian](#) University of Athens, 15784, Greece

*Corresponding author: gt@hcmr.gr

Abstract: Microplastics (MPs) are a contaminant of growing concern due to their widespread distribution and interactions with marine species, such as filter feeders. To investigate the MPs accumulation inby wild and cultured mussels, a Dynamic Energy Budget (DEB) model was developed and validated with the available field data of *Mytilus edulis* (*M. edulis*, wild) from the North Sea and *Mytilus galloprovincialis* (*M. galloprovincialis*, cultured) from the Northern Ionian Sea. Towards a generic DEB model, the site-specific model parameter, half saturation coefficient (X_k) was applied as a power function of food density for the cultured mussel, while for the wild mussel it was calibrated to a constant value. The DEB-accumulation model simulated the uptake and excretion rate of MPs, taking into account of environmental characteristics (temperature and chlorophyll-a). An accumulation of MPs equal to 0.5364 particles individual⁻¹ (fresh tissue mass 1.9 g) and 0.91 particles individual⁻¹ (fresh tissue mass 3.34 g) was simulatedfound for the wild and cultured mussel after 4 years and 1 year respectively, in agreement with the field data. The inverse experiments investigating the depuration time of the wild and cultured mussel in a clean from MPs environment showed a 90% removal of MPs load after 2.53 and 124 days, respectively. Furthermore, sensitivity tests on model parameters and forcing functions highlighted that besides MPs concentration, the accumulation is highly depended on temperature and chlorophyll-a of the surrounding environment. For this reason, an empirical equation was found, directly relating directly the environmental concentration of MPs in seawater, with the seawater's temperature, chlorophyll-a and the MPs accumulation in mussel's soft tissue MPs load, temperature and chlorophyll a.

1. Introduction

Microplastic particles (MPs) are synthetic organic polymers with size below 5 mm (Arthur et al., 2009) that originate from a variety of sources including ~~mainly~~: those particles that are manufactured for particular household or industrial activities, such as facial scrubs, toothpastes and resin pellets used in the plastic industry (primary MPs), and those formed from the fragmentation of larger plastic items (secondary MPs) (GESAMP, 2015). Eriksen et al. (2014) estimated that more than 5 trillion microplastic particles, weighing over 250,000 tons, float in the oceans. Due to their composition, density and shape, MPs are highly persistent in the environment and are, therefore, accumulating in different marine compartments at increasing rates: surface and deeper layers in the water column, as well as at the seafloor and within the sediments (Moore et al., 2001, Lattin et al., 2004, Thompson, 2004, Lusher, 2015). Since the majority of MPs entering the marine environment, originate from the land (i.e. land-fills, littering of beaches and coastal areas, rivers, floodwaters, untreated municipal sewerage, industrial emissions), the threat of MPs pollution in the coastal zone puts considerable pressure on the coastal ecosystems (Cole et al., 2011, Andrady, 2011). In recent years, initiatives under various projects (i.e. CLAIM, DeFishGear) target at evaluating the threat and impact of marine litter pollution; the European framework of JERICO-RI focuses on a sustainable research infrastructure in the coastal area to support the monitoring, science and management of coastal marine areas (<http://www.jerico-ri.eu/>). In the framework of JERICO-NEXT, a recent study addressed the environmental threats and gaps ~~with~~ monitoring programmes in European coastal waters, including the marine litter (i.e. MPs) as one of the most commonly identified threat to the marine environment and highlighted the need for improved monitoring of the MPs distribution and their impacts in European coastal environments (Painting et al., 2019).

Numerous studies have revealed that MPs are ingested either directly or through lower trophic prey by animals ~~at~~ from all levels of the food web; from zooplankton (Cole et al., 2013), small pelagic fishes and mussels (Digka et al., 2018a) to mesopelagic fishes (Wieczorek et al., 2018) and large predators like tuna and swordfish (Romeo et al., 2015). Microplastic ingestion by marine animals can potentially affect animal health and raises toxicity concerns, since plastics can facilitate the transfer of chemical additives and/or hydrophobic organic contaminants to biota (Mato et al., 2001, Rios et al., 2007, Teuten et al., 2007, 2009, Hirai et al., 2011). Human, as a top predator, is also contaminated by MPs (Schwabl et al., 2019). Mussel and small fishes that are commonly consumed whole, without removing digestive tracts, where MPs are concentrated, are among the most likely pathways for MPs to embed in the human diet (Smith et al., 2018). Especially regarding marine organisms (i.e. mussels), it is notable that the levels of their contamination has been added

69 to the European database (www.ecsafeseafooddbase.eu) as an environmental variable of growing
70 concern, reflecting the health status (Marine Strategy Framework Directive (MSFD) Descriptor 10
71 – Marine Litter (Decision 2017/848/EU)) (De Witte et al., 2014, Vandermeersch et al., 2015, Digka
72 et al., 2018a). Today, a series of studies have denoted the presence of MPs in mussels' tissue
73 intended for human consumption (Van Cauwenberghe and Janssen, 2014, Mathalon and Hill, 2014,
74 Li et al., 2016, 2018, Hantoro et al., 2019). For instance, in a recent study, Li et al. (2018) sampled
75 mussels from coastal waters and supermarkets in the U.K and estimated that a plate of 100g mussels
76 contains 70 MPs that will be ingested by the consumer. The presence of MPs in mussels has been
77 also demonstrated during laboratory trials in their faeces, intestinal tract (Von Moos et al., 2012,
78 Van Cauwenberghe et al., 2015, Wegner et al., 2012, Khan and Prezant, 2018), as well as in their
79 circulatory system (Browne et al., 2008). Other laboratory studies showed several effects of
80 microplastic ingestion in laboratory exposed mussels, including histological changes, inflammatory
81 responses, immunological alterations, lysosomal membrane destabilization, reduced filtering
82 activity, neurotoxic effects, oxidative stress effects, increase in hemocyte mortality, dysplasia,
83 genotoxicity and transcriptional responses (reviewed by Li et al., 2019). However, the tested
84 concentrations of MPs in laboratory experiments are frequently unrealistic, being several orders of
85 magnitude higher (2 to 7 orders of magnitude) than the observed seawater concentrations (Van
86 Cauwenberge et al., 2015, Lenz et al. 2016).

87 Mussels, through their extensive filtering activity, feed on planktonic organisms that have
88 similar size with MPs (Browne et al., 2007) and considering also their inability to select particles
89 with high energy value (i.e. phytoplankton) during filtration (Vahl, 1972, Saraiva et al., 2011a),
90 they are directly exposed to MPs' contamination. Recent studies suggest a positive linear
91 correlation between MPs concentration in mussels and surrounding waters (Capolupo et al., 2018,
92 Qu et al. 2018, Li et al. 2019). The filtering activity of mussels, which directly affects the resulting
93 MPs accumulation, is a complicated process that is controlled by other factors (food availability,
94 temperature, tides etc.).

95 The purpose of the present work is to study the accumulation of MPs ~~inby the~~ mussels and
96 reveal relations between ~~the~~ accumulated concentrations in mussels' soft parts and environmental
97 features. In this context, an accumulation model was developed based on Dynamic Energy Budget
98 theory (DEB, Kooijman , 2000) and applied in two different regions, in two different modes of life
99 (wild and cultivated): in the North Sea (~~Mytilus-~~ ~~e~~Edulis (M. edulis), wild) and in the Northern
100 Ionian Sea (~~Mytilus-~~ ~~g~~Galloprovincialis (M. galloprovincialis), cultivated). DEB theory provides all
101 the necessary detail to model the feeding processes and aspects of the mussel metabolism, taking
102 into account the impact of the environmental variability on the simulated individual. Apart from
103 modelling the growth of bivalves (Rosland et al., 2009, Sara et al., 2012, Thomas et al., 2011,

104 Saraiva et al., 2012, Hatzonikolakis et al., 2017, Monaco & McQuaid, 2018), DEB models have
105 been used to study other processes as well, such as bioaccumulation of PCBs (Polychlorinated
106 Biphenyls) and POPs (Persistent Organic Compounds) (Zaldivar, 2008), trace metals (Casas and
107 Bacher, 2006) and the impact of climate change on individual's physiology (Sara et al., 2014).
108 However, to our knowledge this is the first time that a DEB-based model is used to assess the
109 uptake and excretion rates of MPs in mussels.

110
111

112 2. Materials and Methods

113

114 2.1 Study areas and field data

115

116 The North Sea is a marginal large semi-enclosed sea on the continental shelf of north-west
117 Europe with a total surface area of 850,000 km² and is bounded by the coastlines of 9 countries. The
118 sea is shallow (mean depth 90 m), getting deeper towards the north (up to 725 meters) and the semi-
119 diurnal tide (tidal range 0-5 m) is the dominant feature of the region (Otto et al., 1990). Major
120 rivers, such as Rhine, Elbe, Weser, Ems and Thames discharge into the southern part of the sea
121 (Lacroix et al., 2004), making this area a productive ecosystem. In this study, the area is limited
122 along the French, Belgian and Dutch North Sea coast (N 50.98°-51.46°, W 1.75°-3.54°). This is
123 located close to harbors, where shipping, industrial and agricultural activity is high, putting
124 considerable pressure on the ecological systems of the region (Van Cauwenberghe et al., 2015).

125 The MPs concentration in mussels' tissue and seawater that were used to validate and force
126 the model respectively at its North Sea implementation were derived from Van Cauwenberghe et al.
127 (2015). Van Cauwenberghe et al. (2015) examined the presence of MPs in wild mussels (*M. edulis*),
128 and thus collected both biota and water at 6 sampling stations along the French, Belgian and Dutch
129 North Sea coast in late summer of 2011. *M. edulis* (mean shell length: 4 ± 0.5 cm and wet weight
130 (w.w.): 2 ± 0.7 g) and water samples were randomly collected on the local breakwaters, in order to
131 assess the MPs concentration in the organisms and their habitat. MPs were present in all analyzed
132 samples, both organisms and water. Seawater samples (N=12) had MPs (<1mm) on average 0.4 ±
133 0.3 particles L⁻¹ (range: 0.0 – 0.8 particles L⁻¹) and *M. edulis* contained on average 0.2 ± 0.3
134 particles g⁻¹w.w. (or 0.4 ± 0.3 particles individual⁻¹) (Van Cauwenberghe et al., 2015). The size
135 range of MPs found within the mussels was 20-90 µm (size <1 mm).

136 The Northern Ionian Sea is located in the transition zone between the Adriatic and Ionian Sea.
137 The long and complex coastline, presents a high diversity of hydrodynamic and sedimentary
138 features. Rivers discharging into the Northern Ionian Sea include Kalamas/Thyamis (Greece) and
139 Butrinto (Albania) (Skoulikidis et al., 2009), making the area suitable for aquaculture. Small
140 farming sites and shellfish grounds are operating in Thesprotia (northwestern Ionian Sea)
141 (Theodorou et al., 2011). The main source of marine litter inputs in the area originates from
142 anthropogenic activities that mainly include shoreline tourism and recreational activities, poor
143 wastewater management, agricultural practices, fisheries, aquacultures and shipping (Vlachogianni
144 et al., 2017; Digka et al., 2018a). According to Politikos et al. (2020), the area around the Corfu
145 island (Northern Ionian Sea) is characterized as a retention area of litter particles probably due to
146 the prevailing weak coastal circulation. Furthermore, a northward current on the east Ionian Sea
147 facilitates the transfer of litter particles towards the Adriatic Sea, which has been characterized as a
148 hotspot of marine litter and one of the most affected areas in the Mediterranean Sea (Pasquini et al.,
149 2016, Vlachogianni et al., 2017, Liubartseva et al., 2018, Politikos et al., 2020).

150 The field data used to validate the model output in the N. Ionian Sea were obtained from
151 Digka et al. (2018b, 2018a). In the framework of the “DeFishGear” project, mussels (*M.*
152 *galloprovincialis*) were collected by hand from a long line type mussel culture farm in Thesprotia
153 (N 39.606567° E 20.149421°), in summer 2015 (end of June/July) at a sampling depth up to 3 m
154 (Digka et al., 2018a). The average MPs accumulation was calculated from a total population of 40
155 mussels originated from the farm, with 18 of them found contaminated with MPs (46.25%). The
156 average load of MPs (size <1 mm) per mussel (mean shell length 5.0 ± 0.3 cm) was 0.9 ± 0.2
157 particles individual⁻¹ and the size of MPs found in the mussel’s tissue ranged from 55 to 620 μm .
158 Both clean and contaminated mussels were included in the calculated mean value in order to
159 represent the mean state of the contamination level for the individual inhabiting the study area.

160 The seawater concentration of MPs for the N. Ionian Sea implementation was obtained from
161 Digka et al. (2018b) and the DeFishGear project results ([http://www.defishgear.net/project/main-](http://www.defishgear.net/project/main-lines-of-activities)
162 [lines-of-activities](http://www.defishgear.net/project/main-lines-of-activities)). In total, 12 manta net tows were conducted in the region, collecting a total
163 number of $n_1=2,027$ particles on October 2014 and $n_2=1,332$ on April 2015, leading to an average
164 of 280 particles per tow with size <1 mm and >330 μm (Digka et al., 2018b). In order to estimate
165 the mean MPs concentration in the region, expressed as particles per volume, the dimensions of the
166 manta net (W 60 cm H 24 cm, rectangular frame opening, mesh size 330 μm) and the sampling
167 distance of each tow (~2 km) were used by multiplying the sample surface of the net by the trawled
168 distance in meters (Maes et al., 2017), which resulted in a mean MPs concentration of 1.17 particles
169 m^{-3} (233,333 particles km^{-2}). Moreover, in the wider region of the Adriatic Sea, Zeri et al. (2018)
170 found a mean density of $315,009 \pm 568,578$ particles km^{-2} (1.58 ± 2.84 particles m^{-3}), out of which

171 34% sized <1 mm. A relatively high value of standard deviation (one order of magnitude higher
172 than the mean value) is adopted (0.0012 ± 0.024 particles L^{-1}), considering that the mussel farm is
173 established in an enclosed gulf and close to the coast, since, according to Zeri et al. (2018), the
174 abundance of MPs is one order of magnitude higher in inshore (<4 km) compared to offshore
175 waters (>4 km). Furthermore, it may be assumed that the adopted range (standard deviation is also
176 multiplied by a factor of 2) includes also the smaller particles sized between 50 μm and < 330 μm ,
177 which have been found in mussel's tissue (Digka et al., 2018a), but were overlooked during the
178 seawater sampling due to the manta net's mesh size (> 330 μm). According to Enders et al. (2015)
179 the relative abundance of small particles (50- 300 μm) compared to particles larger than 300 μm is
180 approximately 50%.

181

182 2.2 DEB model description

183

184 In the present study, a ~~DEB~~Dynamic Energy Budget (DEB, Kooijman, 2000, 2010) model is
185 used as basis to simulate the accumulation of MPs by mussels. In DEB theory (Kooijman, 2000),
186 the energy assimilated through food by the simulated individual is stored in a reserve compartment
187 from where a fixed energy fraction κ is allocated for growth and somatic maintenance, with a
188 priority for maintenance. The remaining energy ($I - \kappa$) is spent on maturity maintenance and
189 reproduction. The individual's condition is defined by the dynamics of three state variables: energy
190 reserves E (joules), structural volume V (cm^3) and energy allocated to reproduction R (joules). The
191 energy flow through the organism is controlled by the fluctuations of the available food density and
192 temperature characterizing the surrounding environment.

193 The DEB model implemented here is an extended version of the model described in
194 Hatzonikolakis et al. (2017), where the growth of the Mediterranean mussel is simulated ~~by~~ taking
195 into account only the assimilation rate of the individual. Since the present study focuses on
196 ~~simulating~~ the MPs accumulation, it is crucial to include a detailed representation of the mussel's
197 feeding mechanism. In this context, the DEB model was extended by including the clearance (C_r),
198 filtration (\dot{p}_{XIF}) and ingestion (\dot{p}_{XII}) rates of the mussel, following Saraiva et al. (2011a), assuming
199 that all parameters referred to silt (or inedible particles) are applicable also to MPs particles with
200 MPs represented by the silt variable. In this approach, a pre-ingestive selection occurs between
201 filtration and ingestion, returning the rejected material in the water through pseudofaeces (J_{pfi}).
202 Consequently, energy is assimilated through food while the non-assimilated particles are excreted
203 through the faeces production (J_f). The model's equations, variables and parameters are shown in
204 Table 1, 2 and 3 respectively. The scaled functional response f (Eq. 5, Table 1), which regulates the

205 assimilation rate, is modified following Kooijman (2006) to include an inorganic term representing
206 the non-digestible matter i.e. microplastics: $f = X/(X + K_y)$ and $K_y = X_K \cdot (1 + Y/Y_K)$ where Y
207 and Y_k are the concentration of MPs, converted from particles L^{-1} to $g\ m^{-3}$ (Everaert et al., 2018) and
208 the half saturation coefficient of inorganic particles here represented by MPs ($g\ m^{-3}$), respectively.
209 Thus, the assimilation rate that is regulated by f is decreasing when the concentration of MPs is
210 increased. The same approach is followed by other authors who considered inedible particles in the
211 mussel's diet (Ren, 2009, Troost et al., 2010). During the filtration process the same clearance rate
212 for all particles is used ($\{\dot{C}_R\}$), representing the same searching rate for food that depends on the
213 organism maximum capacity ($\{\dot{C}_{Rm}\}$) and environmental particle concentrations (Vahl, 1972,
214 Widdows et al., 1979, Cucci et al., 1989). During the ingestion process the mussel is able to
215 selectively ingest food particles and reject inedible material, in order to increase the organic content
216 of the ingested material (Kiørboe & Møhlenberg, 1981, Jørgensen et al., 1990, Prins et al., 1991,
217 Maire et al., 2007, Ren, 2009, Saraiva et al., 2011a). This selection is reflected by the different
218 binding probabilities adopted for each type of particle (ρ_1 for algae particles and ρ_2 for inorganic
219 particles i.e. MPs, see Eq. 14 and table 3). The equations representing the feeding processes handle
220 each type of particle separately, while there is interference between the simultaneous handling of
221 different particle types (Eq. 12-14, Table 1) (Saraiva et al., 2011a). Finally, during the assimilation
222 process, suspended matter (i.e. MPs) that the mussel is not able to assimilate due to its different
223 chemical composition from the reserve compartment (Saraiva et al., 2011a) or incipient saturation
224 at high algal concentrations (Riisgard et al., 2011) results in the faeces production (Eq. 16, Table 1).
225

226 2.3 Microplastics accumulation sub-model

227
228 With the DEB model as a basis, a sub-model describing the ~~microplastics~~ (MPs) accumulation
229 by the mussel was developed, assuming that the presence of MPs in the ambient water does not
230 cause a significant adverse effect on the organisms' overall energy budget, in accordance with
231 laboratory experiments, conducted in mussel species (Van Cauwenberghe et al., 2015: *Mytilus*
232 *edulis*, Santana et al., 2018: mussel *Perna perna*). Additionally, it was assumed that the mussel
233 filtrates MPs present in the water, without the ability of selecting between the high energetic valued
234 particles and the MPs during the filtration process (Van Cauwenberghe et al., 2015, Von Moos et
235 al., 2012, Browne et al., 2008, Digka et al., 2018a among others). The uptake of MPs from the
236 environment is taken into account through the process of clearance/filtration rate, while the
237 excretion of the contaminant is derived from two processes: (i) pseudofaeces production and (ii)
238 faeces production. The resulting MPs accumulation is influenced by external environmental factors

239 (MPs concentration, food availability, temperature) and internal biological processes (clearance,
240 filtration, ingestion, growth). ~~All these are described by~~ the following differential equation
241 describes the change of the individual MPs accumulation (C , particles individual⁻¹), taking into
242 account the processes mentioned above:

243

$$\frac{dC}{dt} = C_{env} \cdot \dot{C}_R - \dot{J}_{pf2} - k_f \cdot \frac{J_f}{p_{X1I}} \cdot C \quad (\text{Eq. 18})$$

246 where \dot{C}_R is the clearance rate for water (L h⁻¹), containing a concentration of MPs C_{env} (particles L⁻¹).
247 The terms of \dot{J}_{pf2} and $\frac{J_f}{p_{X1I}}$ represent the elimination rate of MPs through pseudofaeces (particles
248 h⁻¹) and the non-dimensional rate of faeces production with respect to the ingestion rate,
249 respectively (see Table 1, Eq. 15-16). The parameter k_f represents the post-ingestive selection
250 mechanism utilized by the mussel to incorporate indigestible material (i.e. MPs) into faeces and was
251 calibrated using the available field data of mussel's MPs accumulation from both study areas (Table
252 3). Mussel is able to discriminate among particles in the gut based on size, density and chemical
253 properties of the particles (i.e. between microalgae and inorganic material) and thus to eliminate
254 them through faeces (Ward et al., 2019a and references therein). In this context, the pseudofaeces
255 production incorporates the rejected MPs prior to the ingestion, while the faeces production
256 includes MPs that are rejected along with the food particles that are not assimilated by the mussel.
257 The model's time step has been set to one hour in order to capture the dynamics of the rapidly
258 changing processes, such as feeding and excretion.

259 ~~The accumulation of MPs in the individual is represented by the state variable C (particles~~
260 ~~individual⁻¹) which is computed at every model time step. This has been set to one hour, in order to~~
261 ~~properly resolve the dynamics of the rapidly changing processes, such as feeding and excretion.~~

262 2.4 Environmental drivers

263

264 Besides MPs concentration in the seawater, the DEB model is forced by sea surface
265 temperature (SST) and food availability, ~~represented~~defined by chlorophyll-a concentrations
266 (CHL-a, an index of phytoplankton biomass). *M. edulis* has been demonstrated to filter suspended
267 particles greater than 1µm, a size class that includes all of the phytoplankton, zooplankton and
268 much of the detritus (Vahl, 1972, Mohlenberg and Riisgard, 1978, Saraiva et al., 2011a, Strohmeier
269 et al., 2012), including even aggregated picoplankton-size particles (i.e. marine snow) (Kach and
270 Ward, 2008, Ward and Kach, 2009). CHL-a has been considered the most reliable food quantifier
271 for the calculation of DEB shellfish parameters (Pouvreau et al., 2006, Sara et al., 2012,

272 Hatzonikolakis et al., 2017 and references therein). Hatzonikolakis et al. (2017) have tested the
273 performance of the model, considering also particulate organic carbon (POC) in the mussel's diet,
274 which, however, did not have an important impact on the model's skill against field data in the
275 Mediterranean Sea study areas. This outcome agrees with Troost et al. (2010) demonstration that
276 POC contributes to the mussel's diet when CHL-a concentrations are low at the southwest of
277 Netherlands. Thus, in the present study, only CHL-a is considered as the available food source for
278 mussels originated from the Southern North Sea and the Northern Ionian Sea. Thus, only CHL-a, is
279 considered as the available food source. For both study areas SST and CHL-a are derived from
280 daily satellite data, a method also used by other authors (i.e. Thomas et al., 2011, Monaco &
281 McQuaid, 2018).

282 In the North Sea, SST data were obtained from daily satellite images provided by Copernicus
283 Marine Environmental Monitoring Service (CMEMS) at 0.04 degree spatial resolution, ~~and~~ CHL-a
284 data obtained from the Globcolour daily multi-sensor product provided by CMEMS ~~Globecolour~~
285 ~~database~~ at 1 km spatial resolution, based on the OC5 algorithm of Gohin et al. (2002)
286 (<http://marine.copernicus.eu/>, generated using CMEMS Products, production center ACRI-ST). The
287 environmental forcing data (SST, CHL-a) were averaged over the study area (51.08°-51.44° N,
288 2.19°-3.45° E), covering the period 2007-2011 (5 years), in order to realistically simulate the wild
289 mussel's growth harvested ~~in at~~ late summer 2011 (Van Cauwenberghe et al., 2015). It is notable
290 that the study area of the North Sea belongs to CASE II waters (coastal region), where algorithms
291 tend to overestimate CHL-a concentrations. In optically-complex Case II waters, CHL-a cannot
292 readily be distinguished from particulate matter and/or yellow substances (dissolved organic matter)
293 and so global chlorophyll algorithms are less reliable (IOCCG, 2000). However, the CHL-a dataset
294 that was used was found in good agreement with available in situ data from ICES database
295 (<https://www.ices.dk/data/Pages/default.aspx>) for the specific study area and time period,(Fig. 1),
296 showing a relatively smaller bias and better time-space coverage, as compared with other tested
297 remote sensing datasets (not shown) (i.e. regional chlorophyll product available for the North West
298 Shelf-Seas in the CMEMS catalogue, <https://resources.marine.copernicus.eu/>).

299 In the North Ionian Sea, daily satellite SST data were also obtained from the CMEMS
300 database for the Mediterranean Sea with 0.04 degree spatial resolution, while CHL-a daily data
301 were derived from the Globcolour multi-sensor (i.e. SeaWiFS, MERIS, MODIS, VIIRS and OLCI-
302 a) merged product (<http://globcolour.info>) at 1 km spatial resolution based on the OC5 algorithm
303 suitable for coastal regions (Gohin et al., 2002)while CHL-a data were derived from the merged
304 product of many satellites (i.e. SeaWiFs, Meris, Modis, Viirs and Olei-a) provided by Globecolour
305 web interface (<http://globcolour.info>) at a daily temporal resolution and 1 km spatial resolution. The
306 forcing data were averaged over the study area (N 39.49°-39.65°, E 20.09°-20.23°) covering the

307 period 2014-2015 (2 years), when the cultured mussel is ready for the market. The chosen CHL-a
308 dataset was found preferable, as compared with other available remote sensing datasets (i.e.
309 CMEMS chlorophyll product for Mediterranean Sea), since it presented a better spatial and
310 temporal coverage (Hourany et al., 2019, Garnesson et al., 2019) and a slightly lower error, as
311 compared with the very few available in situ data in the study area (not shown). Unfortunately,
312 these were very scarce and therefore an extended comparison between remote and in situ data could
313 not be conducted. The satellite derived CHL-a data were estimated based on the OC5 algorithm of
314 Gohin et al. (2002) in both study areas, which is regarded as suitable for coastal waters. Satellite
315 data have facilitated large scale ecological studies by providing maps of phytoplankton functional
316 types and sea surface temperature (Raitsos et al., 2005, 2008, 2012, 2014, Palacz et al., 2013, Di
317 Cicco et al., 2017, Brewin et al., 2017). The daily environmental forcing data are shown in Fig. 1
318 and Fig. 2 for the North Sea and the N. Ionian Sea, respectively. The two coastal environments
319 present some important differences regarding both CHL-a and SST. Specifically, in the N. Ionian
320 Sea, CHL-a is relatively low (annual mean $\sim 0.88 \text{ mg-chl-a m}^{-3}$) and peaks during winter (maximum
321 $\sim 2.64 \text{ mg-chl-a m}^{-3}$ at December 2014), while in the North Sea CHL-a is about four times higher
322 (annual mean $4.25 \text{ mg-chl-a m}^{-3}$), peaking in April every year (maximum range $29.44\text{-}33.38 \text{ mg-chl-}$
323 a m^{-3}), as soon as light availability reaches a critical level (Van Beusekom et al., 2009). The higher
324 productivity during spring season in the North Sea is related with the nutrient inputs from the
325 English Channel, the North Atlantic and particularly the river discharge of nutrient-rich waters
326 along the Belgian-French-Dutch coastline, ~~which that~~ peaks earlier, during winter period (Van
327 Beusekom et al., 2009). The SSTsea surface temperature peaks during August in both areas (Fig. 1
328 and Fig. 2), but is significantly higher in the N. Ionian Sea (maximum 28.8°C), as compared to the
329 North Sea (maximum $18\text{-}19.3^{\circ}\text{C}$).

330 The environmental concentration of MPs, C_{env} (particles L^{-1}) was obtained also at a daily time
331 step as randomly generated values of the Gaussian distribution that is determined by the mean value
332 and standard deviation of the observed field data (0.4 ± 0.3 particles L^{-1} , North Sea, Van
333 Cauwenberghe et al., 2015, 0.0012 ± 0.024 particles L^{-1} , N. Ionian Sea, Digka et al., 2018a).
334 Considering that these values originate from surface waters and that mussels live in the near surface
335 layer (0-5 m), C_{env} is estimated as a mean value of the upper layer with the methods described by
336 Kooi et al. (2016), who studied the vertical distribution of MPs, considering an exponential
337 decrease with depth. Specifically, in the N. Ionian Sea, mussels were collected from a depth up to 3
338 m (Digka et al., 2018a), while in the North Sea (Van Cauwenberghe et al., 2015), there is no
339 information and thus a maximum depth of 5 m is adopted.

340 In the North Sea simulation, the effect of tides is taken into account by considering that the
341 mussel originated from the intertidal zone, is submerged 12 hours during the day (Van

342 Cauwenberghe et al., 2015). In the N. Ionian Sea simulation, tides are not considered, given the
343 very small tide amplitude (few centimeters) in the Mediterranean (i.e. Sara et al., 2011;
344 Hatzonikolakis et al., 2017) and thus the cultured mussel is assumed permanently submerged. *In*
345 *situ* hourly tide data (2007-2011) from the coastal zone of the region (Dunkerque station N
346 51.04820°, E 2.36650°) obtained from Coriolis and Copernicus data provider
347 (<http://marine.copernicus.eu>, <http://www.coriolis.eu.org>), showed that mussels experience
348 alternating periods of aerial exposure and submergence at approximately every 6 hours (2 high and
349 2 low tides). During aerial exposure the model suspends the feeding processes (Sara et al., 2011)
350 and simulates metabolic depression (Monaco & McQuaid, 2018) where, the Arrhenius thermal
351 sensitivity equation (Eq. 9) is corrected by a metabolic depression constant ($M_d = 0.15$), a value
352 representative for *M. galloprovincialis* and here applied also for *M. edulis*. In the present study, the
353 mussel's body temperature change during low tide is ignored, inducing a model error. The mussel's
354 body temperature (i.e. surrounding water temperature for submerged mussels) during air exposure
355 depends on many factors, such as solar radiation, air's temperature, wind speed and wave height,
356 according to studies investigating the temperature effect on intertidal mussels (Kearney et al., 2010,
357 Sara et al., 2011). However, the present study aims to primarily examine the MPs accumulation and
358 thus the intertidal mussel's body temperature was not thoroughly examined. Nonetheless, the time
359 that the mussel is able to filter, ingest and excrete the suspended matter (i.e. food and MPs particles)
360 and the effect on the mussel's growth through the modified relation of $k(T)$ are included, since the
361 assimilation process occurs whether the mussel is submerged or not (Kearney et al., 2010).

362 2.5 Parameter values

363

364 Most of the DEB model parameters were obtained from Van der Veer et al. (2006) and are
365 referred to the blue mussel *M. ~~edulis~~ edulis* in the northeast Atlantic (see Table 3 for the exceptions).
366 This assumption has also been adopted in previous studies which showed that this parameter set for
367 *M. edulis* applies also for *M. galloprovincialis* (i.e. Casas and Bacher, 2006, Hatzonikolakis et al.,
368 2017). The half saturation coefficient X_k represents the density of food at which the food uptake rate
369 reaches half of its maximum value and should be treated as a site – specific parameter (Troost et al.,
370 2010, Pouvreau et al., 2006). In order to estimate the value of X_k , a different approach was followed
371 for each study area.

372 For the North Sea simulation, X_k was tuned so that the simulated individual has the recorded
373 size at the corresponding estimated age (Van Cauwenberghe et al., 2015) growing with the
374 representative growth rates of wild *M. edulis* at the region (Saraiva et al., 2012, Sukhotin et al.,
375 2007). For the N. Ionian Sea simulation, an alternative method was adopted, aiming to generalize

376 the DEB model to overcome the problem of site-specific parameterization. The DEB model was
377 tuned against literature field data for cultured mussels originated from different areas in the
378 Mediterranean and Black Seas, where the average CHL-a concentration ranged between 1.0 and 5.0
379 ~~mg chl-amg~~ m^{-3} , and one X_k value was found for each area. The four areas used, their characteristics
380 and the corresponding value of X_k adopted, are shown in Table 4. These values of X_k are related to
381 the prevailing CHL-a concentration of each area ([CHL-a]) through three different functions:
382 linear: $f(x) = a * [CHL - a] + b$ exponential: $f(x) = a * \exp(b * [CHL - a])$ and power: $f(x) =$
383 $a * [CHL - a]^b + c$. The curve fitting app of Matlab (Matlab R2015a) was used for the
384 determination of a, b and c of each function taking into account the 95% confidence level. The
385 score of each function regarding the somatic/mussel growth simulation in all four regions is tested
386 through target diagrams (Jolliff et al., 2009) by computing the bias and unbiased root-mean-square-
387 deviation (RMSD) between field and simulated data of all 4 regions and the function with the best
388 score is adopted. A similar approach was followed by Alunno-Bruscia et al. (2011) for the oyster
389 *Crassostrea gigas* in six Atlantic ecosystems who expressed the X_k as a linear function of food
390 density (e.g. phytoplankton). Unfortunately, the approach described for the N. Ionian Sea
391 simulation could not be applied in the North Sea, as the limited amount of growth data from the
392 literature for wild *M. edulis* in similar environments did not permit a statistically significant fit of a
393 similar function ($X_k = f(chl - a)$).

394

395 **2.6 Simulation of reproduction-Initialization of the model**

396

397 The reproductive buffer (R) is assumed to be completely emptied at spawning ($R = 0$)
398 (Sprung, 1983, Van Haren et al., 1994). In order to simulate mussel's spawning, the gonado-somatic
399 index (GSI) defined as gonad dry mass over total dry flesh mass was computed at every model's
400 time step (Eq. 17 Table 1; the water content of the fresh tissue mass was assumed 80% according to
401 Thomas et al. (2011)). Spawning was induced by a critical value of GSI (GSI_{th} , Table 3) and a
402 minimum temperature threshold (T_{th}) at each study area, obtained from the literature. In the North
403 Sea implementation, T_{th} was set at 9.6 °C (Saraiva et al., 2012), while in the N. Ionian Sea, at 15 °C
404 (Honkoop and Van der Meer, 1998). This kind of formulation for the spawning event in bivalves
405 has been used in previous studies (i.e. Pouvreau et al., 2006, Troost et al., 2010, Thomas et al.,
406 2011, Monaco & McQuaid, 2018). The simulated abrupt losses of the mussel's tissue mass
407 correspond to spawning events and the model's prediction was compared with the available
408 literature data regarding the spawning period in each study area. Theodorou et al. (2011)
409 demonstrated that the spawning events occur during winter for *M. galloprovincialis* in the mussel

410 farms of Greece, while in the North Sea the spawning period for *M. edulis* is extended from the end
411 of April until the end of June (Sprung, 1983, Cardoso et al., 2007).

412 In both areas, the model was initialized so that the simulated individual is in the juvenile phase
413 ($V < V_p$; Table 3) and the reproductive buffer can be considered to be empty ($R = 0$) (Thomas et al.,
414 2011). As stated by Jacobs et al. (2015) amongst others, juvenile mussels (*M. edulis*) range between
415 1.5-25 mm in size. Specifically, in the North Sea the settlement of mussel larvae (*M. edulis*) takes
416 place in June and the juveniles grow to a maximum size of 25 mm within 4 months (Jacobs et al.,
417 2014). In the N. Ionian Sea, the operating mussel farms follow the life cycle of *M.*
418 *galloprovincialis*, starting the operational cycle each year by dropping seed collectors from late
419 November until March and the juvenile mussels grow up to 6-6.5cm after approximately one year
420 according to the information obtained from the local farms in the region and Theodorou et al.
421 (2011). The initial fresh tissue mass was distributed between the structural volume (V) and reserves
422 energy (E). Energy allocated to those two compartments was firstly constrained by the initial length
423 (L) and then energy allocated to V was in Eq.10 (Table 1). The initial value of E was set so that the
424 simulated individual has an initial weight that corresponds to the juvenile phase ($V < V_p$) (Table 5).
425 Finally, for both model implementations, the initial accumulation of MPs in the mussel's tissue (C)
426 was set to zero.

427

428 **2.7 Simulation Runs**

429 The DEB-accumulation model simulates at an hourly basis the growth and MPs accumulation
430 of the wild mussel from the North Sea and the cultured mussel from the N. Ionian Sea. Initially, a
431 model run is performed at each study area during the periods July 2007 to August 2011 (4 years) for
432 the North Sea simulation and late November 2014 to January 2016 (~ 1 year) for the N. Ionian Sea
433 simulation. Additionally, the inverse simulations were performed in order to evaluate the depuration
434 phase of both cultured and wild mussel, by setting the environmental MPs concentration equal to
435 zero ($C_{env}=0$), after a period of 1 year simulation at the N. Ionian Sea, when the cultured mussel has
436 the appropriate size for market, and after 4 years at the North Sea, when literature field data are
437 available (Van Cauwenberghe et al., 2015). In this simulation, the mussel's gut clearance is
438 achieved by the excretion of MPs through faeces (3rd term of Eq. 18), and thus it is necessary to
439 maintain the existence of food in the mussel's environment in order to ensure that the feeding-
440 excretion processes will occur.

441 Furthermore, to examine the model's uncertainty related to the environmental MPs
442 concentration, a series of 15 and 13 simulations were performed in the North Sea and N. Ionian Sea

443 respectively, adopting different constant values of C_{env} within the observed range of each area.
444 Finally, the effect of the environmental forcing data and some model's parameters on the resulting
445 MPs accumulation by both mussels was explored through sensitivity experiments. These were
446 used to derive a new function that predicts the level of MPs pollution in the environment.

447

448 2.8 Sensitivity tests and Regression analysis

449 The effect of the environmental data (CHL-a, temperature, C_{env}) and two parameters
450 representative of mussel's growth (X_k , Y_k) on the MPs accumulation by the mussel for each study
451 area was examined through sensitivity experiments with the DEB-accumulation model. Each
452 variable (CHL-a, T, C_{env}) and parameter (X_k , Y_k) was perturbed by $\pm 10\%$ to examine their effect on
453 the simulated MPs accumulation, and the results of each run were analyzed using the sensitivity
454 index (SI), SI which calculates the percentage change of the mussel's MPs accumulation $SI =$
455 $\frac{1}{n} \sum_{t=1}^n \frac{|C_t^1 - C_t^0|}{C_t^0} \cdot 100$ (%), where n is the simulated time steps, C_t^0 is the MPs accumulation predicted
456 with the standard simulation at time t and C_t^1 is the MPs accumulation with a perturbed
457 variable/parameter at time t ; for details see Bacher and Gangnery, (2006). The same method has
458 been also applied to other studies, which examined the model's sensitivity on specific
459 variables/parameters regarding the mussel growth (Casas and Bacher, 2006, Rosland et al., 2009,
460 Béjaoui-Omri et al., 2014, Hatzonikolakis et al., 2017). In order to also examine the effect of tides,
461 in the North Sea implementation, the sensitivity experiments were conducted twice: the first time
462 assuming that the mussel is permanently submerged and the second time assuming that the mussel
463 is periodically exposed to the air.

464 Preliminary sensitivity experiments showed that the MPs accumulation is highly depended on
465 the prevailing conditions regarding the CHL-a, temperature and C_{env} and the mussel's growth that is
466 regulated by the half saturation coefficient (X_k). Therefore an attempt was made using the model's
467 output to describe the MPs accumulation as a function of these variables through a custom
468 regression model:

$$469 \quad y = b_1 * W + b_2 * \exp\left(\frac{1}{T}\right) + b_3 * \frac{1}{[CHL-a]} + b_4 * C_{env} \quad (\text{Eq. 19})$$

470 where y (particles/individual) is the response variable and represent the predicted MPs
471 accumulation by the mussel; W (g) the mussel's fresh tissue mass, T (K) the sea surface
472 temperature, CHL-a and C_{env} are the concentrations of chlorophyll-a and MPs in the water
473 respectively, which are the predictor variables. The values of coefficients b_1 , b_2 , b_3 , and b_4 are

474 calculated using the nonlinear regression function (nlinfit, Matlab R2015a) which attempts to find
475 values of the parameters b that minimize the least squared differences between the model's MPs
476 accumulation output C and the predictions of the regression model $y = f(W, T, [chl\ a], C_{env}, b)$.

477 The ultimate aim of this analysis, once coefficients are determined, is to use [Eq. equation 19](#) to
478 obtain the environmental MPs concentration:

$$C_{env} = \frac{1}{b_4} * \left(C - b_1 * W - b_2 * \exp\left(\frac{1}{T}\right) - b_3 * \frac{1}{[CHL-a]} \right)$$

480 (Eq. 20)

481 which could be a very useful tool to predict the MPs concentration in the environment, when all
482 involved variables are known (~~mussel size~~, mussel's accumulated MPs (C), wet weight (W)
483 temperature (T) and CHL-a), using the mussel as a potential bioindicator (Li et al., 2016, Li et al.,
484 2019). The score of this custom model was tested by applying Eq. 20 in our study areas and 6 more
485 areas around the U.K., where information of mussel's wet weight and both mussels' and
486 environment's MPs load is available (Li et al., 2018). CHL-a and temperature, which were not
487 included in Li et al. (2018), were obtained from daily satellite images (same source as in the North
488 Sea, see 2.4 section), covering the period that the mussels were harvested (Li et al., 2018).

489

490 **3. Results**

491

492 **3.1 Growth simulations**

493

494 The growth simulations of *M. edulis* and *M. galloprovincialis* for the North Sea and the N.
495 Ionian Sea are shown in Fig. [34](#) and Fig. [45](#) respectively. In the North Sea implementation, X_k was
496 tuned to a constant value: $X_k = 8 \text{ mg chl-a m}^{-3}$ ($\pm 1.5 \text{ mg m}^{-3}$). The fitted value was slightly higher, as
497 compared to the one ($X_k = 3.88 \text{ mg m}^{-3} \text{ } \mu\text{g chl-a l}^{-1}$) used by Casas and Bacher (2006) in productive
498 areas of the French Mediterranean shoreline (average CHL-a concentration $1.45 \text{ mg m}^{-3} \text{ } \mu\text{g chl-a l}^{-1}$
499 maximum peak at $20 \text{ mg m}^{-3} \text{ } \mu\text{g chl-a l}^{-1}$), as a consequence of given the ~~even~~ higher productivity in
500 the North Sea (average CHL-a concentration $4.25 \text{ mg m}^{-3} \text{ } \mu\text{g chl-a l}^{-1}$; maximum peak at $\sim 33.40 \text{ mg}$
501 $\text{m}^{-3} \text{ } \mu\text{g chl-a l}^{-1}$). The high value of X_k -could also be explained by the presence of silt and other
502 inedible particles (i.e. MPs) which led result to lower quality food in the mussel's diet compared
503 with an assumed "clean of inedible particles" site environment (Kooijman, 2006, Ren, 2009). In the
504 present study the inedible particles (i.e. MPs) have been incorporated in the mussel's diet through

505 the modified relation of the functional response f (Eq. 5, Table 1), which regulates the assimilation
506 rate and thus the mussel's growth. However, the DEB model applied at the French site, did not
507 account inedible particles in the mussel's food. Furthermore, it has been reported that wild mussels
508 grow considerably slower than farmed mussels (~1.7 times) (Sukhotin and Kulakowski, 1992) and
509 thus, a higher value of X_k promotes a lower mussel growth, which is the case of the North Sea
510 mussel. The simulated mussel shell length after 4 years, in August, is 4.35 cm and the fresh tissue
511 mass is 1.87 gr, in agreement with Van Cauwenberghe et al. (2015) and other studies conducted on
512 wild mussels (Sukhotin et al., 2007, Saraiva et al., 2012, MarLIN, 2016). In particular, Saraiva et al.
513 (2012) found that after 16 years of simulation, the wild mussel of the Wadden Sea (North Sea) is 7
514 cm long, while according to Bayne and Worrall (1980) a mussel with shell length 4 cm corresponds
515 to the age of 4 years, in agreement with the current study. The simulated growth presents a strong
516 seasonal pattern, being higher during spring and summer season, as compared to autumn and
517 winter, which is consistent with the seasonal cycle of temperature and CHL-a concentration, for a
518 typical year in the region (Fig. 1). The increase of food availability and temperature during spring
519 (April) results in high mussel growth for a 4-month period, while the decrease of CHL-a from
520 summer until the end of the year, in conjunction with the temperature decrease in autumn, result in
521 a lower mussel growth. Spawning events that occurred each year in late~~between the end of~~ April-
522 early and beginning of May (30 April-2 May) each year, are responsible for the sharp decline in
523 mussel's fresh tissue mass, shown in Fig. 4 (Handa et al., 2011; Zaldivar, 2008) and in agreement
524 with the literature (Sprung, 1983, Cardoso et al., 2007, Saraiva et al., 2012). The predicted weight
525 loss due to spawning was around 7% at the first year of simulation, while the second, third and
526 fourth year the percentage of weight loss increased gradually to 8.3%, 12.6% and 14.4%
527 respectively. Bayne and Worrall (1980) demonstrated that the weight losses on spawning for
528 individuals of 1 g weight vary between 2.1% and 39.8%, presenting a weight-specific increase with
529 size.

530 In the N. Ionian Sea implementation, X_k is applied as a function of CHL-a concentration
531 through the method described in section 2.5. The target diagram showing the performance of each
532 tested function (linear: $f(x) = a * [CHL - a] + b$, where $a = 0.959$ and $b = -1.420$; exponential:
533 $f(x) = a * \exp(b * [CHL - a])$ where $a = 0.2$ and $b = 0.567$; power: $f(x) = a * [CHL - a]^b +$
534 c where $a = 0.01$, $b = 3.529$ and $c = 0.480$) is shown in ~~Figure~~ Figure 53. The linear and power
535 function of X_k present a good skill, with the power function leading to the most successful
536 simulation of the cultured mussel's growth in all four areas (diagram marks for mussel length and
537 fresh tissue mass are closer to the target's center). The power function applied in the N. Ionian Sea,
538 resulted in mussel's shell length 5.8 cm and fresh tissue mass 5.92 gr after one year simulation, in

539 agreement with Theodorou et al. (2011). The spawning event occurred at the beginning of
540 December (Theodorou et al., 2011) and was illustrated by a 12.6% tissue mass decline.
541

542 **3.2 Microplastics accumulation and depuration phase**

543
544 The hourly simulated MPs accumulation by the mussel in the North Sea and N. Ionian Sea are
545 shown in Fig. 6 and Fig. 7 respectively. Calibration of the parameter k_f (1.2 d^{-1}) led to a model
546 which was well fitted to the observed MPs accumulation in the mussel of both study areas. In the
547 North Sea, a 4-year-old wild mussel ($L=4.35 \text{ cm}$, $W=1.87 \text{ g}$) contains 0.5364 particles individual⁻¹
548 in August within the range value found by Van Cauwenberghe et al. (2015) (0.4 ± 0.3 particles
549 individual⁻¹), although the model overestimated the data range reproducing a seasonal increase that
550 was not observed. This is most likely due to the fact ~~It is worth noting~~ that Van Cauwenberghe et al.
551 (2015) allowed a 24 h clearance period, before analyzing the mussels' tissue for MPs, ~~possibly~~
552 resulting in slightly lower MPs accumulation than the model's prediction. The MPs egested through
553 faeces by the 4 year old mussel after 24 h were 0.2 ± 0.2 particles individual⁻¹ (Van Cauwenberghe
554 et al., 2015), which agree also with model's output (0.3 particles individual⁻¹, Fig. 8) regarding the
555 depuration phase and could compensate for the observed difference in mussel's MPs load between
556 the simulated and field data. In the N. Ionian Sea, the simulated MPs accumulation by the cultured
557 mussel with $L = 4.858 \text{ cm}$ and $W = 3.343 \text{ g}$ was 0.91 particles individual⁻¹ in the end of JuneJuly, in
558 agreement with field observations obtained from Digka et al. (2018a) (0.9 ± 0.2 particles individual⁻¹
559 ¹). Overall, the developed model simulated the MPs accumulation by both mussels in the two
560 different areas, using the same parameter set (see Table 3 for the exceptions), under the assumption
561 that parameters referred to silt particles (i.e. inedible particles) may be used to describe also the
562 MPs accumulation. Both simulations were in good agreement with the available field data, with a
563 small deviation for the North Sea.~~In both regions, the model computed MPs accumulation,~~
564 ~~assuming that the mussel treats MPs as silt particles (i.e. inedible particles) and is in agreement with~~
565 ~~the available field data.~~ -This may lead to the assumptions ~~suggests~~ that mussels ~~probably~~ present a
566 common behavior against all inedible particles. In model's results, based on the uptake and
567 excretion rates of MPs by the mussels in both study areas, the majority of MPs are rejected through
568 pseudofaeces and fewer through faeces production (not shown). This is in agreement with Woods et
569 al. (2018) who found that most microplastic fibers (71%) were quickly rejected as pseudofaeces and
570 $< 1\%$ excreted in faeces.

571 The small-scale (daily) fluctuations of MPs in the mussel (wild and cultivated) reflect the
572 adopted random variability of the environmental MPs concentration C_{env} and the daily fluctuations

573 | of the environmental forcing (CHL-a, temperature). The large-scale (seasonal) variability follows
574 | mainly the variability of the clearance rate. The seasonal variability of the CHL-a concentration and
575 | temperature greatly determines the variability of the clearance rate and hence the variability of MPs
576 | in the individual. Moreover, the model predicts that mussel's energy needs are increased as it grows
577 | and therefore the clearance rate is increased, resulting in higher MPs accumulation.

578 | The simulated time needed to clean the mussel's gut from the MPs load for both areas is
579 | shown in Fig. 8. In both areas, the cleaning follows an exponential decay, in agreement with
580 | laboratory experiments by Woods et al. (2018). In particular, the model predicts a 90% mussel's
581 | cleaning after 284330 hours (~124 days) and 5663 hours (~2.53 days) for the N. Ionian Sea and
582 | North Sea respectively. The cleaning process is more rapid in the North Sea simulation, which can
583 | be attributed to the higher CHL-a concentration found in this area, leading to increased production
584 | of faeces by the mussel and hence faster excretion of the accumulated MPs. In the N. Ionian Sea, on
585 | the other hand, the rate of the mussel's cleaning is slower, due to the limited food availability.

586

587 | **3.3 Model's uncertainty regarding the environmental microplastics concentration**

588

589 | The MPs concentration in the environment presents a strong variability in both temporal and
590 | spatial scales. To examine the model's uncertainty related to the environmental MPs concentration
591 | (C_{env}), a series of 15 and 13 simulations were performed in the North Sea and N. Ionian Sea
592 | respectively, adopting different values of C_{env} within the observed range of each area. In the North
593 | Sea, the adopted C_{env} ranged between 0.1 and 0.8 particles L^{-1} with a step of 0.05 (15 runs), while in
594 | the N. Ionian Sea C_{env} ranged between 0.0012 and 0.0252 particles L^{-1} with a step of 0.002 (13
595 | runs). -The mean seasonal values and standard deviation of the 15 simulations in the North Sea and
596 | the mean monthly values and standard deviation of the 13 simulations in the N. Ionian Sea were
597 | computed and plotted in Fig. 9 and Fig. 10, respectively. Each error bar represents the uncertainty
598 | of the simulated accumulation at the specific time, related to the environmental MPs concentration.

599 | In both case studies, the uncertainty of the model appears to increase as the MPs accumulation
600 | is increased. -As the mussel grows in the North Sea, the mean value and standard deviation of MPs
601 | accumulation is increased during the same season every year, illustrating the effect of the mussel's
602 | weight. Moreover, the seasonal variability of the MPs accumulation appears to be related
603 | withshould be caused by the seasonality of CHL-a concentration. This is apparent during each
604 | year's spring: when CHL-a concentration peaks at its maximum value (~30 $mg\ m^{-3}$; see Fig. 1), the
605 | filtration rate is decreased (Riisgard et al., 2003, 2011), leading to lower MPs accumulation by the
606 | mussel and thus lower model's uncertainty. In the N. Ionian Sea, the effect of the mussel's weight is

607 more apparent in the early months (~ 6 months), resulting on higher MPs accumulation and model
608 uncertainty as the mussel grows. Afterwards, the seasonality of both CHL-a concentration and
609 temperature plays the major role. During summer, when the CHL-a concentration is progressively
610 decreased, reaching minimum values (~0.7 mg /m³) and temperature is increased (>20° C), the
611 filtration rate is significantly decreased or stopped, resulting in lower MPs accumulation and lower
612 model's uncertainty. This is in line with studies reporting that the mussel suspends the filtering
613 activity and thus closes its valves until better conditions occur (Pascoe et al., 2009, Rissgard et al.,
614 2011). Overall, the available field data lie within the model's uncertainty, apart from the North Sea
615 case, where the range of field data variability and model uncertainty dot not overlap significantly at
616 the time of the observations for both study areas.

617 Moreover, to evaluate the scenario adopted with the set-up of the previous experiments
618 (random C_{env} at a daily time step) 3 additional model runs are performed in each study area,
619 adopting each time different stochastic sequences of daily random C_{env} values within the observed
620 range, which is considered to reflect the high spatial and temporal variability of the environmental
621 MPs concentration. The mean value and standard deviation of these “stochastic” runs lie most of the
622 time within the standard deviation of the overall model's uncertainty in both case study areas (Fig. 9
623 and Fig. 10).

624

625 **3.4 Sensitivity and Regression analysis results**

626

627 The results of the sensitivity experiments regarding the MPs accumulation by the mussels are
628 shown in Fig. 11 and 12 for the North Sea and N. Ionian Sea respectively. The comparison between
629 the intertidal and subtidal mussel of the North Sea revealed that both +10% and -10% perturbation
630 of CHL-a and X_k have a slightly lower effect on the MPs accumulation by the intertidal mussel
631 which is probably attributed to the intermittent feeding periods experienced by the individual due to
632 the tide effect. As far as the temperature effect, both +10% and -10% perturbed value led to higher
633 sensitivity on the MPs accumulation by the intertidal mussel, due to the adopted modified
634 temperature relation during low tide. Especially, if the mussel's body temperature change during air
635 exposure would be considered, the perturbed temperature will probably affect even more the MPs
636 accumulation on the intertidal than the subtidal mussel. The sensitivityeffect of the C_{env} is slightly
637 higher and lower on the MPs accumulation by the intertidal mussel when perturbed either +10%
638 orand -10% is almost the same for the intertidal and subtidal mussel, respectively, however the
639 difference of the sensitivity index (%) between the two mussels (intertidal vs. subtidal) is small,

640 indicating that the environmental MPs concentration affects similarly both mussels, regardless the
641 continuous or intermittent feeding-excretion process.

642 The comparison between the mussel sensitivity indexes in the N. Ionian and the North Sea
643 (in conditions of submergence) study areas reveals some important differences. Generally, most of
644 the perturbed (either +10% or -10%) variables and parameters (i.e. CHL-a, temperature, X_k) present
645 higher sensitivity on the MPs accumulation by the mussel from the N. Ionian Sea. This is attributed
646 to the prevailing environmental conditions and specifically the lower food availability (CHL-a) and
647 the higher temperature range in the N. Ionian Sea compared to the North Sea, which greatly
648 determine the feeding processes, the mussel's growth and hence the MPs accumulation. The
649 perturbed C_{env} in both study areas appears to affect similarly the MPs accumulation on both mussels
650 (\sim 10%), with the small difference (<2%) probably attributed to the higher abundance of seawater's
651 MPs present in the North Sea compared to the N. Ionian Sea. Finally, the half saturation coefficient
652 for the inorganic particles (Y_k) has no effect on the MPs accumulation of both North Sea and N.
653 Ionian Sea mussels, indicating that the amount of inedible particles (i.e. MPs) is relatively low in
654 both areas and thus the Y_k does not affect the way that the organic particles are being ingested
655 (Kooijman, 2006). According to Ren (2009), when the inorganic matter is low, the $K(y)$ (Eq. 5;
656 Table 1) is approximately equal to X_k and then Y_k is the least sensitive parameter for the ingestion
657 rate and thus growth.

658 The DEB-accumulation model output was used to determine the coefficients in Eq. 19 by the
659 nonlinear regression analysis: $b_1 = 0.1909 (\pm 0.0006)$, $b_2 = 0.0412 (\pm 0.0019)$, $b_3 = 0.1315 (\pm$
660 $0.0021)$ and $b_4 = 1.1060 (\pm 0.0253)$. The accurate estimation of the confidence intervals for the
661 estimated coefficients (b_1, b_2, b_3, b_4) is indicated by the low confidence intervals, while the mean
662 squared error of the regression model appears also sufficiently small~~are small enough which~~
663 ~~indicates an accurate estimation of them and the mean squared error of the regression model is~~
664 ~~small enough~~ (MSE=0.0523). Subsequently, as shown in Figure 13, Eq. ~~uation~~ 20 may be used to
665 predict the MPs concentration of the environment where mussels live. ~~, being~~ In most cases, the
666 predicted MPs concentration is found within the standard deviation of the field data. Two
667 exceptions are shown in Hastings-A and Plymouth areas. The reasons behind these discrepancies
668 may be related to the environmental conditions prevailing in each area at the sampling time. For
669 example, Eq. 20 does not take into account the impact of tides that may affected the mussel's MPs
670 load (C) and the lack of information on the exact sampling date led to using a mean SST and CHL-a
671 value representative of the given sampling time period (Li et al., 2018). Although, Eq. 20 does not
672 account for the tide effect, however, the sensitivity analysis (Fig. 11) showed that the effect of C_{env}
673 on the mussel's MPs accumulation was the same for both intertidal and subtidal mussel in the North
674 Sea. This result may also apply at the two exceptions areas, leading to the assumption that the

675 discrepancies are due to the lack of the ambient temperature and CHL-a information during the
676 sampling date. In any case However, this is just a first rough demonstration of the method and
677 should be implemented in more environments in order to be further validated.

678
679

680 4. Discussion

681

682 A DEB-accumulation model was developed and validated with ~~the only available~~ data
683 available from the North Sea and the N. Ionian Sea, to study the MPs accumulation by wild *M.*
684 *edulis* and cultured *M. galloprovincialis*, ~~as they~~ grown in different, representative environments.
685 Although the study is limited by scarce validation data, it should be noted the MPs accumulation
686 model parameter set, except one tuning parameter (k_f), was extracted from the literature (Table 3),
687 assuming it is notable that the accumulation submodel's parameters are extracted from literature
688 (Table 3) illustrating that mussels adopt a common defensive mechanism against inedible particles
689 (i.e. silt, MPs). Thus, the theoretical background constructed by Saraiva et al., (2011a) (based on
690 Kooijman, 2010) regarding the feeding and excretion processes of the mussel remains unspoiled.
691 Through the strong theoretical background of DEB theory, this study highlights that the
692 accumulation of MPs by the mussel is highly depended on the prevailing environmental conditions
693 which control the amount of MPs that the mussel filtrates and excretes.

694 Towards a generic DEB model Beginning with the generalization of the DEB model
695 regarding the site specific parameter X_k in the N. Ionian Sea simulation, the applied function of the
696 half saturation coefficient ($f(x) = a * [CHL - a]^b + c$) successfully captures the physiological
697 responses and thus the growth rate of the cultured mussel at the N. Ionian Sea implementation. In
698 the current study, ~~a demonstration of this method~~ ledis conducted leading to a robust and generic
699 DEB growth model able to simulate ~~robust enough with a sufficiently generic nature for the~~
700 ~~simulation of~~ the mussel growth in representative mussel habitats of the Mediterranean Sea,
701 covering a range of productivity and sea surface temperature. This approach supports and takes a
702 step further of Bourles et al. (2008) suggestion about a suggested for oyster growth (*Crassostrea*
703 *gigas*) that a seasonally varied half saturation coefficient, demonstrating an improvement could
704 improve the accuracy of the food quantifier. The applied function of X_k considers the daily CHL-a
705 fluctuations, and thus the seasonal variation of the seawater composition. ~~because seawater~~
706 ~~composition is closely related to the season.~~ As more field data becomes available from various
707 environments, the applied ~~such an~~ approach could result to more generic formulations for the site-

708 specific parameter X_k , so that the model could be applied in several areas of interest, where field
709 growth data are absent and/or to simulate the potential mussel growth in the 2D space.

710 The simulation of MPs accumulation by the mussels, using the DEB-accumulation model, is
711 in good agreement with the available field data (Fig. 3 and Fig. 4). The simulated values lie within
712 the observed field data range (mean \pm SD), although the seasonal increase reproduced by the model
713 at the North Sea implementation did not exactly overlap with the field data at the time of
714 observations. This could be attributed to the clearance period (24 h) that allowed mussels to excrete
715 MPs through faeces (0.2 ± 0.2 particles individual⁻¹) before the mussel's tissue analysis (Van
716 Cauwenberghe et al., 2015). The measured loss of mussel's MPs is in agreement with the model's
717 result on the depuration experiment after 24 h. The MPs accumulation by the cultivated mussel
718 (fresh tissue mass 3.3342 g) originated from the N. Ionian Sea with mean $C_{env} = 0.0012 \pm 0.024$
719 particles L⁻¹, is 0.91 particles individual⁻¹ and by the wild mussel (fresh tissue mass 1.87 g) from the
720 North Sea with mean $C_{env} = 0.4 \pm 0.3$ particles L⁻¹ is 0.5364 particles individual⁻¹. If these
721 concentrations are expressed per gram of wet tissue of mussels, the cultivated mussel contamination
722 (0.27 particles g⁻¹w.w.) is comparable with the wild mussel (0.2834 particles g⁻¹w.w.), despite the
723 much lower environmental MPs concentration (C_{env}) in the N. Ionian Sea than the North Sea. This
724 comparison aims to highlight the significant impact of the prevailing environmental conditions
725 (CHL-a and temperature) on the MPs accumulation by the mussels, although they originate from
726 different areas and lived different time period. The generally high abundance of CHL-a in the North
727 Sea simulation, contributes to a reduction of the filtering activity and hence of the MPs
728 accumulation. The threshold algal concentration for reduction of the mussel's filtration rate
729 (incipient saturation) has been found to lie between 6.3 and 10.0 $\text{mg m}^{-3} \mu\text{g chl-a L}^{-1}$ (Riisgard et al.,
730 2011), which is a range comparable to the CHL-a concentrations in the North Sea ~~case~~.
731 ~~Furthermore, in the N. Ionian Sea simulation, the filtration, ingestion, pseudofaeces and faeces~~
732 ~~production rates are decreased during the summer season when the CHL-a and temperature has~~
733 ~~downward and upward trend respectively, gradually leading to a decline of the mussel's MPs~~
734 ~~accumulation.~~ Van Cauwenberghe and Janssen (2014) found that cultivated *M. edulis* from the
735 North Sea contained on average 0.36 ± 0.07 particles g⁻¹w.w., a slightly higher similar value with
736 that found in the present study for the wild mussel of the North Sea (0.2834 particles g⁻¹w.w.). This
737 could be attributed to mussel farms acting as a potential source of MPs contamination for the
738 mussels due to plastic materials (i.e. plastic sock nets and polypropylene long lines) used during
739 cultivation (Mathalon and Hill, 2014, Santana et al., 2018). probably highlights the small
740 contribution of mussel farms as a source of MPs pollution (Santana et al., 2018). Moreover, the
741 intertidal wild mussel (present study) is assumed to filter and excrete MPs half of the time in
742 comparison with the submerged cultured mussel in the North Sea, resulting though in similar

743 accumulation level. The model also predicts the time needed for the 90% gut clearance of both
744 cultured (N. Ionian Sea) and wild (North Sea) mussel to be almost 284330 hours and 5663 hours
745 (equivalent to 124 and 2.53 days) respectively, when MPs contamination is removed from their
746 habitat. This is in line with a series of studies which demonstrated that the depuration time varies
747 between 6-72 hours and can last up to 40 days depending on several factors such as species,
748 environmental conditions (Bayne et al., 1987), size and type of MPs (Browne et al., 2008, Ward and
749 Kach, 2009, Woods et al., 2018, Birnstiel et al., 2019).

750 The strong dependence of food (CHL-a), temperature and seawater's MPs concentration on
751 the MPs accumulation by the mussel, regarding its wet weight, is demonstrated through sensitivity
752 experiments that were used to derive a rather simple nonlinear regression model (Eq. 19). The
753 comparison of the regression model's with the DEB model's output resulted in a quite accurate
754 estimation of the coefficients, which in turn sparked the idea of a 'new' relationship (Eq. 20) that
755 could potentially predict the MPs concentration in the environment (C_{env}) when certain conditions
756 are known (CHL-a, T, C_{env} , W). The latter equation was applied in 8 areas in total (2 from the
757 present study areas and 6 from Li et al. (2018)), with relatively good results since there is general
758 overlapping of regressed and observed MPs concentration in the environment (C_{env}), except for
759 Hastings-A and Plymouth areas, probably due to missing information on the environmental
760 conditions (CHL-a, SST) during the samplingthe predicted value is within the observed range of
761 field data in most regions, suggesting thatmaking the mussels can be used as potential bioindicators.
762 Mussels have been previously proposed as bioindicators for marine microplastic pollution (<1 mm),
763 although the efficient gut clearance and selective feeding behavior limit their quantitative ability
764 (Lusher et al., 2017, Brate et al., 2018, Beyer et al., 2017, Fossi et al., 2018, Li et al., 2019).The
765 very recent study by Ward et al. (2019b) demonstrated that bivalves are poor bioindicators of MPs
766 pollution due to the particle selection during feeding and excretion processes that is based on the
767 physical characteristics of the MPs. Considering that the MPs accumulation is site-dependent~~d~~ and
768 that sampling of mussels is usually easier than seawater (Karlsson et al., 2017, Brate et al., 2018),
769 models like the one described in Eq. 20, ~~that~~ besides the MPs accumulation, take into account also
770 characteristics of the environment, ~~that~~which are crucial for the way that mussels accumulate MPs,
771 This methodpossibly could be possibly used at global level and allow comparisons between various
772 environments. However, the method described should be validated in more environments with more
773 frequent field data to be able to provide secure results.

774 In addition toDespite the scarce validation data regarding the MPs accumulation in mussels,
775 in this study has some morethere are some other limitations. First of all, the data regarding the
776 concentration of MPs in the mussels' environment areis also scarce; since MPs is a relatively recent
777 subject of study, the existing knowledge of the spatial and temporal distribution is still quite limited

778 (Law and Thompson, 2014, Browne, 2015, Anderson et al., 2016, de Sa et al., 2018, Smith et al.,
779 2018, Troost et al., 2018). To overcome the lack of environmental MPs time series, a function of
780 randomly generated values within the observed range of each area was applied and its uncertainty
781 was examined through an ensemble forecasting. Specifically, the model's uncertainty due to the
782 environmental MPs concentration (C_{env}) was tested by performing a series of model runs forced by
783 an envelope of representative values of C_{env} . ~~and The~~ results (section 3.3) showed ed that the adopted
784 stochastic scenario simulates d quite satisfactorily ~~realistically~~ the MPs accumulation by the mussels,
785 lying within the observed field range, although a slight overestimation was found in the North Sea
786 and in agreement with the available field data. The approach used is assumed to represent the
787 natural variability ~~be close to reality~~ since it has been reported that MPs quantification in the water is
788 rather a complicated procedure due to the influence of many factors such as tides, wind, wave
789 action, ocean currents, river inputs and hydrodynamic features lead ~~resulting~~ to high spatially and
790 temporally variability of MPs distribution even in very small scales (Messinetti et al., 2018,
791 Goldstein et al., 2013). In addition, the nature of the variable C_{env} makes it difficult to estimate,
792 presenting large observational errors, not only due to the intense physical variation but also due to
793 different sampling and analysis techniques that were used. In a future work the DEB-accumulation
794 model could be coupled with a high-resolution MPs distribution model (Kalaroni et al., 2019),
795 being extensively validated against field data that will have been collected and processed according
796 to a common scientifically defined protocol, to overcome this limitation. Moreover, the approach
797 followed in calculating the value of MPs concentration in the near surface layer (0-5m depth) (Kooi
798 et al., 2016), resulted in a representative value of the upper ocean layer. In depth knowledge of the
799 MPs distribution, both horizontally and vertically, is essential to understand and mitigate their
800 impact not only on the various marine compartments but also on the organisms inhabiting those
801 compartments (Van Sebille et al., 2015, Kooi et al., 2016). For that reason, it is important to
802 enhance the monitoring activity especially in the vulnerable coastal environments, adopting
803 integrated cross-disciplinary approaches and monitoring of biological, physical and chemical
804 parameters which provide information on the ecosystem function, in order to improve the
805 assessment of emerging pollutants (i.e. MPs) and their impacts on biota (objective of JERICO-RI
806 framework).

807 ~~Our~~ Further, the assumption that the mussel has the same filtration rate for all particles
808 independently of their chemical composition, size and shape, is a simplification and an open
809 contradictory theme of discussion (see Saraiva et al., 2011a for details). However, in our model
810 application through the model, a pre-ingestive particle selection by the mussel is implied based on
811 the organic-inorganic content of the suspended matter illustrating the different binding probabilities
812 applied for algal and MPs particles during the ingestion process. Through an investigation of wild

813 mussel's faeces and pseudofaeces production in laboratory conditions, Zhao et al. (2018) found that
814 the length of MPs was significantly longer in pseudofaeces than in the digestive gland and faeces.
815 Furthermore, Van Cauwenberghe et al. (2015) demonstrated that mussel's faeces contained larger
816 MPs (15–500 µm) compared to the mussel's tissue (20–90 µm). Apparently, smaller sized MPs
817 seem to be dominant within the mussels in comparison with the size of the MPs in the ambient
818 environment (Li et al., 2018, Qu et al., 2018, Digka et al., 2018b), implying that the mussel is more
819 prone to ingest and retain smaller sized MPs. As an example, Digka et al. (2018b) confirmed that
820 the smaller MPs (<1 mm) occupy the 62.3%, 96.9% and 100% of the total MPs in seawater,
821 sediments and mussels from the N. Ionian Sea respectively. In a future work this selection pattern
822 regarding size, could be simulated by suitable preference weights among different MPs sizes. This
823 will improve the knowledge of the feeding and excretion mechanisms used by the mussels against
824 MPs pollution and the assessment of the ecological footprint (Rist et al., 2019).

825 Our Moreover, the assumption that the contamination by MPs does not affect the energy
826 budget in terms of growth might also be a simplification as this is a subject currently under
827 investigation. Van Cauwenberghe et al. (2015) found that although mussels *M. edulis* exposed to
828 MPs increased their energy consumption, the energy reserves was not affected compared to the
829 control organisms, implying that mussels are able to adopt a defensive mechanism against the
830 suspended inorganic particles (i.e. MPs) (Ward and Shumway, 2004). Furthermore, MPs exposure
831 showed no significant effect on mussel's (*Perna perna*) energy budget, despite its long duration and
832 relatively realistic intensity, leading to the hypothesis that ~~concluding to the assumption of~~ mussels's
833 can acclimate to the MPs exposure ~~acclimation~~ to maintain their ~~its~~ health (Santana et al., 2018). On
834 the contrary, other authors ~~who mainly intended to predict future effects~~, suggested a significant
835 energy shift from reproduction to structural growth and elevated maintenance costs, probably
836 attributed to the reduced energy intake, when the organisms (i.e. oyster *Crassostrea gigas*) were
837 contaminated with high and unrealistic concentration of MPs (Sussarellu et al., 2016). Moreover,
838 Gardon et al. (2018) showed that the overall energy balance of oyster *Pinctada margaritifera* was
839 significantly impacted by the reduced assimilation efficiency in correlation with the exposed dose
840 of MPs and for that reason energy had to be withdrawn from reproduction to compensate for the
841 energy loss. In future dedicated experiments exploring the effects on all components of a DEB
842 model should be carried out considering long-term realistic MPs exposure.

843 Our use of the tide data led to some model bias ~~Furthermore, the tide data as considered in the~~
844 ~~present study impose model's bias~~, since the model does not take into account of the mussel's body
845 temperature change when this is exposed to air ~~was not taken into consideration~~. Assessing the
846 mussel's body temperature requires ~~demand~~ extended experiments in field conditions (Tagliarolo
847 and McQuaid, 2015, Monaco and McQuaid, 2018). The ~~A very recent~~ study by Seuront et al. (2019)

848 along the French coast of the eastern English Channel found no significant correlation between air's
849 and mussel's body temperature, but ~~demonstrated a rather positively~~ significant positive correlation
850 between the body temperature and with the hard substrate's (i.e. rocks) temperature. However, in the
851 present study the tide effect on processes that are affected by the thermal equation ($k(T)$) is
852 considered indirectly through the metabolic depression (details in section 2.4). Sara et al. (2011)
853 ~~following the method developed by Kearney et al. (2010), who~~ coupled a DEB model with a
854 biophysical model (Kearney et al., 2010), incorporating ~~the~~ the change of mussel's body temperature
855 during emersion, by using information of various climatological variables (i.e. solar radiation, air
856 temperature, wind speed, wave height), but ~~the ignored the~~ temperature sensitivity on the
857 physiological processes ~~was ignored~~. In a future study, a combined similar approach by coupling the
858 present DEB-accumulation model with a biophysical model, which includes both the tide effect on
859 the physiological processes and the mussel's body temperature respectively, could be followed and
860 lead to a more detailed simulation of the intertidal mussel's body temperature.

861 5. Conclusions

862
863 In a future study the model should be corroborated further by using a larger dataset
864 of validated against more frequent field data regarding the MPs accumulation, with sampling of
865 mussels of among various sizes and life stages. Currently, the model is mainly limited by the
866 insufficient validation, as a larger dataset could be also used for a better model calibration, as for now
867 ~~it cannot be reliable in conducting predictions within accepted precision~~. However, this study
868 provides a new approach in studying the accumulation of MPs by filter feeders and reveals the
869 relations between characteristics of the mussel's surrounding environment and the MPs
870 accumulation, which is presented with high seasonal fluctuations. Additionally, in a future study the
871 DEB-accumulation model will be coupled to with a ~~coupled~~ hydrodynamic-biochemical model (e.g.,
872 Petihakis et al., 2002, 2012, Triantafyllou et al., 2003, Tsiaras et al., 2014, Ciavatta et al., 2019,
873 Kalaroni et al., 2020) and a MPs distribution model (Kalaroni et al., 2019) that will provide fields of
874 temperature, food availability and MPs concentration respectively at the Mediterranean scale, and
875 eventually lead to an integrated representation of the MPs accumulation by mussels (Daewel et al.,
876 2008). This fully coupled model will be downscaled to the Cretan Sea SuperSite, while the
877 parameterization of important biological processes will be redesigned based on the new data which
878 will be acquired in the framework of the JERICO S3 project (<http://www.jerico-ri.eu>). The present
879 study highlights the urgent need for adopting a multi-disciplinary monitoring activity by measuring
880 physical, biological and chemical parameters that are crucial for mapping the MPs distribution,
881 assessing the contamination level of the marine organisms and investigating the impact on the

882 health status. Overall, despite the ~~significant~~ limitations ~~that were~~ mentioned ~~before~~, taken into
883 account that plastics are one of the global hot issues, this particular study could help ~~for the~~ design
884 ~~of~~ next efforts, since it provides indications on the future priority related issues.

885

886 **Author Contribution:**

887 **Natalia Stamataki, Yannis Hatzonikolakis, Kostas Tsiaras, Catherine Tsangaris, George**
888 **Petihakis, Sarantis Sofianos, George Triantafyllou**

889

890 G.T. conceived the basic idea of the present study and was responsible for the management and
891 coordination of the research planning and execution. N.S. and Y.H. developed the model code with
892 the contribution of K.T.. N.S. collected the existing information on the subject and performed the
893 simulations of the present study with the help of Y.H. when needed. G.T., G.P., K.T., Y.H. and N.S.
894 contributed to the interpretation of the results. C.T. provided the field data of the mussel's
895 microplastic accumulation in the North Ionian Sea. N.S. prepared the manuscript, with critical
896 review, commentary and revision contributed from all co-authors.

897

898 **Competing interests:**

899 The authors declare that they have no conflict of interest.

900

901 **Acknowledgments:**

902

903 This work was partially funded by the national project 'Blue growth with innovation and
904 application in Greek Seas' (MIS 5002438) and the EU H2020 CLAIM project (G.A. n° 774586).

905 This study has been conducted using E.U. Copernicus Marine Service Information
906 (<http://marine.copernicus.eu/>). Part of this work was supported by the JERICO- NEXT project. This
907 project has received funding from the European Union's Horizon 2020
908 research and innovation programme under grant agreement no. 654410.

909

910

911

912

References

- 914 Alunno-Bruscia, M., Bourlès, Y., Maurer, D., Robert, S., Mazurié, J., Gangnery, A., Gouilletquer, P. and
 915 Pouvreau, S.: A single bio-energetics growth and reproduction model for the oyster *Crassostrea gigas* in six Atlantic
 916 ecosystems, *J. Sea Res.*, 66(4), 340–348, doi:10.1016/j.seares.2011.07.008, 2011.
- 917 Anderson, J. C., Park, B. J. and Palace, V. P.: Microplastics in aquatic environments: Implications for Canadian
 918 ecosystems, *Environ. Pollut.*, 218, 269–280, doi:10.1016/j.envpol.2016.06.074, 2016.
- 919 Andrady, A. L.: Microplastics in the marine environment, *Mar. Pollut. Bull.*, 62(8), 1596–1605,
 920 doi:10.1016/j.marpolbul.2011.05.030, 2011.
- 921 Arthur, C., J. Baker and H. Bamford (eds). Proceedings of the International Research Workshop on the
 922 Occurrence, Effects and Fate of Microplastic Marine Debris. Sept 9-11, 2008. NOAA Technical Memorandum NOS-
 923 OR&R-30, 2009
- 924 Bacher, C. and Gangnery, A.: Use of dynamic energy budget and individual based models to simulate the
 925 dynamics of cultivated oyster populations, *J. Sea Res.*, 56(2), 140–155, doi:10.1016/j.seares.2006.03.004, 2006.
- 926 Bayne, B. and Worrall, C.: Growth and Production of Mussels *Mytilus edulis* from Two Populations, *Mar. Ecol.*
 927 *Prog. Ser.*, 3, 317–328, doi:10.3354/meps003317, 1980.
- 928 Bayne, B. L., Hawkins, A. J. S. and Navarro, E.: Feeding and digestion by the mussel *Mytilus edulis* L.
 929 (*Bivalvia: Mollusca*) in mixtures of silt and algal cells at low concentrations, *J. Exp. Mar. Bio. Ecol.*, 111(1), 1–22,
 930 doi:10.1016/0022-0981(87)90017-7, 1987.
- 931 Béjaoui-Omri, A., Béjaoui, B., Harzallah, A., Aloui-Béjaoui, N., El Bour, M. and Aleya, L.: Dynamic energy
 932 budget model: a monitoring tool for growth and reproduction performance of *Mytilus galloprovincialis* in Bizerte
 933 Lagoon (Southwestern Mediterranean Sea), *Environ. Sci. Pollut. Res.*, 21(22), 13081–13094, doi:10.1007/s11356-014-
 934 3265-1, 2014.
- 935 Beyer, J., Green, N. W., Brooks, S., Allan, I. J., Ruus, A., Gomes, T., Bråte, I. L. N. and Schøyen, M.: Blue
 936 mussels (*Mytilus edulis* spp.) as sentinel organisms in coastal pollution monitoring: A review, *Mar. Environ. Res.*,
 937 130, 338–365, doi:10.1016/j.marenvres.2017.07.024, 2017.
- 938 Birnstiel, S., Soares-Gomes, A. and da Gama, B. A. P.: Depuration reduces microplastic content in wild and
 939 farmed mussels, *Mar. Pollut. Bull.*, 140, 241–247, doi:10.1016/j.marpolbul.2019.01.044, 2019.
- 940 Bourlès, Y., Alunno-Bruscia, M., Pouvreau, S., Tollu, G., Leguay, D., Arnaud, C., Gouilletquer, P. and
 941 Kooijman, S. A. L. M.: Modelling growth and reproduction of the Pacific oyster *Crassostrea gigas*: Advances in the
 942 oyster-DEB model through application to a coastal pond, *J. Sea Res.*, 62(2–3), 62–71,
 943 doi:10.1016/j.seares.2009.03.002, 2009.
- 944 Bråte, I. L. N., Hurley, R., Iversen, K., Beyer, J., Thomas, K. V., Steindal, C. C., Green, N. W., Olsen, M. and
 945 Lusher, A.: *Mytilus* spp. as sentinels for monitoring microplastic pollution in Norwegian coastal waters: A qualitative
 946 and quantitative study, *Environ. Pollut.*, 243, 383–393, doi:10.1016/j.envpol.2018.08.077, 2018.
- 947 [Brewin, R., Ciavatta, S., Sathyendranath, S., Jackson, T., Tilstone, G. and Curran, K.: Uncertainty in Ocean-
 948 Color Estimates of Chlorophyll for Phytoplankton Groups, *Front. Mar. Sci.*, 4, doi:10.3389/fmars.2017.00104, 2017.](#)
- 949 [Browne, M. A., Galloway, T. and Thompson, R.: Microplastic-an emerging contaminant of potential concern?,
 950 *Integr. Environ. Assess. Manag.*, 3\(4\), 559–561, doi:10.1002/ieam.5630030412, 2007.](#)
- 951 Browne, M. A., Dissanayake, A., Galloway, T. S., Lowe, D. M. and Thompson, R. C.: Ingested microscopic
 952 plastic translocates to the circulatory system of the mussel, *Mytilus edulis* (L.), *Environ. Sci. Technol.*, 42(13), 5026–
 953 5031, doi:10.1021/es800249a, 2008.
- 954 ~~[Browne, M. A., Galloway, T. and Thompson, R.: Microplastic-an emerging contaminant of potential concern?,
 955 *Integr. Environ. Assess. Manag.*, 3\(4\), 559–561, doi:10.1002/ieam.5630030412, 2007.](#)~~
- 956 Browne, M. A.: Sources and pathways of microplastics to habitats, *Mar. Anthropog. Litter*, 229–244,
 957 doi:10.1007/978-3-319-16510-3_9, 2015.
- 958 Capolupo, M., Franzellitti, S., Valbonesi, P., Lanzas, C. S. and Fabbri, E.: Uptake and transcriptional effects of
 959 polystyrene microplastics in larval stages of the Mediterranean mussel *Mytilus galloprovincialis*, *Environ. Pollut.*, 241,
 960 1038–1047, doi:10.1016/j.envpol.2018.06.035, 2018.
- 961 Cardoso, J. F. M. F., Dekker, R., Witte, J. I. J. and van der Veer, H. W.: Is reproductive failure responsible for
 962 reduced recruitment of intertidal *Mytilus edulis* L. in the western Dutch Wadden Sea?, *Senckenbergiana Maritima*,
 963 37(2), 83–92, doi:10.1007/BF03043695, 2007.

964 Casas, S. and Bacher, C.: Modelling trace metal (Hg and Pb) bioaccumulation in the Mediterranean mussel,
965 *Mytilus galloprovincialis*, applied to environmental monitoring, *J. Sea Res.*, 56(2), 168–181,
966 doi:10.1016/j.seares.2006.03.006, 2006.

967 Ciavatta, S., Kay, S., Brewin, R. J. W., Cox, R., Di Cicco, A., Nencioli, F., Polimene, L., Sammartino, M.,
968 Santoleri, R., Skákala, J. and Tsapakis, M.: Ecoregions in the Mediterranean Sea Through the Reanalysis of
969 Phytoplankton Functional Types and Carbon Fluxes, *J. Geophys. Res. Ocean.*, 124(10), 6737–6759,
970 doi:10.1029/2019JC015128, 2019.

971 [Cole, M., Lindeque, P., Halsband, C. and Galloway, T. S.: Microplastics as contaminants in the marine
972 environment: A review, *Mar. Pollut. Bull.*, 62\(12\), 2588–2597, doi:10.1016/j.marpolbul.2011.09.025, 2011.](#)

973 Cole, M., Lindeque, P., Fileman, E., Halsband, C., Goodhead, R., Moger, J. and Galloway, T. S.: Microplastic
974 ingestion by zooplankton, *Environ. Sci. Technol.*, 47(12), 6646–6655, doi:10.1021/es400663f, 2013.

975 ~~Cole, M., Lindeque, P., Halsband, C. and Galloway, T. S.: Microplastics as contaminants in the marine
976 environment: A review, *Mar. Pollut. Bull.*, 62(12), 2588–2597, doi:10.1016/j.marpolbul.2011.09.025, 2011.~~

977 Cucci, T. L., Shumway, S. E., Brown, W. S. and Newell, C. R.: Using phytoplankton and flow cytometry to
978 analyze grazing by marine organisms, *Cytometry*, 10(5), 659–669, doi:10.1002/cyto.990100523, 1989.

979 Daewel, U., Peck, M. A., Kühn, W., St. John, M. A., Alekseeva, I. and Schrum, C.: Coupling ecosystem and
980 individual-based models to simulate the influence of environmental variability on potential growth and survival of
981 larval sprat (*Sprattus sprattus* L.) in the North Sea, *Fish. Oceanogr.*, 17(5), 333–351, doi:10.1111/j.1365-
982 2419.2008.00482.x, 2008.

983 de Sá, L. C., Oliveira, M., Ribeiro, F., Rocha, T. L. and Futter, M. N.: Studies of the effects of microplastics on
984 aquatic organisms: What do we know and where should we focus our efforts in the future?, *Sci. Total Environ.*, 645,
985 1029–1039, doi:10.1016/j.scitotenv.2018.07.207, 2018.

986 De Witte, B., Devriese, L., Bekaert, K., Hoffman, S., Vandermeersch, G., Cooreman, K. and Robbens, J.: Quality
987 assessment of the blue mussel (*Mytilus edulis*): Comparison between commercial and wild types, *Mar. Pollut. Bull.*,
988 85(1), 146–155, doi:10.1016/j.marpolbul.2014.06.006, 2014.

989 [Di Cicco, A., Sammartino, M., Marullo, S. and Santoleri, R.: Regional Empirical Algorithms for an Improved
990 Identification of Phytoplankton Functional Types and Size Classes in the Mediterranean Sea Using Satellite Data,
991 *Front. Mar. Sci.*, 4, doi:10.3389/fmars.2017.00126, 2017.](#)

992 Digka, N., Tsangaris, C., Kaberi, H., Adamopoulou, A. and Zeri, C.: Microplastic Abundance and Polymer
993 Types in a Mediterranean Environment, Springer Water., 2018b.

994 Digka, N., Tsangaris, C., Torre, M., Anastasopoulou, A. and Zeri, C.: Microplastics in mussels and fish from the
995 Northern Ionian Sea, *Mar. Pollut. Bull.*, 135, 30–40, doi:10.1016/j.marpolbul.2018.06.063, 2018a.

996 [El Hourany, R., Abboud-Abi Saab, M., Faour, G., Mejia, C., Crépon, M., & Thiria, S.: Phytoplankton Diversity
997 in the Mediterranean Sea From Satellite Data Using Self-Organizing Maps, *J. Geophys. Res. Ocean.*, 124\(8\), 5827–
998 5843, doi:10.1029/2019jc015131, 2019.](#)

999 Enders, K., Lenz, R., Stedmon, C. A. and Nielsen, T. G.: Abundance, size and polymer composition of marine
1000 microplastics $\geq 10 \mu\text{m}$ in the Atlantic Ocean and their modelled vertical distribution, *Mar. Pollut. Bull.*, 100(1), 70–81,
1001 doi:10.1016/j.marpolbul.2015.09.027, 2015.

1002 Eriksen, M., Lebreton, L. C. M., Carson, H. S., Thiel, M., Moore, C. J., Borerro, J. C., Galgani, F., Ryan, P. G.
1003 and Reisser, J.: Plastic Pollution in the World's Oceans: More than 5 Trillion Plastic Pieces Weighing over 250,000
1004 Tons Afloat at Sea, *PLoS One*, 9(12), doi:10.1371/journal.pone.0111913, 2014.

1005 Everaert, G., Van Cauwenberghe, L., De Rijcke, M., Koelmans, A. A., Mees, J., Vandegehuchte, M. and Janssen,
1006 C. R.: Risk assessment of microplastics in the ocean: Modelling approach and first conclusions, *Environ. Pollut.*, 242,
1007 1930–1938, doi:10.1016/j.envpol.2018.07.069, 2018.

1008 Fossi, M. C., Pedà, C., Compa, M., Tsangaris, C., Alomar, C., Claro, F., Ioakeimidis, C., Galgani, F., Hema, T.,
1009 Deudero, S., Romeo, T., Battaglia, P., Andaloro, F., Caliani, I., Casini, S., Panti, C. and Baini, M.: Bioindicators for
1010 monitoring marine litter ingestion and its impacts on Mediterranean biodiversity, *Environ. Pollut.*, 237, 1023–1040,
1011 doi:10.1016/j.envpol.2017.11.019, 2018.

1012 Gardon, T., Reisser, C., Soyeux, C., Quillien, V. and Le Moullac, G.: Microplastics Affect Energy Balance and
1013 Gametogenesis in the Pearl Oyster *Pinctada margaritifera*, *Environ. Sci. Technol.*, 52(9), 5277–5286,
1014 doi:10.1021/acs.est.8b00168, 2018.

1015 [Garnesson, P., Mangin, A., Fanton d'Andon, O., Demaria, J., & Bretagnon, M.: The CMEMS
1016 GlobColour chlorophyll a product based on satellite observation: multi-sensor merging and flagging strategies, *Ocean
1017 Sci.*, 15\(3\), 819–830, doi:10.5194/os-15-819-2019, 2019.](#)

1018 GESAMP Joint Group of Experts on the Scientific Aspects of Marine Environmental Protection: Sources, fate
1019 and effects of microplastics in the marine environment: a global assessment”, edited by P. J. Kershaw and ed), Reports
1020 Stud. GESAMP, 90(90), 96, doi:10.13140/RG.2.1.3803.7925, 2015.

1021 *GlobColour data (<http://globcolour.info>) used in this study has been developed, validated, and distributed by*
1022 *ACRI-ST, France.*

1023 Gohin, F., Druon, J. N. and Lampert, L.: A five channel chlorophyll concentration algorithm applied to Sea
1024 WiFS data processed by SeaDAS in coastal waters, *Int. J. Remote Sens.*, 23(8), 1639–1661,
1025 doi:10.1080/01431160110071879, 2002.

1026 Goldstein, M. C., Titmus, A. J. and Ford, M.: Scales of spatial heterogeneity of plastic marine debris in the
1027 northeast Pacific Ocean, *PLoS One*, 8(11), 80020, doi:10.1371/journal.pone.0080020, 2013.

1028 Handå, A., Alver, M., Edvardsen, C. V., Halstensen, S., Olsen, A. J., Øie, G., Reitan, K. I., Olsen, Y. and
1029 Reinertsen, H.: Growth of farmed blue mussels (*Mytilus edulis* L.) in a Norwegian coastal area; comparison of food
1030 proxies by DEB modeling, *J. Sea Res.*, 66(4), 297–307, doi:10.1016/j.seares.2011.05.005, 2011.

1031 Hantoro, I., Löhr, A. J., Van Belleghem, F. G. A. J., Widianarko, B. and Ragas, A. M. J.: Microplastics in coastal
1032 areas and seafood: implications for food safety, *Food Addit. Contam. - Part A Chem. Anal. Control. Expo. Risk*
1033 *Assess.*, 36(5), 674–711, doi:10.1080/19440049.2019.1585581, 2019.

1034 Hatzonikolakis, Y., Tsiaras, K., Theodorou, J. A., Petihakis, G., Sofianos, S. and Triantafyllou, G.: Simulation of
1035 mussel *Mytilus galloprovincialis* growth with a dynamic energy budget model in Maliakos and Thermaikos Gulfs
1036 (Eastern mediterranean), *Aquac. Environ. Interact.*, 9, 371–383, doi:10.3354/aei00236, 2017.

1037 Hirai, H., Takada, H., Ogata, Y., Yamashita, R., Mizukawa, K., Saha, M., Kwan, C., Moore, C., Gray, H.,
1038 Laursen, D., Zettler, E. R., Farrington, J. W., Reddy, C. M., Peacock, E. E. and Ward, M. W.: Organic micropollutants
1039 in marine plastics debris from the open ocean and remote and urban beaches, *Mar. Pollut. Bull.*, 62(8), 1683–1692,
1040 doi:10.1016/j.marpolbul.2011.06.004, 2011.

1041 [International Ocean-Colour Coordinating Group – IOCCG, Remote sensing of ocean colour in coastal, and other](#)
1042 [optically-complex waters, Rep. Int. Ocean-Colour Coord. Group 3, edited by S. Sathyendranath, Dartmouth, N. S.,](#)
1043 [Canada, 2000.](#)

1044 Jacobs, P., Beauchemin, C. and Riegman, R.: Growth of juvenile blue mussels (*Mytilus edulis*) on suspended
1045 collectors in the Dutch Wadden Sea, *J. Sea Res.*, 85, 365–371, doi:10.1016/j.seares.2013.07.006, 2014.

1046 Jacobs, P., Troost, K., Riegman, R. and van der Meer, J.: Length- and weight-dependent clearance rates of
1047 juvenile mussels (*Mytilus edulis*) on various planktonic prey items, *Helgol. Mar. Res.*, 69(1), 101–112,
1048 doi:10.1007/s10152-014-0419-y, 2015.

1049 Jolliff, J. K., Kindle, J. C., Shulman, I., Penta, B., Friedrichs, M. A. M., Helber, R. and Arnone, R. A.: Summary
1050 diagrams for coupled hydrodynamic-ecosystem model skill assessment, *J. Mar. Syst.*, 76(1–2), 64–82,
1051 doi:10.1016/j.jmarsys.2008.05.014, 2009.

1052 Jørgensen, C., Larsen, P. and Riisgård, H.: Effects of temperature on the mussel pump, *Mar. Ecol. Prog. Ser.*,
1053 64(1/2), 89–97, doi:10.3354/meps064089, 1990.

1054 [Kach, D. and Ward, J.: The role of marine aggregates in the ingestion of picoplankton-size particles by](#)
1055 [suspension-feeding molluscs, Mar. Biol., 153\(5\), 797–805, doi:10.1007/s00227-007-0852-4, 2007.](#)

1056 Kalaroni S, Hatzonikolakis Y, Tsiaras K, Gkanasos A, Triantafyllou G.: Modelling the Marine Microplastic
1057 Distribution from Municipal Wastewater in Saronikos Gulf (E. Mediterranean). *Oceanogr Fish Open Access J.*; 9(1):
1058 555752. DOI: 10.19080/OFOAJ.2019.09.555752, 2019.

1059 Kalaroni, S., Tsiaras, K., Petihakis, G., Economou-Amilli, A. and Triantafyllou, G.: Modelling the
1060 Mediterranean pelagic ecosystem using the POSEIDON ecological model. Part I: Nutrients and chlorophyll-a
1061 dynamics, *Deep. Res. Part II Top. Stud. Oceanogr.*, 171, 104647, doi:10.1016/j.dsr2.2019.104647, 2020.

1062 Karayücel, S., Çelik, M. Y., Karayücel, I. and Erik, G.: Karadeniz’de Sinop İlinde Akdeniz Midyesinin (*Mytilus*
1063 *galloprovincialis* Lamarck, 1819) Sal Sisteminde Büyümesi ve Üretimi, *Turkish J. Fish. Aquat. Sci.*, 10(1), 9–17,
1064 doi:10.4194/trjfas.2010.0102, 2010.

1065 Karlsson, T. M., Vethaak, A. D., Almroth, B. C., Ariese, F., van Velzen, M., Hassellöv, M. and Leslie, H. A.:
1066 Screening for microplastics in sediment, water, marine invertebrates and fish: Method development and microplastic
1067 accumulation, *Mar. Pollut. Bull.*, 122(1–2), 403–408, doi:10.1016/j.marpolbul.2017.06.081, 2017.

1068 Kearney, M., Simpson, S. J., Raubenheimer, D. and Helmuth, B.: Modelling the ecological niche from functional
1069 traits, *Philos. Trans. R. Soc. B Biol. Sci.*, 365(1557), 3469–3483, doi:10.1098/rstb.2010.0034, 2010.

1070 Khan, M. B. and Prezant, R. S.: Microplastic abundances in a mussel bed and ingestion by the ribbed marsh
1071 mussel *Geukensia demissa*, *Mar. Pollut. Bull.*, 130, 67–75, doi:10.1016/j.marpolbul.2018.03.012, 2018.

1072 Kjørboe, T. and Møhlenberg, F.: Particle Selection in Suspension-Feeding Bivalves, *Mar. Ecol. Prog. Ser.*, 5,
1073 291–296, doi:10.3354/meps005291, 1981.

1074 Kooi, M., Reisser, J., Slat, B., Ferrari, F. F., Schmid, M. S., Cunsolo, S., Brambini, R., Noble, K., Sirks, L. A.,
1075 Linders, T. E. W., Schoeneich-Argent, R. I. and Koelmans, A. A.: The effect of particle properties on the depth profile
1076 of buoyant plastics in the ocean, *Sci. Rep.*, 6(1), doi:10.1038/srep33882, 2016.

1077 ~~Kooijman SALM: *Dynamic Energy Budget Theory for Metabolic Organisation*. Cambridge University Press,
1078 Cambridge, 2010.~~

1079 Kooijman, S. A. L. M.: *Dynamic Energy and Mass Budgets in Biological Systems*. Cambridge: Cambridge
1080 University Press, 2000.

1081 Kooijman, S. A. L. M.: Pseudo-faeces production in bivalves, *J. Sea Res.*, 56(2), 103–106,
1082 doi:10.1016/j.seares.2006.03.003, 2006.

1083 ~~Kooijman SALM: *Dynamic Energy Budget Theory for Metabolic Organisation*. Cambridge University Press,
1084 Cambridge, 2010.~~

1085 Lacroix, G., Ruddick, K., Ozer, J. and Lancelot, C.: Modelling the impact of the Scheldt and Rhine/Meuse
1086 plumes on the salinity distribution in Belgian waters (southern North Sea), *J. Sea Res.*, 52(3), 149–163,
1087 doi:10.1016/j.seares.2004.01.003, 2004.

1088 Lattin, G. L., Moore, C. J., Zellers, A. F., Moore, S. L. and Weisberg, S. B.: A comparison of neustonic plastic
1089 and zooplankton at different depths near the southern California shore, *Mar. Pollut. Bull.*, 49(4), 291–294,
1090 doi:10.1016/j.marpolbul.2004.01.020, 2004.

1091 Law, K. L. and Thompson, R. C.: Microplastics in the seas, *Science* (80-.), 345(6193), 144–145,
1092 doi:10.1126/science.1254065, 2014.

1093 Lenz, R., Enders, K. and Nielsen, T. G.: Microplastic exposure studies should be environmentally realistic, *Proc.*
1094 *Natl. Acad. Sci. U. S. A.*, 113(29), E4121–E4122, doi:10.1073/pnas.1606615113, 2016.

1095 ~~Li, J., Qu, X., Su, L., Zhang, W., Yang, D., Kolandhasamy, P., Li, D. and Shi, H.: *Microplastics in mussels along*
1096 *the coastal waters of China*, *Environ. Pollut.*, 214, 177–184, doi:10.1016/j.envpol.2016.04.012, 2016.~~

1097 Li, J., Green, C., Reynolds, A., Shi, H. and Rotchell, J. M.: Microplastics in mussels sampled from coastal waters
1098 and supermarkets in the United Kingdom, *Environ. Pollut.*, 241, 35–44, doi:10.1016/j.envpol.2018.05.038, 2018.

1099 Li, J., Lusher, A. L., Rotchell, J. M., Deudero, S., Turra, A., Bråte, I. L. N., Sun, C., Shahadat Hossain, M., Li,
1100 Q., Kolandhasamy, P. and Shi, H.: Using mussel as a global bioindicator of coastal microplastic pollution, *Environ.*
1101 *Pollut.*, 244, 522–533, doi:10.1016/j.envpol.2018.10.032, 2019.

1102 ~~Li, J., Qu, X., Su, L., Zhang, W., Yang, D., Kolandhasamy, P., Li, D. and Shi, H.: *Microplastics in mussels along*
1103 *the coastal waters of China*, *Environ. Pollut.*, 214, 177–184, doi:10.1016/j.envpol.2016.04.012, 2016.~~

1104 Liubartseva, S., Coppini, G., Lecci, R. and Clementi, E.: Tracking plastics in the Mediterranean: 2D Lagrangian
1105 model, *Mar. Pollut. Bull.*, 129(1), 151–162, doi:10.1016/j.marpolbul.2018.02.019, 2018.

1106 ~~Lusher, A.: *Microplastics in the marine environment: Distribution, interactions and effects*, *Mar. Anthropog.*
1107 *Litter*, 245–307, doi:10.1007/978-3-319-16510-3_10, 2015.~~

1108 Lusher, A., Bråte, I. L. N., Hurley, R., Iversen, K. and Olsen, M.: Testing of methodology for measuring
1109 microplastics in blue mussels (*Mytilus* spp) and sediments, and recommendations for future monitoring of
1110 microplastics, 87, (7209), doi:10.13140/RG.2.2.24399.59041, 2017.

1111 ~~Lusher, A.: *Microplastics in the marine environment: Distribution, interactions and effects*, *Mar. Anthropog.*
1112 *Litter*, 245–307, doi:10.1007/978-3-319-16510-3_10, 2015.~~

1113 Maes, T., Van der Meulen, M. D., Devriese, L. I., Leslie, H. A., Huvet, A., Frère, L., Robbens, J. and Vethaak,
1114 A. D.: Microplastics baseline surveys at the water surface and in sediments of the North-East Atlantic, *Front. Mar.*
1115 *Sci.*, 4(MAY), doi:10.3389/fmars.2017.00135, 2017.

1116 Maire, O., Amouroux, J. M., Duchêne, J. C. and Grémare, A.: Relationship between filtration activity and food
1117 availability in the Mediterranean mussel *Mytilus galloprovincialis*, *Mar. Biol.*, 152(6), 1293–1307,
1118 doi:10.1007/s00227-007-0778-x, 2007.

1119 MarLIN: The Marine Life Information Network - Common mussel (*Mytilus edulis*). Available from:
1120 <https://www.marlin.ac.uk/species/detail/1421>, 2016.

1121 Mathalon, A. and Hill, P.: Microplastic fibers in the intertidal ecosystem surrounding Halifax Harbor, Nova
1122 Scotia, *Mar. Pollut. Bull.*, 81(1), 69–79, doi:10.1016/j.marpolbul.2014.02.018, 2014.

1123 Mato, Y., Isobe, T., Takada, H., Kanehiro, H., Ohtake, C. and Kaminuma, T.: Plastic resin pellets as a transport
1124 medium for toxic chemicals in the marine environment, *Environ. Sci. Technol.*, 35(2), 318–324,
1125 doi:10.1021/es0010498, 2001.

1126 Messinetti, S., Mercurio, S., Parolini, M., Sugni, M. and Pennati, R.: Effects of polystyrene microplastics on
1127 early stages of two marine invertebrates with different feeding strategies, *Environ. Pollut.*, 237, 1080–1087,
1128 doi:10.1016/j.envpol.2017.11.030, 2018.

1129 [Möhlenberg, F., & Riisgård, H. : Efficiency of particle retention in 13 species of suspension feeding bivalves, *Ophelia*, 17\(2\), 239–246, doi:10.1080/00785326.1978.10425487, 1978.](#)

1130

1131 Monaco, C. J. and McQuaid, C. D.: Applicability of Dynamic Energy Budget (DEB) models across steep
1132 environmental gradients, *Sci. Rep.*, 8(1), doi:10.1038/s41598-018-34786-w, 2018.

1133 Moore, C. J., Moore, S. L., Leecaster, M. K. and Weisberg, S. B.: A comparison of plastic and plankton in the
1134 North Pacific Central Gyre, *Mar. Pollut. Bull.*, 42(12), 1297–1300, doi:10.1016/S0025-326X(01)00114-X, 2001.

1135 Otto, L., Zimmerman, J. T. F., Furnes, G. K., Mork, M., Saetre, R. and Becker, G.: Review of the physical
1136 oceanography of the North Sea, *Netherlands J. Sea Res.*, 26(2–4), 161, doi:10.1016/0077-7579(90)90091-T, 1990.

1137 Painting, S. J., Collingridge, K. A., Durand, D., Grémare, A., Créach, V., Arvanitidis, C. and Bernard, G.:
1138 Marine monitoring in Europe: is it adequate to address environmental threats and pressures?, *Ocean Sci. Discuss.*,
1139 16(1), 1–31, doi:10.5194/os-2019-75, 2019.

1140 Palacz, A. P., St. John, M. A., Brewin, R. J. W., Hirata, T. and Gregg, W. W.: Distribution of phytoplankton
1141 functional types in high-nitrate, low-chlorophyll waters in a new diagnostic ecological indicator model,
1142 *Biogeosciences*, 10(11), 7553–7574, doi:10.5194/bg-10-7553-2013, 2013.

1143 Pascoe, P. L., Parry, H. E. and Hawkins, A. J. S.: Observations on the measurement and interpretation of
1144 clearance rate variations in suspension-feeding bivalve shellfish, *Aquat. Biol.*, 6(1–3), 181–190, doi:10.3354/ab00123,
1145 2009.

1146 Pasquini, G., Ronchi, F., Strafella, P., Scarcella, G. and Fortibuoni, T.: Seabed litter composition, distribution
1147 and sources in the Northern and Central Adriatic Sea (Mediterranean), *Waste Manag.*, 58, 41–51,
1148 doi:10.1016/j.wasman.2016.08.038, 2016.

1149 Petihakis, G., Triantafyllou, G., Allen, I. J., Hoteit, I. and Dounas, C.: Modelling the spatial and temporal
1150 variability of the Cretan Sea ecosystem, *J. Mar. Syst.*, 36(3–4), 173–196, doi:10.1016/S0924-7963(02)00186-0, 2002.

1151 Petihakis, G., Triantafyllou, G., Korres, G., Tsiaras, K. and Theodorou, A.: Ecosystem modelling: Towards the
1152 development of a management tool for a marine coastal system part-II, ecosystem processes and biogeochemical
1153 fluxes, *J. Mar. Syst.*, 94(SUPPL.), 49–64, doi:10.1016/j.jmarsys.2011.11.006, 2012.

1154 Politikos, D. V., Tsiaras, K., Papatheodorou, G. and Anastasopoulou, A.: Modeling of floating marine litter
1155 originated from the Eastern Ionian Sea: Transport, residence time and connectivity, *Mar. Pollut. Bull.*, 150, 110727,
1156 doi:10.1016/j.marpolbul.2019.110727, 2020.

1157 Pouvreau, S., Bourles, Y., Lefebvre, S., Gangnery, A. and Alunno-Bruscia, M.: Application of a dynamic energy
1158 budget model to the Pacific oyster, *Crassostrea gigas*, reared under various environmental conditions, *J. Sea Res.*,
1159 56(2), 156–167, doi:10.1016/j.seares.2006.03.007, 2006.

1160 Prins, T. C., Smaal, A. C. and Pouwer, A. J.: Selective ingestion of phytoplankton by the bivalves *Mytilus edulis*
1161 *L.* and *Cerastoderma edule* (*L.*), *Hydrobiol. Bull.*, 25(1), 93–100, doi:10.1007/BF02259595, 1991.

1162 Qu, X., Su, L., Li, H., Liang, M. and Shi, H.: Assessing the relationship between the abundance and properties of
1163 microplastics in water and in mussels, *Sci. Total Environ.*, 621, 679–686, doi:10.1016/j.scitotenv.2017.11.284, 2018.

1164 [Raitsos, D. E., Reid, P. C., Lavender, S. J., Edwards, M. and Richardson, A. J.: Extending the SeaWiFS
1165 chlorophyll data set back 50 years in the northeast Atlantic, *Geophys. Res. Lett.*, 32\(6\), 1–4,
1166 doi:10.1029/2005GL022484, 2005.](#)

1167 [Raitsos, D. E., Lavender, S. J., Maravelias, C. D., Haralabous, J., Richardson, A. J. and Reid, P. C.: Identifying
1168 four phytoplankton functional types from space: An ecological approach, *Limnol. Oceanogr.*, 53\(2\), 605–613,
1169 doi:10.4319/lo.2008.53.2.0605, 2008.](#)

1170 Raitsos, D. E., Korres, G., Triantafyllou, G., Petihakis, G., Pantazi, M., Tsiaras, K. and Pollani, A.: Assessing
1171 chlorophyll variability in relation to the environmental regime in Pagasitikos Gulf, Greece, *J. Mar. Syst.*, 94(SUPPL.),
1172 16–22, doi:10.1016/j.jmarsys.2011.11.003, 2012.

1173 ~~[Raitsos, D. E., Lavender, S. J., Maravelias, C. D., Haralabous, J., Richardson, A. J. and Reid, P. C.: Identifying
1174 four phytoplankton functional types from space: An ecological approach, *Limnol. Oceanogr.*, 53\(2\), 605–613,
1175 doi:10.4319/lo.2008.53.2.0605, 2008.](#)~~

1176 Raitsos, D. E., Pradhan, Y., Lavender, S. J., Hoteit, I., Mcquatters-Gollop, A., Reid, P. C. and Richardson, A. J.:
1177 From silk to satellite: Half a century of ocean colour anomalies in the Northeast Atlantic, *Glob. Chang. Biol.*, 20(7),
1178 2117–2123, doi:10.1111/gcb.12457, 2014.

1179 [Raitso, D. E., Reid, P. C., Lavender, S. J., Edwards, M. and Richardson, A. J.: Extending the SeaWiFS](#)
1180 [chlorophyll data set back 50 years in the northeast Atlantic, *Geophys. Res. Lett.*, 32\(6\), 1–4,](#)
1181 [doi:10.1029/2005GL022484, 2005.](#)

1182 Ren, J. S.: Effect of food quality on energy uptake, *J. Sea Res.*, 62(2–3), 72–74,
1183 doi:10.1016/j.seares.2008.11.002, 2009.

1184 [Riisgård, H. U., Kittner, C. and Seerup, D. F.: Regulation of opening state and filtration rate in filter-feeding](#)
1185 [bivalves \(*Cardium edule*, *Mytilus edulis*, *Mya arenaria*\) in response to low algal concentration, *J. Exp. Mar. Bio. Ecol.*,](#)
1186 [284\(1–2\), 105–127, doi:10.1016/S0022-0981\(02\)00496-3, 2003.](#)

1187 Riisgård, H. U., Egede, P. P. and Barreiro Saavedra, I.: Feeding Behaviour of the Mussel, *Mytilus edulis* : New
1188 Observations, with a Minireview of Current Knowledge , *J. Mar. Biol.*, 2011, 1–13, doi:10.1155/2011/312459, 2011.

1189 [Riisgård, H. U., Kittner, C. and Seerup, D. F.: Regulation of opening state and filtration rate in filter-feeding](#)
1190 [bivalves \(*Cardium edule*, *Mytilus edulis*, *Mya arenaria*\) in response to low algal concentration, *J. Exp. Mar. Bio. Ecol.*,](#)
1191 [284\(1–2\), 105–127, doi:10.1016/S0022-0981\(02\)00496-3, 2003.](#)

1192 Rios, L. M., Moore, C. and Jones, P. R.: Persistent organic pollutants carried by synthetic polymers in the ocean
1193 environment, *Mar. Pollut. Bull.*, 54(8), 1230–1237, doi:10.1016/j.marpolbul.2007.03.022, 2007.

1194 Rist, S., Steensgaard, I. M., Guven, O., Nielsen, T. G., Jensen, L. H., Møller, L. F. and Hartmann, N. B.: The fate
1195 of microplastics during uptake and depuration phases in a blue mussel exposure system, *Environ. Toxicol. Chem.*,
1196 38(1), 99–105, doi:10.1002/etc.4285, 2019.

1197 Romeo, T., Pietro, B., Pedà, C., Consoli, P., Andaloro, F. and Fossi, M. C.: First evidence of presence of plastic
1198 debris in stomach of large pelagic fish in the Mediterranean Sea, *Mar. Pollut. Bull.*, 95(1), 358–361,
1199 doi:10.1016/j.marpolbul.2015.04.048, 2015.

1200 Rosland, R., Strand, Alunno-Bruscia, M., Bacher, C. and Strohmeier, T.: Applying Dynamic Energy Budget
1201 (DEB) theory to simulate growth and bio-energetics of blue mussels under low seston conditions, *J. Sea Res.*, 62(2–3),
1202 49–61, doi:10.1016/j.seares.2009.02.007, 2009.

1203 Santana, M. F. M., Moreira, F. T., Pereira, C. D. S., Abessa, D. M. S. and Turra, A.: Continuous Exposure to
1204 Microplastics Does Not Cause Physiological Effects in the Cultivated Mussel *Perna perna*, *Arch. Environ. Contam.*
1205 *Toxicol.*, 74(4), 594–604, doi:10.1007/s00244-018-0504-3, 2018.

1206 Sarà, G., Kearney, M. and Helmuth, B.: Combining heat-transfer and energy budget models to predict thermal
1207 stress in Mediterranean intertidal mussels, *Chem. Ecol.*, 27(2), 135–145, doi:10.1080/02757540.2011.552227, 2011.

1208 [Sarà, G., Reid, G. K., Rinaldi, A., Palmeri, V., Troell, M. and Kooijman, S. A. L. M.: Growth and reproductive](#)
1209 [simulation of candidate shellfish species at fish cages in the Southern Mediterranean: Dynamic Energy Budget \(DEB\)](#)
1210 [modelling for integrated multi-trophic aquaculture, *Aquaculture*, 324–325, 259–266,](#)
1211 [doi:10.1016/j.aquaculture.2011.10.042, 2012.](#)

1212 Sarà, G., Milanese, M., Prusina, I., Sarà, A., Angel, D. L., Glamuzina, B., Nitzan, T., Freeman, S., Rinaldi, A.,
1213 Palmeri, V., Montalto, V., Lo Martire, M., Gianguzza, P., Arizza, V., Lo Brutto, S., De Pirro, M., Helmuth, B.,
1214 Murray, J., De Cantis, S. and Williams, G. A.: The impact of climate change on mediterranean intertidal communities:
1215 Losses in coastal ecosystem integrity and services, *Reg. Environ. Chang.*, 14(SUPPL.1), 5–17, doi:10.1007/s10113-
1216 012-0360-z, 2014.

1217 [Sarà, G., Reid, G. K., Rinaldi, A., Palmeri, V., Troell, M. and Kooijman, S. A. L. M.: Growth and reproductive](#)
1218 [simulation of candidate shellfish species at fish cages in the Southern Mediterranean: Dynamic Energy Budget \(DEB\)](#)
1219 [modelling for integrated multi-trophic aquaculture, *Aquaculture*, 324–325, 259–266,](#)
1220 [doi:10.1016/j.aquaculture.2011.10.042, 2012.](#)

1221 Saraiva, S., der Meer, J. van, Kooijman, S. A. L. M. and Sousa, T.: DEB parameters estimation for *Mytilus*
1222 *edulis*, *J. Sea Res.*, 66(4), 289–296, doi:10.1016/j.seares.2011.06.002, 2011b.

1223 Saraiva, S., van der Meer, J., Kooijman, S. A. L. M. and Sousa, T.: Modelling feeding processes in bivalves: A
1224 mechanistic approach, *Ecol. Modell.*, 222(3), 514–523, doi:10.1016/j.ecolmodel.2010.09.031, 2011a.

1225 Saraiva, S., Van Der Meer, J., Kooijman, S. A. L. M., Witbaard, R., Philippart, C. J. M., Hippler, D. and Parker,
1226 R.: Validation of a Dynamic Energy Budget (DEB) model for the blue mussel *Mytilus edulis*, *Mar. Ecol. Prog. Ser.*,
1227 463, 141–158, doi:10.3354/meps09801, 2012.

1228 Schwabl, P., Koppel, S., Königshofer, P., Bucsics, T., Trauner, M., Reiberger, T. and Liebmann, B.: Detection of
1229 various microplastics in human stool: A prospective case series, *Ann. Intern. Med.*, 171(7), 453–457,
1230 doi:10.7326/M19-0618, 2019.

1231 Seuront, L., Nicastro, K. R., Zardi, G. I. and Goberville, E.: Decreased thermal tolerance under recurrent heat
1232 stress conditions explains summer mass mortality of the blue mussel *Mytilus edulis*, *Sci. Rep.*, 9(1),
1233 doi:10.1038/s41598-019-53580-w, 2019.

1234 Skoulidakis, N. T., Economou, A. N., Gritzalis, K. C. and Zogaris, S.: Rivers of the Balkans, *Rivers Eur.*, 421–
1235 466, doi:10.1016/B978-0-12-369449-2.00011-4, 2009.

1236 Smith, M., Love, D. C., Rochman, C. M. and Neff, R. A.: Microplastics in Seafood and the Implications for
1237 Human Health, *Curr. Environ. Heal. reports*, 5(3), 375–386, doi:10.1007/s40572-018-0206-z, 2018.

1238 Sprung, M.: Reproduction and fecundity of the mussel *mytilus edulis* at helgoland (North sea), *Helgoländer*
1239 *Meeresuntersuchungen*, 36(3), 243–255, doi:10.1007/BF01983629, 1983.

1240 Strohmeier, T., Strand, Ø., Alunno-Bruscia, M., Duinker, A. and Cranford, P.: Variability in particle retention
1241 efficiency by the mussel *Mytilus edulis*, *J. Exp. Mar. Bio. Ecol.*, 412, 96–102, doi:10.1016/j.jembe.2011.11.006, 2012.

1242 Sukhotin, A. A. and Kulakowski, E. E.: Growth and population dynamics in mussels (*Mytilus edulis* L.) cultured
1243 in the White Sea, *Aquaculture*, 101(1–2), 59–73, doi:10.1016/0044-8486(92)90232-A, 1992.

1244 Sukhotin, A. A., Strelkov, P. P., Maximovich, N. V. and Hummel, H.: Growth and longevity of *Mytilus edulis*
1245 (L.) from northeast Europe, *Mar. Biol. Res.*, 3(3), 155–167, doi:10.1080/17451000701364869, 2007.

1246 Sussarellu, R., Suquet, M., Thomas, Y., Lambert, C., Fabioux, C., Pernet, M. E. J., Goïc, N. Le, Quillien, V.,
1247 Mingant, C., Epelboin, Y., Corporeau, C., Guyomarch, J., Robbins, J., Paul-Pont, I., Soudant, P. and Huvet, A.: Oyster
1248 reproduction is affected by exposure to polystyrene microplastics, *Proc. Natl. Acad. Sci. U. S. A.*, 113(9), 2430–2435,
1249 doi:10.1073/pnas.1519019113, 2016.

1250 Tagliarolo, M. and McQuaid, C. D.: Sub-lethal and sub-specific temperature effects are better predictors of
1251 mussel distribution than thermal tolerance, *Mar. Ecol. Prog. Ser.*, 535, 145–159, doi:10.3354/meps11434, 2015.

1252 Teuten, E. L., Rowland, S. J., Galloway, T. S. and Thompson, R. C.: Potential for plastics to transport
1253 hydrophobic contaminants, *Environ. Sci. Technol.*, 41(22), 7759–7764, doi:10.1021/es071737s, 2007.

1254 Teuten, E. L., Saquing, J. M., Knappe, D. R. U., Barlaz, M. A., Jonsson, S., Björn, A., Rowland, S. J.,
1255 Thompson, R. C., Galloway, T. S., Yamashita, R., Ochi, D., Watanuki, Y., Moore, C., Viet, P. H., Tana, T. S.,
1256 Prudente, M., Boonyatumanond, R., Zakaria, M. P., Akkavong, K., Ogata, Y., Hirai, H., Iwasa, S., Mizukawa, K.,
1257 Hagino, Y., Imamura, A., Saha, M. and Takada, H.: Transport and release of chemicals from plastics to the
1258 environment and to wildlife, *Philos. Trans. R. Soc. B Biol. Sci.*, 364(1526), 2027–2045, doi:10.1098/rstb.2008.0284,
1259 2009.

1260 Theodorou, J. A., Viaene, J., Sorgeloos, P. and Tzovenis, I.: Production and Marketing Trends of the Cultured
1261 Mediterranean Mussel *Mytilus galloprovincialis* Lamarck 1819, in Greece , *J. Shellfish Res.*, 30(3), 859–874,
1262 doi:10.2983/035.030.0327, 2011.

1263 Thomas, Y., Mazurié, J., Alunno-Bruscia, M., Bacher, C., Bouget, J. F., Gohin, F., Pouvreau, S. and Struski, C.:
1264 Modelling spatio-temporal variability of *Mytilus edulis* (L.) growth by forcing a dynamic energy budget model with
1265 satellite-derived environmental data, *J. Sea Res.*, 66(4), 308–317, doi:10.1016/j.seares.2011.04.015, 2011.

1266 Thompson, R. C., Olson, Y., Mitchell, R. P., Davis, A., Rowland, S. J., John, A. W. G., McGonigle, D. and
1267 Russell, A. E.: Lost at Sea: Where Is All the Plastic?, *Science* (80-.), 304(5672), 838, doi:10.1126/science.1094559,
1268 2004.

1269 Triantafyllou, G., Petihakis, G. and Allen, I. J.: Assessing the performance of the Cretan Sea ecosystem model
1270 with the use of high frequency M3A buoy data set, *Ann. Geophys.*, 21(1), 365–375, doi:10.5194/angeo-21-365-2003,
1271 2003.

1272 Troost, T. A., Wijsman, J. W. M., Saraiva, S. and Freitas, V.: Modelling shellfish growth with dynamic energy
1273 budget models: An application for cockles and mussels in the Oosterschelde (southwest Netherlands), *Philos. Trans. R.*
1274 *Soc. B Biol. Sci.*, 365(1557), 3567–3577, doi:10.1098/rstb.2010.0074, 2010.

1275 Troost, T. A., Desclaux, T., Leslie, H. A., van Der Meulen, M. D. and Vethaak, A. D.: Do microplastics affect
1276 marine ecosystem productivity?, *Mar. Pollut. Bull.*, 135, 17–29, doi:10.1016/j.marpolbul.2018.05.067, 2018.

1277 ~~Troost, T. A., Wijsman, J. W. M., Saraiva, S. and Freitas, V.: Modelling shellfish growth with dynamic energy~~
1278 ~~budget models: An application for cockles and mussels in the Oosterschelde (southwest Netherlands), *Philos. Trans. R.*~~
1279 ~~*Soc. B Biol. Sci.*, 365(1557), 3567–3577, doi:10.1098/rstb.2010.0074, 2010.~~

1280 Tsiaras, K. P., Petihakis, G., Kourafalou, V. H. and Triantafyllou, G.: Impact of the river nutrient load variability
1281 on the North Aegean ecosystem functioning over the last decades, *J. Sea Res.*, 86, 97–109,
1282 doi:10.1016/j.seares.2013.11.007, 2014.

1283 Vahl, O.: Efficiency of particle retention in *mytilus edulis* L, *Ophelia*, 10(1), 17–25,
1284 doi:10.1080/00785326.1972.10430098, 1972.

1285 van Beusekom, J. E. E., Loebel, M. and Martens, P.: Distant riverine nutrient supply and local temperature drive
1286 the long-term phytoplankton development in a temperate coastal basin, *J. Sea Res.*, 61(1–2), 26–33,
1287 doi:10.1016/j.seares.2008.06.005, 2009.

1288 Van Cauwenberghe, L. and Janssen, C. R.: Microplastics in bivalves cultured for human consumption, *Environ.*
1289 *Pollut.*, 193, 65–70, doi:10.1016/j.envpol.2014.06.010, 2014.

1290 Van Cauwenberghe, L., Claessens, M., Vandegehuchte, M. B. and Janssen, C. R.: Microplastics are taken up by
1291 mussels (*Mytilus edulis*) and lugworms (*Arenicola marina*) living in natural habitats, *Environ. Pollut.*, 199, 10–17,
1292 doi:10.1016/j.envpol.2015.01.008, 2015.

1293 van der Veer, H. W., Cardoso, J. F. M. F. and van der Meer, J.: The estimation of DEB parameters for various
1294 Northeast Atlantic bivalve species, *J. Sea Res.*, 56(2), 107–124, doi:10.1016/j.seares.2006.03.005, 2006.

1295 van Haren, R. J. F., Schepers, H. E. and Kooijman, S. A. L. M.: Dynamic energy budgets affect kinetics of
1296 xenobiotics in the marine mussel *Mytilus edulis*, *Chemosphere*, 29(2), 163–189, doi:10.1016/0045-6535(94)90099-X,
1297 1994.

1298 Van Sebille, E., Wilcox, C., Lebreton, L., Maximenko, N., Hardesty, B. D., Van Franeker, J. A., Eriksen, M.,
1299 Siegel, D., Galgani, F. and Law, K. L.: A global inventory of small floating plastic debris, *Environ. Res. Lett.*, 10(12),
1300 124006, doi:10.1088/1748-9326/10/12/124006, 2015.

1301 Vandermeersch, G., Lourenço, H. M., Alvarez-Muñoz, D., Cunha, S., Diogène, J., Cano-Sancho, G., Sloth, J. J.,
1302 Kwadijk, C., Barcelo, D., Allegaert, W., Bekaert, K., Fernandes, J. O., Marques, A. and Robbens, J.: Environmental
1303 contaminants of emerging concern in seafood - European database on contaminant levels, *Environ. Res.*, 143, 29–45,
1304 doi:10.1016/j.envres.2015.06.011, 2015.

1305 Vlachogianni, T., Anastasopoulou, A., Fortibuoni, T., Ronchi, F. and Zeri, C.: Marine Litter Assessment in the
1306 Adriatic & Ionian Seas. IPA-Adriatic DeFishGear Project, MIO-ECSDE, HCMR and ISPRA. pp. 168 (ISBN: 978-
1307 960-6793-25-7), 2017.

1308 Von Moos, N., Burkhardt-Holm, P. and Köhler, A.: Uptake and effects of microplastics on cells and tissue of the
1309 blue mussel *Mytilus edulis* L. after an experimental exposure, *Environ. Sci. Technol.*, 46(20), 11327–11335,
1310 doi:10.1021/es302332w, 2012.

1311 Ward, J. E. and Kach, D. J.: Marine aggregates facilitate ingestion of nanoparticles by suspension-feeding
1312 bivalves, *Mar. Environ. Res.*, 68(3), 137–142, doi:10.1016/j.marenvres.2009.05.002, 2009.

1313 Ward, J. E. and Shumway, S. E.: Separating the grain from the chaff: Particle selection in suspension- and
1314 deposit-feeding bivalves, *J. Exp. Mar. Bio. Ecol.*, 300(1–2), 83–130, doi:10.1016/j.jembe.2004.03.002, 2004.

1315 [Ward, J., Rosa, M. and Shumway, S.: Capture, ingestion, and egestion of microplastics by suspension-feeding](#)
1316 [bivalves: a 40-year history, *Anthr. Coasts*, 2\(1\), 39–49, doi:10.1139/anc-2018-0027, 2019a.](#)

1317 Ward, J. E., Zhao, S., Holohan, B. A., Mladinich, K. M., Griffin, T. W., Wozniak, J. and Shumway, S. E.:
1318 Selective Ingestion and Egestion of Plastic Particles by the Blue Mussel (*Mytilus edulis*) and Eastern Oyster
1319 (*Crassostrea virginica*): Implications for Using Bivalves as Bioindicators of Microplastic Pollution, *Environ. Sci.*
1320 *Technol.*, 53(15), 8776–8784, doi:10.1021/acs.est.9b02073, 2019b.

1321 Wegner, A., Besseling, E., Foekema, E. M., Kamermans, P. and Koelmans, A. A.: Effects of nanopolystyrene on
1322 the feeding behavior of the blue mussel (*Mytilus edulis* L.), *Environ. Toxicol. Chem.*, 31(11), 2490–2497,
1323 doi:10.1002/etc.1984, 2012.

1324 Widdows, J., Fieth, P. and Worrall, C. M.: Relationships between seston, available food and feeding activity in
1325 the common mussel *Mytilus edulis*, *Mar. Biol.*, 50(3), 195–207, doi:10.1007/BF00394201, 1979.

1326 Wieczorek, A. M., Morrison, L., Croot, P. L., Allcock, A. L., MacLoughlin, E., Savard, O., Brownlow, H. and
1327 Doyle, T. K.: Frequency of microplastics in mesopelagic fishes from the Northwest Atlantic, *Front. Mar. Sci.*, 5(FEB),
1328 doi:10.3389/fmars.2018.00039, 2018.

1329 Woods, M. N., Stack, M. E., Fields, D. M., Shaw, S. D. and Matrai, P. A.: Microplastic fiber uptake, ingestion,
1330 and egestion rates in the blue mussel (*Mytilus edulis*), *Mar. Pollut. Bull.*, 137, 638–645,
1331 doi:10.1016/j.marpolbul.2018.10.061, 2018.

1332 Zaldivar, J. M.: A general bioaccumulation DEB model for mussels. JRC Scientific and Technical Reports, EUR
1333 23626. Office for Official Publications of the European Communities: Luxembourg, ISBN 978-92-79-10943-0 , ii, 31
1334 pp, 2008.

1335 Zeri, C., Adamopoulou, A., Bojanić Varezić, D., Fortibuoni, T., Kovač Viršek, M., Kržan, A., Mandić, M.,
1336 Mazziotti, C., Palatinus, A., Peterlin, M., Prvan, M., Ronchi, F., Siljic, J., Tutman, P. and Vlachogianni, T.: Floating
1337 plastics in Adriatic waters (Mediterranean Sea): From the macro- to the micro-scale, *Mar. Pollut. Bull.*, 136, 341–350,
1338 doi:10.1016/j.marpolbul.2018.09.016, 2018.

1339 Zhao, S., Ward, J. E., Danley, M. and Mincer, T. J.: Field-Based Evidence for Microplastic in Marine Aggregates
 1340 and Mussels: Implications for Trophic Transfer, Environ. Sci. Technol., 52(19), 11038–11048,
 1341 doi:10.1021/acs.est.8b03467, 2018.

1342

1343

1344 **Tables & Figures**

1345
$$\frac{dE}{dt} = \dot{p}_a - \dot{p}_c \quad (1)$$

1346
$$\frac{dV}{dt} = \frac{k \cdot \dot{p}_c - [\dot{p}_M] \cdot V}{[E_g]} \quad (2)$$

1347
$$\frac{dR}{dt} = (1 - k) \cdot \dot{p}_c - \left[\frac{1-k}{k} \right] \cdot \min(V, V_p) \cdot [\dot{p}_M] \quad (3)$$

1348
$$\dot{p}_a = \{\dot{p}_{Am}\} \cdot f \cdot k(T) \cdot V^{\frac{2}{3}} \quad (4)$$

1349
$$f = \frac{X}{X + K_y}, \quad \text{where } K_y = X_K \cdot \left(1 + \frac{Y}{Y_K}\right) \quad (5)$$

1350
$$\dot{p}_c = \frac{[E]}{[E_g] + k \cdot [E]} \cdot \left(\frac{[E_g] \cdot \{\dot{p}_{Am}\} \cdot k(T) \cdot V^{\frac{2}{3}}}{[E_m]} + [\dot{p}_M] \cdot V \right) \quad (6)$$

1351
$$[E] = \frac{E}{V} \quad (7)$$

1352
$$[\dot{p}_M] = k(T) \cdot [\dot{p}_M]_m \quad (8)$$

1353
$$k(T) = \frac{\exp\left(\frac{T_A - T_A}{T_I - T}\right)}{1 + \exp\left(\frac{T_{AL} - T_{AL}}{T - T_L}\right) + \exp\left(\frac{T_{AH} - T_{AH}}{T_H - T}\right)} \quad (9)$$

1354
$$L = \frac{V^{\frac{1}{3}}}{\delta_m} \quad (10)$$

1355
$$W = d \cdot \left(V + \frac{E}{[E_g]} \right) + \frac{R}{\mu_E} \quad (11)$$

1356
$$\dot{C}_R = \frac{\{\dot{C}_{Rm}\}}{1 + \sum_i^n \frac{X_i \cdot \{\dot{C}_{Rm}\}}{\{\dot{p}_{XiFm}\}}} \cdot k(T) \cdot V^{\frac{2}{3}}, \quad i = \begin{cases} 1 & \text{for CHL} - a \\ 2 & \text{for MPs} \end{cases} \quad (12)^a$$

1357
$$\dot{p}_{XiF} = \dot{C}_R \cdot X_i \quad (13)^a$$

1358
$$\dot{p}_{XiI} = \frac{\rho_{Xi} \cdot \dot{p}_{XiF}}{1 + \sum_i^n \frac{\rho_{Xi} \cdot \dot{p}_{XiF}}{\{\dot{p}_{XiIm}\}}} \quad (14)^a$$

1359
$$\dot{J}_{pfi} = \dot{p}_{XiF} - \dot{p}_{XiI} \quad (15)^a$$

1360
$$\dot{J}_f = \dot{p}_{X1I} - \dot{p}_A \quad (16)$$

1361
$$GSI = \frac{\frac{R}{\mu E}}{d \cdot \left(V + \frac{E}{[Eg]} \right) + \frac{R}{\mu E}} \quad (17)$$

1362 *Table 1. Dynamic energy budget model: equations. See Table 2 for model variables, Table 3 for parameters and Table*
 1363 *4 for initial values*

1364 *^a notation refers to feeding equations handling each type of suspended matter separately (i=1 for algae and i=2 for*
 1365 *microplastics) where units transformation is applied when it is necessary (see Table 3).*

1366

1367	Variable	Description	Units
1368	V	Structural volume	cm^3
1369	E	Energy reserves	J
1370	R	Energy allocated to development	
1371		and reproduction	J
1372	C	Microplastics accumulation	particles individual ⁻¹
1373	\dot{p}_a	Assimilation energy rate	J d^{-1}
1374	\dot{p}_c	Utilization energy rate	J d^{-1}
1375	\dot{C}_R	Clearance rate	$\text{m}^3 \text{d}^{-1}$
1376	C_{env}	Microplastics concentration	particles L^{-1}
1377	\dot{p}_{XiF}	Filtration rate	J d^{-1} or g d^{-1}
1378	\dot{p}_{XiI}	Ingestion rate	J d^{-1} or g d^{-1}
1379	\dot{J}_{pfi}	Pseudofaeces production rate	J d^{-1} or g d^{-1}
1380	\dot{J}_f	Faeces production rate	J d^{-1}
1381	f	Functional response function	-
1382	X_i	Food or MPs density	mg chl a m^{-3} or g m^{-3}
1383	$[\dot{p}_M]$	Maintenance costs	$\text{J cm}^{-3} \text{d}^{-1}$
1384	T	Temperature	K
1385	$k(T)$	Temperature dependence	-
1386	L	Shell length	cm
1387	W	Fresh tissue mass	g
1388	GSI	Gonado-somatic index	-

1389 *Table 2. Dynamic energy budget model: variables*

1390

1391	Parameter	Units	Description	Value	Reference
1392	$\{\dot{p}_{Am}\}$	$\text{J cm}^{-2} \text{d}^{-1}$	Maximum surface area-specific assimilation rate	147.6	Van der Veer et al. (2006)
1393	$\{\dot{C}_{Rm}\}$	$\text{m}^3 \text{cm}^{-2} \text{d}^{-1}$	Maximum surface area-specific clearance rate	0.096	Saraiva et al. (2011a)
1394	$\{\dot{p}_{X_1Fm}\}$	$\text{mg chl-a cm}^{-2} \text{d}^{-1}$	Algal maximum surface area-specific filtration rate*	0.1152	Rosland et al. (2009)
1395	$\{\dot{p}_{X_2Fm}\}$	$\text{g cm}^{-2} \text{d}^{-1}$	Silt maximum surface area-specific filtration rate	3.5	Saraiva et al. (2011a)
1396	$\{\dot{p}_{X_1Im}\}$	mg chl-a d^{-1}	Algae maximum ingestion rate*	$3.12 \cdot 10^6$	Saraiva et al. (2011b)
1397	$\{\dot{p}_{X_2Im}\}$	g d^{-1}	Silt maximum ingestion rate	0.11	Saraiva et al. (2011b)
1398	ρ_1	-	Algae binding probability	0.99	Saraiva et al. (2011a)
1399	ρ_2	-	Inorganic material binding probability	0.45	Saraiva et al. (2011a)
1400	k_f	d^{-1}	Post-igestive losses through faeces	Calibrated	-
1401	X_K	mg chl-a m^{-3}	Half saturation coefficient	Calibrated	-
1402	T_A	K	Arrhenius temperature	5800	Van der Veer et al. (2006)
1403	T_I	K	Reference temperature	293	Van der Veer et al. (2006)
1404	T_L	K	Lower boundary of tolerance rate	275	Van der Veer et al. (2006)
1405	T_H	K	Upper boundary of tolerance rate	296	Van der Veer et al. (2006)
1406	T_{AL}	K	Rate of decrease of upper boundary	45430	Van der Veer et al. (2006)
1407	T_{AH}	K	Rate of decrease of lower boundary	31376	Van der Veer et al. (2006)
1408	$[\dot{p}_M]_m$	$\text{J cm}^{-3} \text{d}^{-1}$	Volume specific maintenance costs	24	Van der Veer et al. (2006)
1409	$[E_G]$	J cm^{-3}	Volume specific growth costs	1900	Van der Veer et al. (2006)
1410	$[E_m]$	J cm^{-3}	Maximum energy density	2190	Van der Veer et al. (2006)
1411	k	-	Fraction of utilized energy spent on maintenance/growth	0.7	Van der Veer et al. (2006)
1412	V_p	cm^3	Volume at start of reproductive stage	0.06	Van der Veer et al. (2006)
1413	GSI_{th}	-	Gonado-somatic index triggering spawning	0.28	Van der Veer et al. (2006)
1414	δ_m	-	Shape coefficient	0.25	Casas & Bacher (2006)
1415	d	g cm^{-3}	Specific density	1.0	Kooijman (2000)
1416	μ_E	J g^{-1}	Energy content of reserves	6750	Casas & Bacher (2006)
1417	λ	J mg chl-a^{-1}	Conversion factor	2387.73	Rosland et al. (2009)

1418

Table 3. Dynamic energy budget model: parameters

1419 *units mol C converted to mg CHL-a by multiplying with the factor $\frac{12 \cdot 10^3}{50}$ assuming Carbon:CHL-a ratio of 50
 1420 (Hatzonikolakis et al., 2017).

1421
 1422
 1423

Area	X _k value (mg m ⁻³)	CHL-a range (mg m ⁻³)	CHL-a mean (mg m ⁻³)	Temperature range(°C)	Length after one year±SD (cm)	Reference
Maliakos Gulf	0.72	0.87-5.59	1.80	12.0-26.0	7.06 ± 0.46	Hatzonikolakis et al., 2017
Thermaikos Gulf	0.56	1.04-2.76	1.89	11.5-24.5	7.0 ± 0.47	Hatzonikolakis et al., 2017
Black Sea	Calibrated: 0.96	0.53-16.30	3.07	6.5-25.0	7.5 ± 0.1	Karayucel et al., 2010
Bizerte lagoon	3.829	4.00-7.70	5.20	12.0-28.0	7.26 ± 0.46	Béjaoui-Omri et al., 2014

1424
 1425
 1426
 1427
 1428

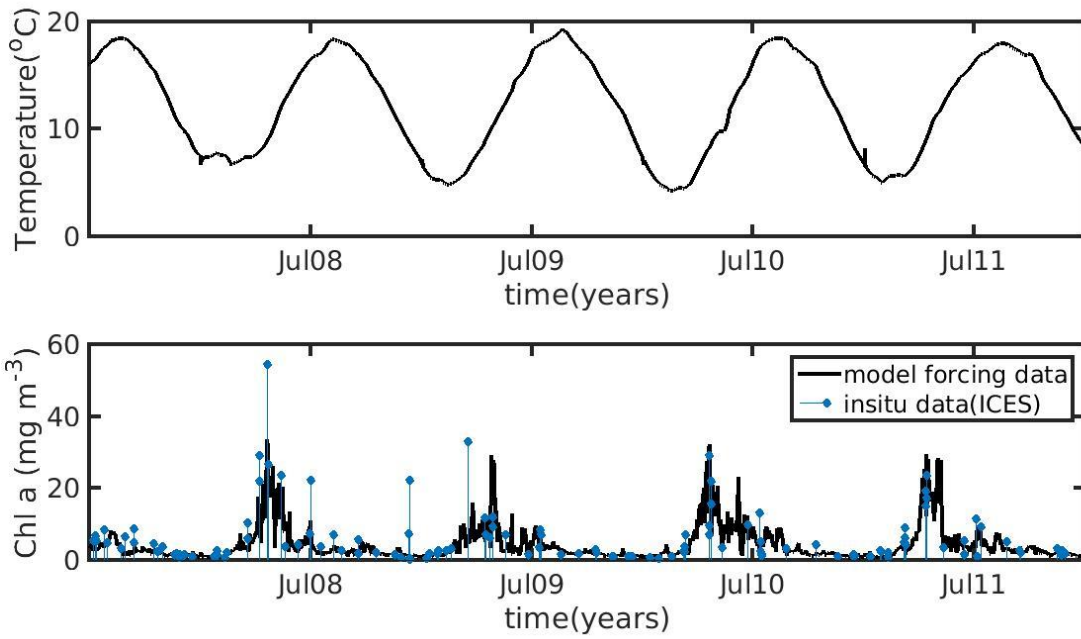
Table 4. Half saturation tuned values (X_k) and mussel growth data (Length) in different areas of the Mediterranean and Black Seas.

1429
 1430
 1431
 1432
 1433
 1434
 1435
 1436
 1437
 1438

Northern Ionian Sea		North Sea	
Variable	Value	Variable	Value
Start date	20 Nov 2010	Start date	1 Jul 2007
L	0.85 cm	L	0.15 cm
W	0.1938 g	W	0.0055 g
V	0.0096 cm ³	V	5.3·10 ⁻⁵ cm ³
E	350 J	E	10 J
R	0 J	R	0 J
C	0 particles individual ⁻¹	C	0 particles individual ⁻¹

1439 Table 5. Dynamic energy budget-accumulation model: initial values. L: shell length; W: fresh tissue mass; V: structural
 1440 volume; E: energy reserves; R: energy allocated to reproduction; C: Microplastics accumulation

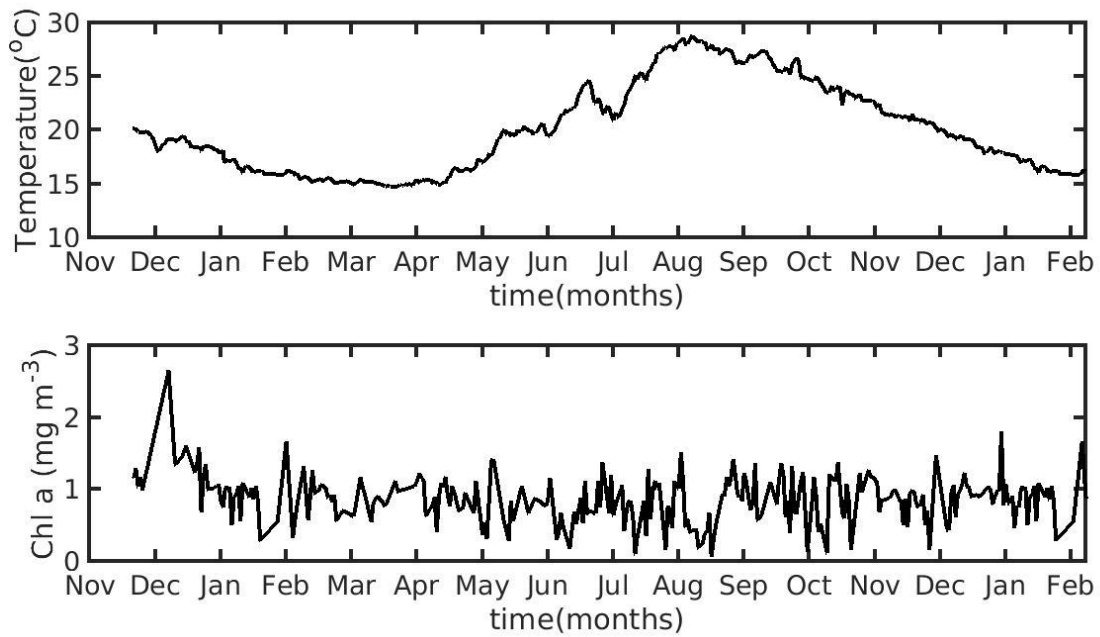
1441
 1442
 1443
 1444



1445

1446 *Fig. 1. Environmental data used for the forcing of the Dynamic Energy Budget model(DEB) in the North Sea*
 1447 *simulation, showing temperature (top) and chlorophyll a concentration against in situ data from the ICES database*
 1448 *(bottom).*

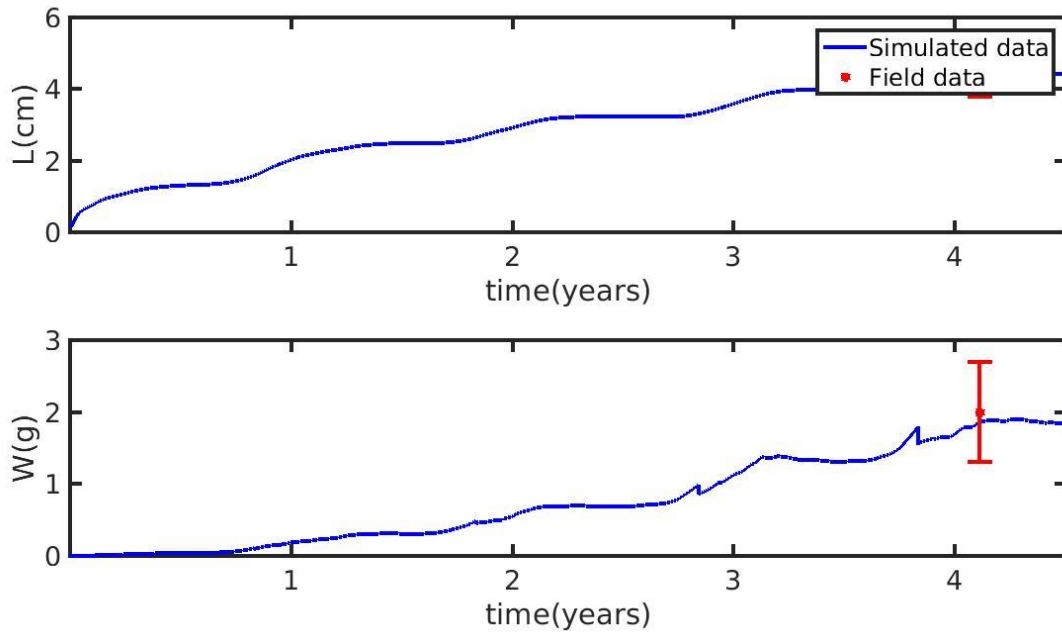
1449



1450

1451 *Fig. 2. Environmental data used for the forcing of the dynamic energy budget model in the Northern Ionian Sea*
 1452 *simulation, showing temperature (top) and chlorophyll a concentration (bottom).*

1453



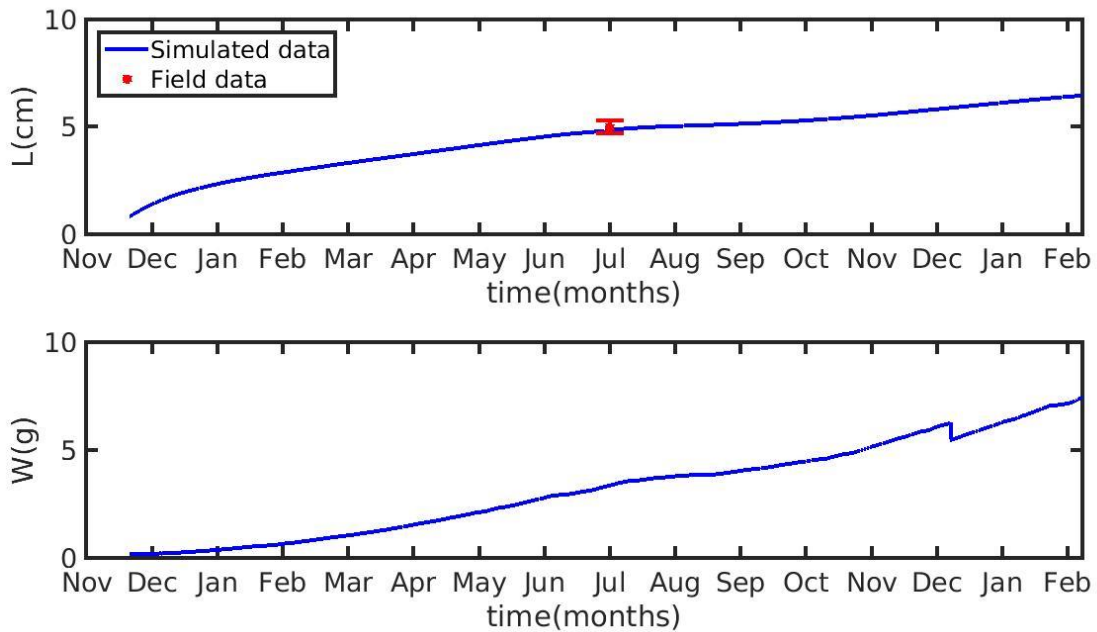
1454

1455

1456

1457

Fig. 3. Simulated mussel shell length (L) (top) and fresh tissue mass (W) (bottom) against North Sea data (red star: mean \pm SD), using chlorophyll a ($X=[CHL-a]$) in the mussel diet.

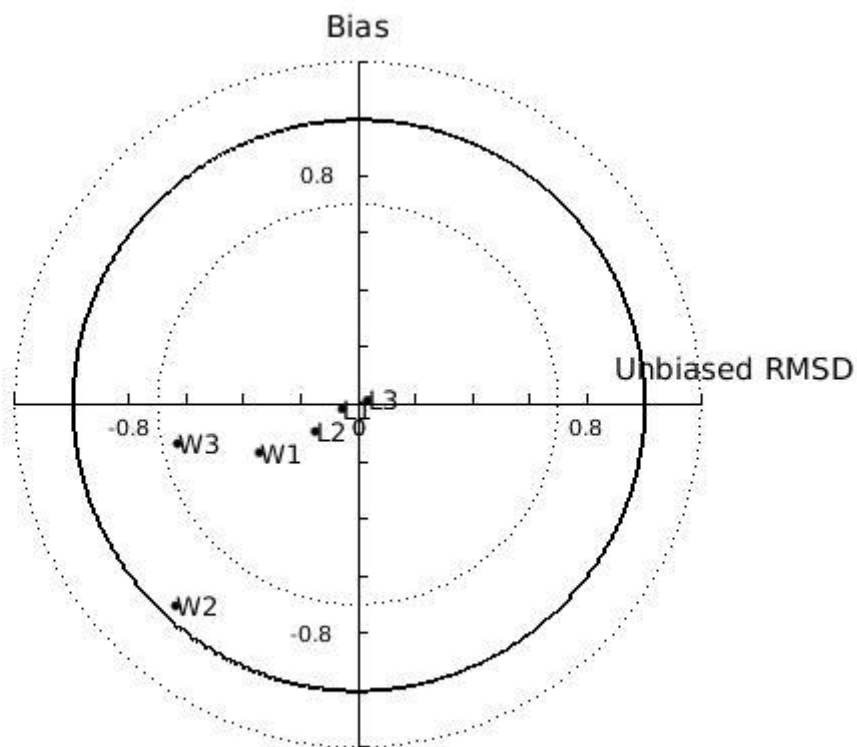


1458

1459

1460

Fig. 4. Simulated mussel shell length (L) (top) and fresh tissue mass (W) (bottom) against North Sea data (red star: mean \pm SD), using chlorophyll a ($X=[CHL-a]$) in the mussel diet

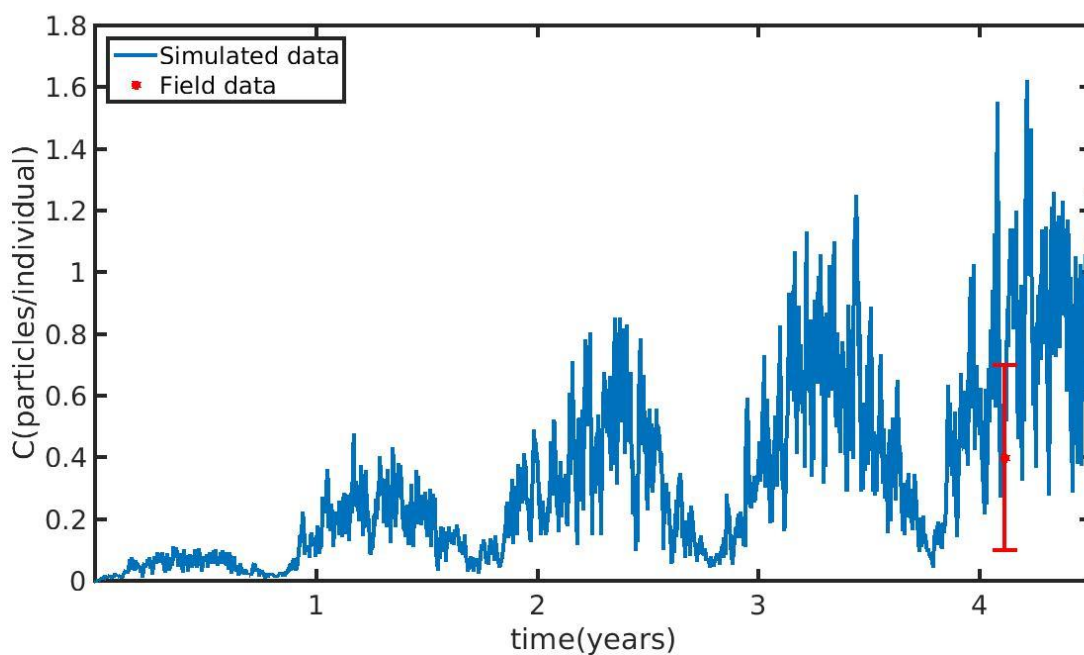


1461

1462 | *Fig. 53. Target diagram of simulated shell length (L) and fresh mass tissue weight (W) against field data from*
 1463 *Thermaikos and Maliakos Gulf (eastern Mediterranean Sea), Black Sea and Bizerte Lagoon (southwestern*
 1464 *Mediterranean Sea), using the **power** (L_1 , W_1), **exponential** (L_2 , W_2) and **linear** (L_3 , W_3) function of the half saturation*
 1465 *coefficient. The model bias is indicated on the y-axis while the unbiased root-mean-square-deviation (RMSD) is*
 1466 *indicated on the x-axis.*

1467

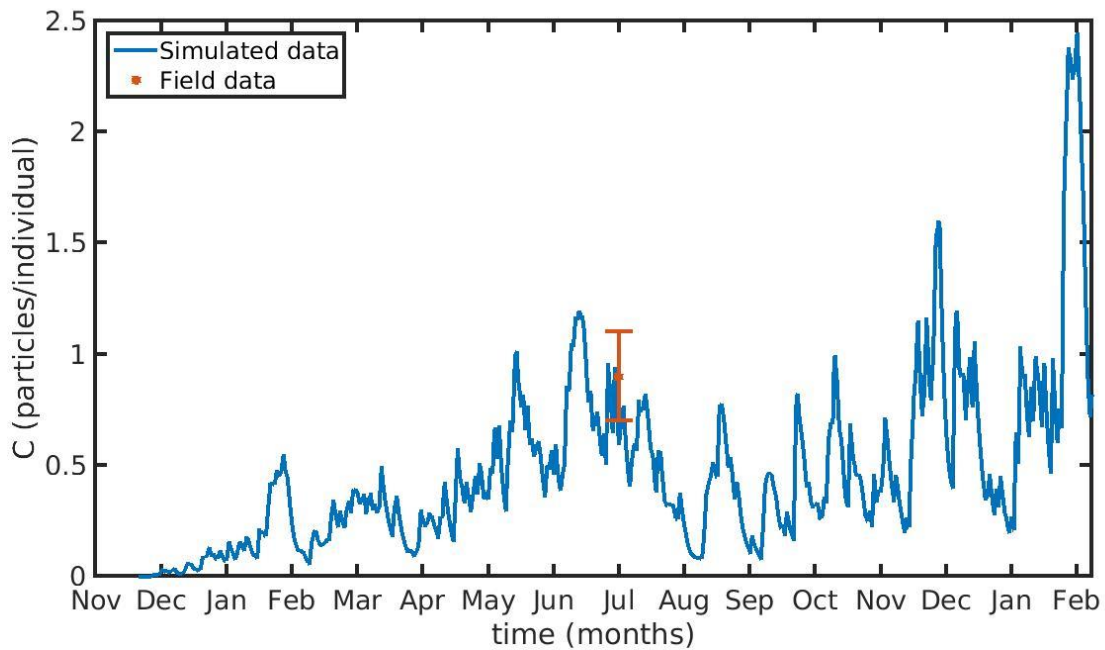
1468



1469

1470 Fig.6. Microplastics (MPs) accumulation by the mussel (blue line) against field data (red star: mean \pm SD), using daily
1471 environmental concentration of MPs (C_{env} mean value \pm SD: 0.4 ± 0.3 particles L^{-1}) in the North Sea.

1472

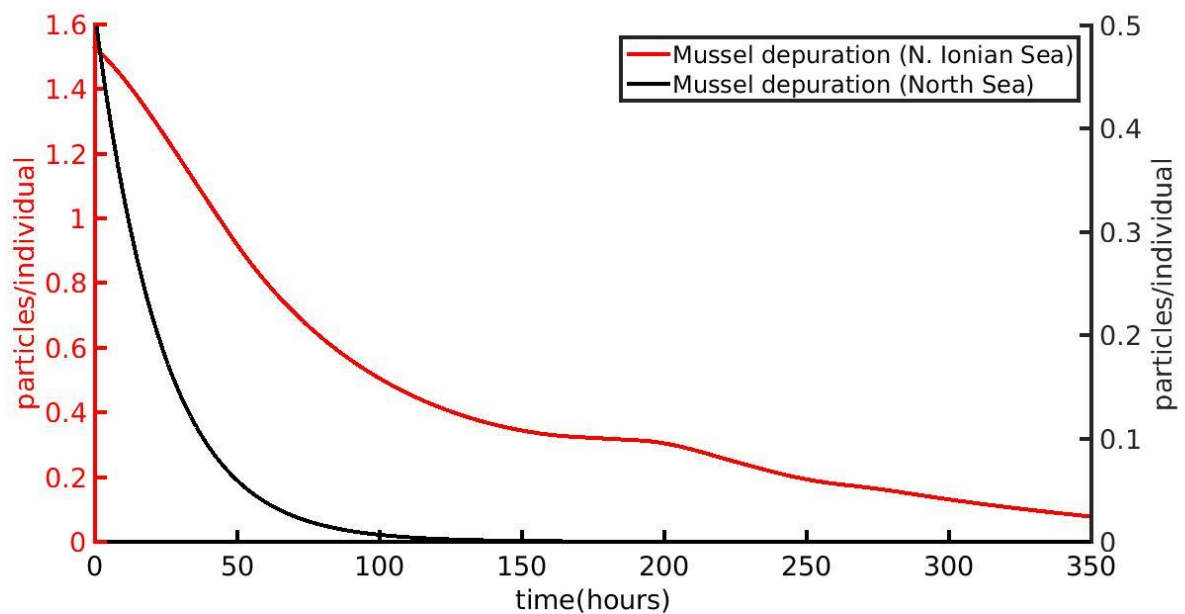


1473

1474 Fig. 7. Microplastics (MPs) accumulation by the mussel (blue line) against field data (red star: mean value \pm SD),
1475 using daily environmental concentration of MPs (C_{env} mean value \pm SD: 0.0012 ± 0.024 particles L^{-1}) in the Northern
1476 Ionian Sea.

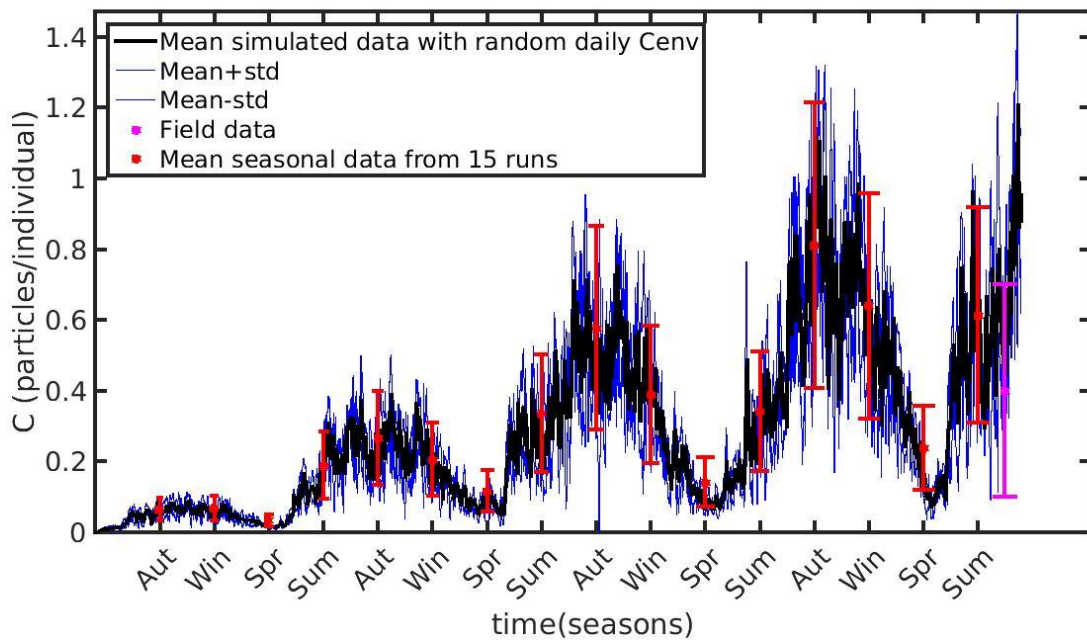
1477

1478



1479

1480 Fig. 8. Depuration phase of the cultured *Mytilus galloprovincialis* (red line) and wild *Mytilus edulis* (black line) using
1481 zero environmental concentration of microplastics ($C_{env}=0$) after 1 year and 4 years of simulation time at the Northern
1482 Ionian Sea and North Sea respectively.

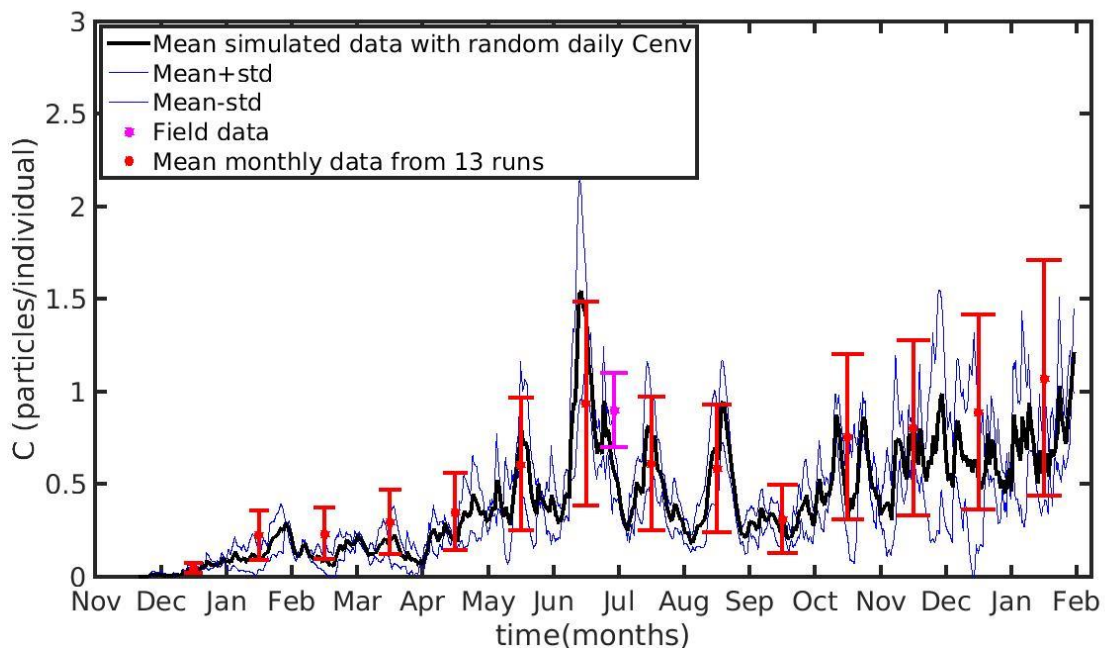


1484

1485 *Fig.9. Mean seasonally values and standard deviation of microplastics (MPs) accumulation (red error bars: mean*
 1486 *value \pm SD) by the mussel in North Sea derived from 15 model runs with different constant values of environmental*
 1487 *MPs concentration (C_{env} range: 0.1-0.8 particles L^{-1}); Mean hourly simulated data (black line) and standard deviation*
 1488 *(blue lines) of microplastics accumulation derived from 3 model runs with stochastic sequences of daily random C_{env}*
 1489 *values.*

1490

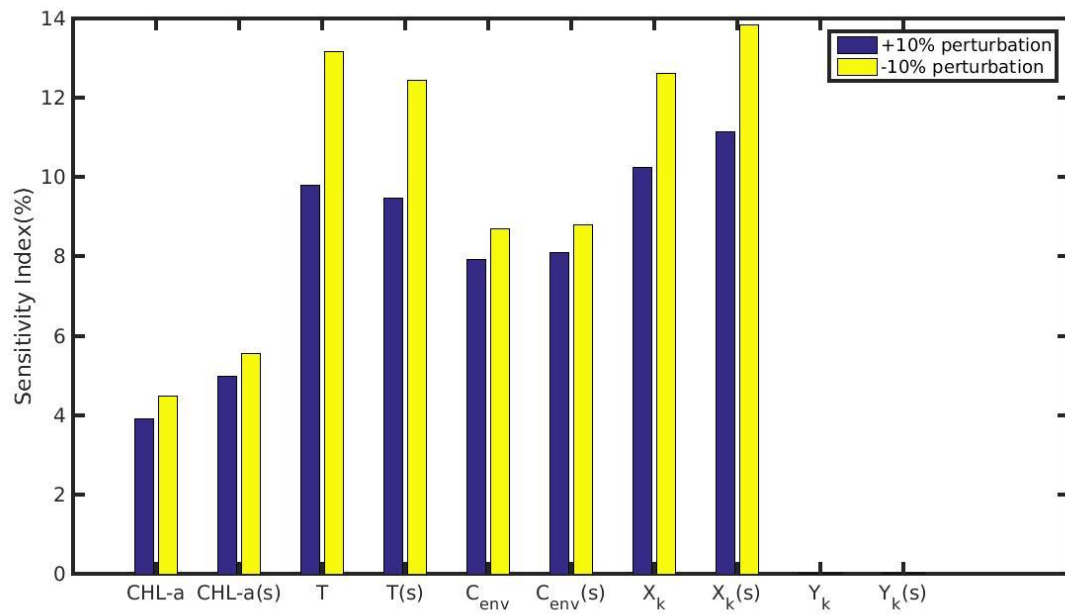
1491



1492

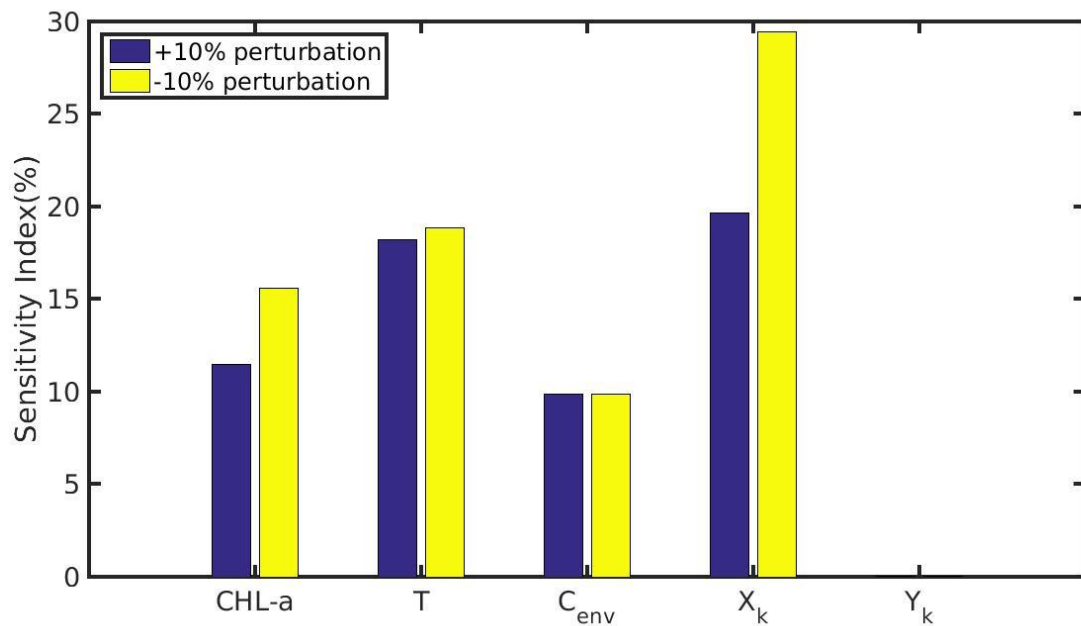
1493 *Fig. 10. Mean monthly values and standard deviation of microplastics accumulation (red error bars: mean value \pm SD)*
 1494 *by the mussel in Northern Ionian Sea derived from 13 model runs with different constant values of environmental MPs*
 1495 *concentration (C_{env} range: 0.0012-0.024 particles L^{-1}); Mean hourly simulated data (back line) and standard deviation*

1496 (blue lines) of microplastics accumulation derived from 3 model runs with stochastic sequences of daily random C_{env}
 1497 values.
 1498



1499
 1500 *Fig. 11. Sensitivity index of MPs accumulation on the wild mussel of the North Sea when variables (CHL-a,*
 1501 *temperature, C_{env}) and parameters (X_k , Y_k) are perturbed $\pm 10\%$. The notation (s) refers to the permanently submerged*
 1502 *mussel.*

1503
 1504

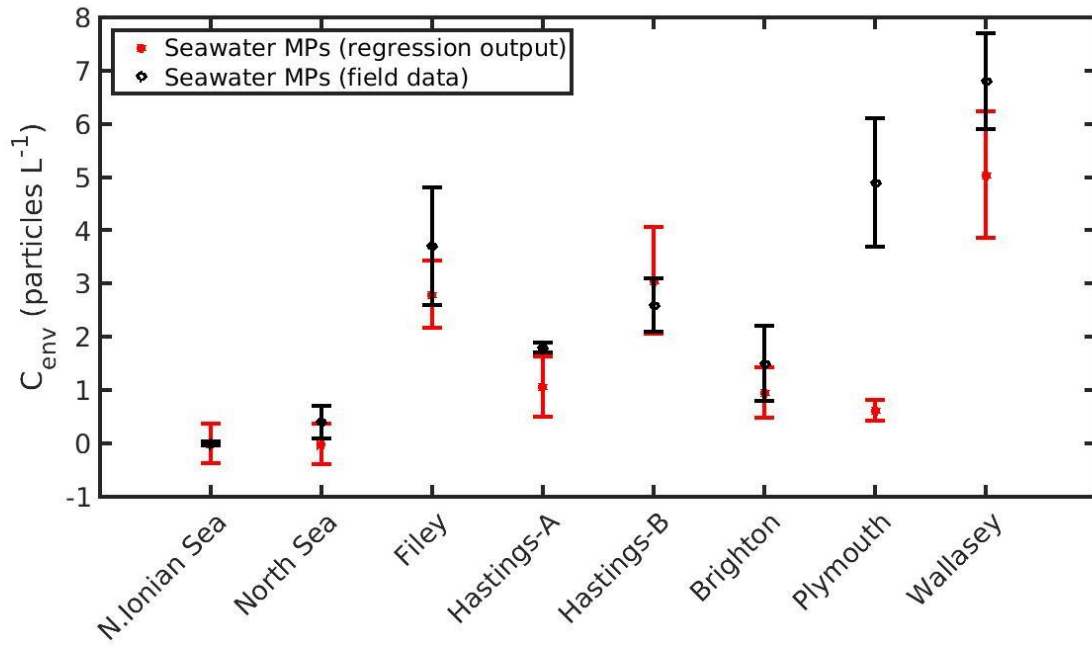


1505
 1506 *Fig. 12. Sensitivity index of MPs accumulation on the cultured mussel of the Northern Ionian Sea when variables*
 1507 *(CHL-a, temperature, C_{env}) and parameters (X_k , Y_k) are perturbed $\pm 10\%$.*

1508

1509

1510



1511

1512

1513

1514

Fig. 13. Prediction of seawater microplastics concentration by using Eq. 20 for the Northern Ionian Sea, North Sea (present study) and 6 areas around U.K. (Filey, Hastings-A&B, Brighton, Plymouth, Wallasey; Li et al. (2018)).